(12) INTERNATIONAL APPLICATION PUBLISHED UNDER THE PATENT COOPERATION TREATY (PCT)

(19) World Intellectual Property Organization
International Bureau

(43) International Publication Date
13 August 2020 (13.08.2020)

WIPO | PCT

(10) International Publication Number
WO 2020/161477 A1

(51) International Patent Classification:
A61K 31/506 (2006.01) *A61P 9/04* (2006.01)
A61K 31/437 (2006.01) *A61P 9/12* (2006.01)
A61P 1/16 (2006.01) *A61P 11/00* (2006.01)
A61P 9/00 (2006.01) *A61P 21/00* (2006.01)

(21) International Application Number:
PCT/GB2020/050243

(22) International Filing Date:
03 February 2020 (03.02.2020)

(25) Filing Language: English

(26) Publication Language: English

(30) Priority Data:
1901507.2 04 February 2019 (04.02.2019) GB

(71) Applicants: **ST GEORGE'S HOSPITAL MEDICAL SCHOOL** [GB/GB]; Cranmer Terrace, Tooting, London SW17 0RE (GB). **UNIVERSITY OF READING** [GB/GB]; Whiteknights House, Reading RG6 6AH (GB).

(72) Inventors: **MEIJLES, Daniel**; c/o St George's Hospital Medical School, University of London, Cranmer Terrace, London Greater London SW17 0RE (GB). **CLERK, Angela**; c/o St George's Hospital Medical School, University of London, Cranmer Terrace, London Greater London SW17 0RE (GB).

(74) Agent: **J A KEMP LLP**; 14 South Square, Gray's Inn, London Greater London WC1R 5JJ (GB).

(81) Designated States *(unless otherwise indicated, for every kind of national protection available)*: AE, AG, AL, AM, AO, AT, AU, AZ, BA, BB, BG, BH, BN, BR, BW, BY, BZ, CA, CH, CL, CN, CO, CR, CU, CZ, DE, DJ, DK, DM, DO, DZ, EC, EE, EG, ES, FI, GB, GD, GE, GH, GM, GT, HN, HR, HU, ID, IL, IN, IR, IS, JO, JP, KE, KG, KH, KN, KP, KR, KW, KZ, LA, LC, LK, LR, LS, LU, LY, MA, MD, ME, MG, MK, MN, MW, MX, MY, MZ, NA, NG, NI, NO, NZ, OM, PA, PE, PG, PH, PL, PT, QA, RO, RS, RU, RW, SA, SC, SD, SE, SG, SK, SL, ST, SV, SY, TH, TJ, TM, TN, TR, TT, TZ, UA, UG, US, UZ, VC, VN, WS, ZA, ZM, ZW.

(84) Designated States *(unless otherwise indicated, for every kind of regional protection available)*: ARIPO (BW, GH, GM, KE, LR, LS, MW, MZ, NA, RW, SD, SL, ST, SZ, TZ, UG, ZM, ZW), Eurasian (AM, AZ, BY, KG, KZ, RU, TJ, TM), European (AL, AT, BE, BG, CH, CY, CZ, DE, DK, EE, ES, FI, FR, GB, GR, HR, HU, IE, IS, IT, LT, LU, LV, MC, MK, MT, NL, NO, PL, PT, RO, RS, SE, SI, SK, SM, TR), OAPI (BF, BJ, CF, CG, CI, CM, GA, GN, GQ, GW, KM, ML, MR, NE, SN, TD, TG).

Published:
— *with international search report (Art. 21(3))*

(54) Title: TREATMENT OF FIBROSIS WITH RAF INHIBITORS

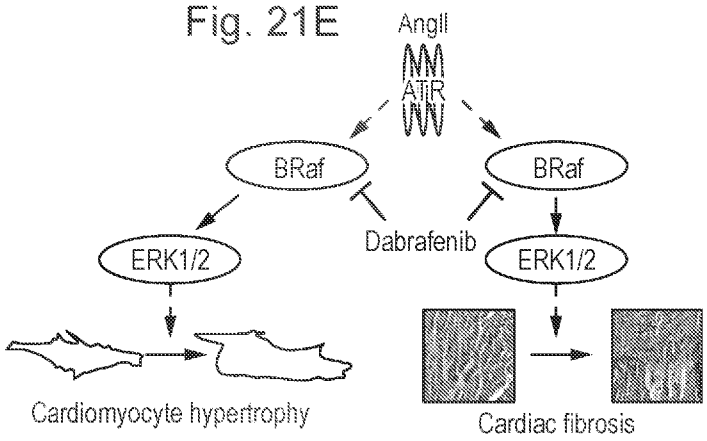

(57) Abstract: The present invention relates to the treatment or prevention of fibrosis associated with the activity of Raf kinases, for example cardiac fibrosis.

WO 2020/161477 A1

TREATMENT OF FIBROSIS WITH RAF INHIBITORS

FIELD OF THE INVENTION

The present invention relates to the treatment or prevention of fibrosis associated with the activity of Raf kinases, e.g. BRaf.

BACKGROUND OF THE INVENTION

Fibrosis can occur in many tissues of the body, for example the heart, liver, lungs and kidney. Activation of pathways such as the extracellular signal regulated kinase 1/2 (ERK1/2) pathway ultimately lead to fibroblast proliferation, which results in the deposition of extracellular matrix into surrounding connective tissue, i.e. fibrosis. Whilst fibrosis is important in normal tissue repair, excessive fibroblast proliferation is harmful and can, depending on the location of the fibrosis within the body, lead to (for example) shortness of breath, heart failure or loss of kidney function.

One of the most important diseases associated with fibrosis is cardiac fibrosis and/or heart failure, with hypertension as a major contributing factor. Initially, the heart adapts to the increased work-load to maintain cardiac output. This is achieved in part by hypertrophy of terminally-differentiated contractile cardiomyocytes which increase in size, adapting and increasing the myofibrillar apparatus. In the longer term, this is not sustained, contractile function is compromised and heart failure develops. Pathological changes include cardiomyocyte cell death, and capillary rarefaction. This is associated with inflammation and increased fibrosis. Strategies to reduce cardiomyocyte death, improve contractility, increase angiogenesis and reduce fibrosis are all necessary to treat heart failure.

The extracellular signal regulated kinase 1/2 (ERK1/2) cascade is a key growth-promoting pathway in all cells. It is best characterised in proliferating cells in which ERK1/2 activation promotes cell division. ERK1/2 are phosphorylated/activated by MKK1/2 that are phosphorylated/activated by upstream Raf kinases (ARaf, BRaf, cRaf) or, in the context of inflammation, Cot/Tpl2. Raf kinases are regulated at multiple levels. Of particular importance, activation requires interaction with activated Ras which induces a conformational change in Raf proteins. They also operate as homo- or heterodimers and are subject to activating and inhibitory phosphorylations.

In the heart, the ERK1/2 cascade is strongly implicated in promoting cardiomyocyte hypertrophy and, independent of this, is potently cardioprotective. All Raf kinases are activated in cultured cardiomyocytes by hypertrophic stimuli such as endothelin-1. Studies in genetically-modified mice indicate cRaf is required for cardiac hypertrophy (Muslin *et al.*, Trends Cardiovasc. Med., (2005), 15:225-229). One report suggested BRaf may be pro-hypertrophic (Kramann *et al.*, Cardiovasc. Res., (2014), 102:88-96), but BRaf itself was not studied, the conclusions relying on use of an inhibitor at a concentration likely to inhibit all Raf isoforms (King *et al.*, Cancer Res., (2006), 66:11100-11105).

Genetic mutations that activate ERK1/2 are known to cause cancer, and oncogenic mutations are highly prevalent in BRaf. BRaf inhibitors such as dabrafenib (N-{3-[5-(2-amino-4-pyrimidinyl)-2-(1,1-dimethylethyl)-1,3-thiazol-4-yl]-2-fluorophenyl}-2,6-difluorobenzenesulfonamide) are in clinical use (Roring *et al.*, Crit. Rev. Oncog., (2012), 17:97-121), and the use of a number of BRaf-inhibiting benzene sulphonamide thiazole and oxazole compounds, including dabrafenib, to treat a range of human cancers associated with BRaf mutations is described in US 2009/0298815 A1.

Although dabrafenib was developed to target oncogenic $BRaf^{V600E/K}$, it also inhibits wild-type BRaf and cRaf. As a Type 1.5 inhibitor, dabrafenib binds to and inhibits the "DFG-in" conformation of the kinase, generally viewed as the active conformation. However, dabrafenib stabilises another part of the structure in an "out" (i.e., inactive) conformation. Type 1 and Type 1.5 inhibitors may, paradoxically, activate ERK1/2 at low concentrations. This is potentially because they bind to one partner in a Raf dimer, locking the other in an active conformation that can activate MKK1/2 in the presence of activated Ras (the Raf paradox). At high concentrations, both partners are inhibited.

SUMMARY OF THE INVENTION

It has now been found that dabrafenib can be used to treat fibrosis, including cardiac fibrosis. Without being limited to theory, it is considered that the efficacy is achieved via inhibition of Raf kinases, for instance BRaf, cRaf and/or ARaf (ARaf, BRaf and cRaf are hereafter referred to collectively as Raf). Efficacy is not limited to patients having mutated forms of the underlying genes and in particular is achieved in patients who do not carry, for instance, any BRaf mutation. It has further been found that the efficacy of dabrafenib may be especially high relative to other potential BRaf inhibitors (e.g. SB590885, a Type 1 inhibitor

with greater preference for BRaf). A particular surprising finding of the present invention is that dabrafenib is active in reducing cardiac fibrosis, particularly that associated with hypertension. More generally, it has been found that inhibitors targeting BRaf (a known class of active agents previously studied and applied primarily in oncology), and/or other Raf kinases, may be suitable for the treatment of fibrosis, including but not limited to cardiac fibrosis.

Accordingly, the present invention provides a compound for use in treating or preventing fibrosis, for example cardiac fibrosis, kidney fibrosis, liver fibrosis, pulmonary fibrosis, or muscular fibrosis, in a patient, which compound is N-{3-[5-(2-amino-4-pyrimidinyl)-2-(1,1-dimethylethyl)-1,3-thiazol-4-yl]-2-fluorophenyl}-2,6-difluorobenzenesulfonamide, or a pharmaceutically acceptable salt thereof. Preferably, the compound is for use as described herein in treating or preventing fibrosis by inhibiting BRaf (possibly in conjunction with cRaf and/or ARaf) activity. Preferably, the compound is for use as described herein in treating or preventing cardiac fibrosis in a patient wherein the patient does not have a BRaf mutation, by inhibiting BRaf activity (or Raf activity), which compound is N-{3-[5-(2-amino-4-pyrimidinyl)-2-(1,1-dimethylethyl)-1,3-thiazol-4-yl]-2-fluorophenyl}-2,6-difluorobenzenesulfonamide, or a pharmaceutically acceptable salt thereof.

It has been found that, despite a requirement for BRaf in cardiomyocytes, global reduction in Raf signalling in the heart is beneficial. Therefore it is also a finding of the present invention Raf (including BRaf) kinase inhibitors related to dabrafenib such as vemurafenib, encorafenib, lifirafenib, LY3009120, PLX8394, LXH254, MLN2480, Raf709, TAK632 and PLX7904 may also potentially be therapeutically useful for reducing (e.g. cardiac) fibrosis.

Accordingly, the present invention also provides a compound for use in treating or preventing fibrosis, for example cardiac fibrosis, kidney fibrosis, liver fibrosis, pulmonary fibrosis, or muscular fibrosis, in a patient, which compound is a Raf inhibitor or a pharmaceutically acceptable salt thereof. The Raf inhibitor may, for example, be vemurafenib, encorafenib, lifirafenib, LY3009120, PLX8394, LXH254, MLN2480, Raf709, TAK632 or PLX7904. Preferably, the compound is for use as described herein in treating or preventing cardiac fibrosis in a patient wherein the patient does not have a BRaf mutation, wherein the compound is a BRaf (and/or ARaf, and/or cRaf) inhibitor, as described herein, or a pharmaceutically acceptable salt thereof.

BRIEF DESCRIPTION OF THE FIGURES

Figure 1: Generation of mice with tamoxifen-inducible cardiomyocyte-specific $BRaf^{V600E}$ knock-in. **A**, Representation of breeding strategy using the Myh6-MER-Cre-MER (MCM) line for a tamoxifen (Tam) inducible system for cardiomyocyte-specific genetic modification. Mice were crossed with floxed $BRaf^{V600E}$ mice producing double heterozygote $BRaf^{V600E/MCM}$ mice for experiments. **B,** Genotyping for MCM (upper panel) and $BRaf^{V600E}$ (lower panel). For MCM, a common forward primer was used with specific reverse primers for wild-type (W; 295 bp product) and transgenic (M; ~300 bp product) mice. For the floxed $BRaf^{V600E}$ transgene for knock-in, a single primer pair was used producing different sized products for wild-type (185 bp) and transgenic (308 bp) mice. **C**, Confirmation of recombination for $BRaf^{V600E}$ knock-in was based on introduction of an Xba1 restriction site in the mRNA following recombination. cDNA prepared from RNA extracted from the hearts was PCR amplified and subject to Xba1 digestion. This resulted in the appearance of an additional band (indicated by arrow) following treatment with tamoxifen (Tam), but not vehicle (Veh). **D**, Immunoblot analysis of Raf isoforms in samples of $BRaf^{V600E/MCM}$ mouse hearts treated with vehicle (Veh) or tamoxifen (Tam) (positions of relative molecular mass markers are on the right) shows that recombination did not affect total levels of protein.

Figure 2: Activated BRaf in cardiomyocytes signals through MKK1/2 to promote changes in gene expression. **A**, Protocol for study of mice with cardiomyocyte-specific knock-in of $BRaf^{V600E}$ by tamoxifen (Tam; 40 mg/kg, i.p.) relative to vehicle (Veh). Mice were heterozygote for both floxed $BRaf^{V600E}$ and Myh6-directed tamoxifen-inducible Cre ($BRaf^{V600E/MCM}$). BL, baseline. **B**, Immunoblotting of phosphorylated and total MKK1/2 and ERK1/2 in mouse hearts. Left panels, representative blots (positions of relative molecular mass markers are on the right); right panel, quantification for MKK1/2 at 1 (n=6) or 10 d (n=4); for each of 1d and 10d $BRaf^{V600E/MCM}$ + Veh is the left boxplot, $BRaf^{V600E/MCM}$ + Tam is the right boxplot. **C - E**, qPCR for expression of ERK1/2-dependent (**C**), hypertrophic genes (**D**) or remodelling genes (**E**) in mouse hearts (1 d, n= 6; 10 d, n=4); for each gene Tamoxifen is the upper boxplot, Vehicle is the lower boxplot. * $p<0.05$, ** $p<0.005$, *** $p<0.0005$ relative to vehicle alone (unpaired t test). Boxplots are 10-90 percentiles; boxes show the interquartile range with the median marked.

Figure 3: Tamoxifen-treatment of $Cre^{MCM/WT}$ mice (i.e. heterozygous for Myh6-MER-Cre-MER only) had no significant effect on the heart. $Cre^{MCM/WT}$ or $BRaf^{V600E/MCM}$ mice were treated with vehicle (Veh) or tamoxifen (Tam; 40 mg/kg i.p.). **A,** Immunoblot analysis of phosphorylated or total MKK1/2 or ERK1/2 from vehicle- or tamoxifen-treated mouse $Cre^{MCM/WT}$ hearts. Immunoblots are shown in the upper panels with densitometric analysis in the lower panels (n=4). **B**, mRNA expression was measured by qPCR (vehicle, n=8; tamoxifen, n=9). **C**, Echocardiographic data for mice treated with vehicle (Veh) with/without tamoxifen. LV, left ventricular; ID, internal diameter; PW, posterior wall; (s), systole; (d), diastole; at each time interval, boxplots are for $Cre^{MCM/WT}$ + Veh, $BRaf^{V600E/MCM}$ + Veh, $Cre^{MCM/WT}$ + Tam in order from left to right. * $p<0.05$ relative to vehicle alone (unpaired t test). Boxplots are 10-90 percentiles; boxes show the interquartile range with the median marked.

Figure 4: BRaf signalling promotes cardiac hypertrophy. $BRaf^{V600E/MCM}$ or $Cre^{MCM/WT}$ mice were treated with tamoxifen (Tam; 40 mg/kg, i.p.) or vehicle (Veh). **A** and **B**, Echocardiography of hearts showing representative images of individual mice (**A**) with quantification of echocardiograms (n=9 per group) (**B**). LV, left ventricle; ID, internal diameter; PW, posterior wall; (s), systole; (d), diastole; at each time interval, boxplots are for $BRaf^{V600E/MCM}$ + Veh, $BRaf^{V600E/MCM}$ + Tam, $Cre^{MCM/WT}$ + Tam in order from left to right. Boxplots are 10-90 percentiles; boxes show the interquartile range with the median marked (n=9) . *$p<0.05$, **$p<0.005$, ***$p<0.0005$ *vs* vehicle (2-way ANOVA with Holm-Sidak's post-test). **C**, Sections of $BRaf^{V600E/MCM}$ mouse hearts (10 d) stained with H&E (left) or Masson's Trichrome (right). **D**, Quantification of cardiomyocyte cross-sectional area (n=4). **E**, Immunoblotting of Col1a1 in $BRaf^{V600E/MCM}$ mouse hearts (10 d) (left panel; positions of relative molecular mass markers are indicated on the left; monomeric (M), dimeric (D) and trimeric (T) forms of Col1a1 are indicated on the right). Boxplots are 10-90 percentiles; boxes show the interquartile range with the median marked (n=3). **$p<0.005$ *vs* vehicle. (unpaired t test).

Figure 5: SB590885 induces Raf paradox signalling to ERK1/2 in rat hearts and cardiac cells. A-C, Immunoblot analysis of phosphorylated and total ERK1/2 in Langendorff-perfused adult rat hearts (**A**) or cultured cells (**B** and **C**). **A**, Rat hearts were perfused without or with 1 μM SB590885 (SB59; 1 μM, 15 min); in the graph, left hand data are Control, right hand data are SB590885. **B**, Neonatal rat cardiomyocytes or adult human

fibroblasts were exposed to the indicated concentrations of SB590885 (20 min); fibroblast data points on the graph are the lower values at 0.01 and 0.1 μM but the higher values at 1 and 10 μM. **C**, Neonatal rat cardiomyocytes were exposed to 1 μM SB590885 for the times shown. **D**, Assay of Raf kinase activities from neonatal rat cardiomyocytes exposed to the indicated concentrations of SB590885 (SB59) or 100 nM endothelin-1 (ET-1) for the times shown. Activities were assayed using GST-MKK1 following immunoprecipitation (IP) of cRaf or BRaf. Phosphorylation of GST-MKK1 was detected with antibodies to phosphorylated MKK1/2. Assay samples were also immunoblotted for total MKK1/2, BRaf and cRaf. Representative blots are shown (positions of relative molecular mass markers are on the right) with densitometric quantification. **E**, Immunoblot analysis of extracts from neonatal rat cardiomyocytes exposed to 0.1 μM SB590885 or 100 nM ET-1 for the times indicated. Total extracts were immunoblotted for phosphorylated or total BRaf and cRaf. Representative blots of 4 independent cardiomyocyte preparations are shown (positions of relative molecular mass markers are on the right). Densitometric data are means ± SEM (n=3-4 independent cell or heart preparations). *p<0.05, **p<0.005, ***p<0.0005, ****p<0.0001, vs control, #### p<0.0001 vs ET-1 (one-way ANOVA with Tukey post-test).

Figure 6: The Raf paradox-inducer, SB590885, increases nuclear-localised activated ERK1/2, induces ERK1/2-dependent gene expression and promotes cardiomyocyte hypertrophy. **A**, Rat neonatal cardiomyocytes were exposed to SB590885 at the concentrations and for the times shown. Cytosolic and nuclear fractions were immunoblotted for phosphorylated or total ERK1/2 (positions of relative molecular mass markers are on the right). Densitometric analysis for 0.1 μM SB590885 is shown. Data are means ± SEM (n=3 independent cell preparations). *p<0.05, **p<0.005, ***p<0.0005 relative to 0 min (one-way ANOVA with Holm-Sidak post-test). **B**, Cardiomyocytes were untreated or exposed to 0.1 μM SB590885 (1 h) with/without 2 μM PD184352. mRNA expression was measured by qPCR (n=4); for each gene, left hand data are PD184352, central data are SB590885, right hand data are PD184352 + SB590885. *p<0.05, ***p<0.0005, ****p<0.0001 *vs* control (dashed line); ## p<0.005 vs SB590885 alone (one-way ANOVA with Holm-Sidak's post-test). **C**, Cardiomyocytes were exposed to 1 μM SB590885 (24 h) and immunostained for troponin T. Images are representative of 6 independent myocyte preparations with analysis of cell size shown in the right panels. **p<0.005 vs control (unpaired t test).

Figure 7: SB590885 promotes cardiac hypertrophy *in vivo*. **A** and **B**, Echocardiography of hearts from wild-type mice treated with vehicle or SB590885 (0.5 mg/kg/d, 3 d) with representative images from individual mice (**A**) and quantification (vehicle, n=10; SB590885, n=12) (**B**). LV, left ventricle; ID, internal diameter; PW, posterior wall; (s), systole; (d), diastole; in each graph, left hand data are Vehicle, right hand data are SB590885. **C**, H&E staining of vehicle- or SB590885-treated (7 d) mouse heart sections with quantification of cardiomyocyte size (n=4). *p<0.05, **p<0.005, ***p<0.0005 vs vehicle (unpaired t test). Boxplots are 10-90 percentiles; boxes show the interquartile range with the median marked. **D**, Schematic representation of the conclusions from this study.

Figure 8: Generation of mice with tamoxifen-inducible cardiomyocyte-specific BRaf knockout. A, Representation of breeding strategy using the Myh6-Mer-Cre-Mer (MCM) line for tamoxifen-inducible cardiomyocyte-specific BRaf knock-out. Mice homozygous for the floxed BRaf gene and heterozygous for MCM were generated. $BRaf^{KO/KO}/Cre^{MCM/WT}$ mice were treated with 40 mg/kg (i.p.) Tam or vehicle 3 d before minipumps were implanted for delivery of 0.8 mg/kg/d AngII or vehicle. **B**, Genotyping for floxed $BRaf^{KO/KO}$ for knock-out used a single primer pair producing different sizes of products for wild-type (357 bp) and transgenic (413 bp) mice. **C**, Confirmation of BRaf gene deletion using cDNA prepared from RNA extracted from the hearts. PCR amplification produced a 550 bp product in vehicle treated samples with a smaller product following recombination. Representative images are shown.

Figure 9: Cardiomyocyte-specific BRaf knock-out inhibits cardiac adaptation to angiotensin II in mouse hearts *in vivo*. **A**, Protocol for study of mice with inducible cardiomyocyte-specific knock-out of BRaf. Mice were homozygote for $BRaf^{KO}$ and heterozygote for Myh6-directed tamoxifen- (Tam-) inducible Cre ($BRaf^{KO/KO}/Cre^{MCM/WT}$). Mice were treated with 40 mg/kg (i.p.) Tam or vehicle 3 d before minipumps were implanted for delivery of 0.8 mg/kg/d AngII or vehicle. **B** and **C**, RNA (**B**) or protein (**C**) was extracted from mouse hearts after treatment with Tam or vehicle (Control, Con). Raf isoform mRNA expression was measured by qPCR (**B**). Samples were immunoblotted for ARaf, BRaf and cRaf (together) or Gapdh (**C**). In **B** and right panel of **C**, for each of ARaf/BRaf/cRaf, left hand data are Control, right hand data are Tamoxifen. In **C**, left panels show representative blots (positions of relative molecular mass markers are on the right); the right panel provides quantification of Raf isoforms relative to Gapdh. * p<0.05 *vs* vehicle (unpaired t test). **D - F**,

Echocardiography of hearts showing representative images of individual mice before and after (7 d) treatment (**D**) with enlargement of the posterior wall (**E**), and quantification (**F**). (N.B. Diastolic dimensions are shown; systolic dimensions are provided in *Figure 10*). LV, left ventricle; AW, anterior wall; PW, posterior wall; IVS, interventricular septum; ID, internal diameter; in each graph of **F**, left hand data are Control, central data are AngII, right hand data are Tam + AngII. Results are means ± SEM with individual values shown. *p<0.05 , **p<0.005, ***p<0.0005, **** p<0.0001 *vs* Control, # p<0.05 , ## p<0.005 *vs* AngII (one-way ANOVA with Holm-Sidak's post-test).

Figure 10: Cardiomyocyte-specific BRaf knock-out reduces cardiac hypertrophy induced by angiotensin II in mouse hearts *in vivo*: systolic measurements. $BRaf^{KO/KO}/Cre^{MCM/WT}$ mice were treated with 40 mg/kg (i.p.) Tam or vehicle 3 d before minipumps were implanted for delivery of 0.8 mg/kg/d AngII or vehicle. Echocardiography of hearts showing systolic measurements. LV, left ventricle; ID, internal diameter; PW, posterior wall, AW anterior wall, IVS, interventricular septum; for each graph, left hand data are Control, central data are AngII, right hand data are Tamoxifen + AngII. Results are means ± SEM with individual values shown. *p<0.05 , **p<0.005, **** p<0.0001 *vs* Control, # p<0.05 *vs* AngII (one-way ANOVA with Holm-Sidak's post-test).

Figure 11: Tamoxifen alone had no effect on cardiac function/dimensions in $BRaf^{KO/KO}/Cre^{MCM/WT}$ mice. $BRaf^{KO/KO}/Cre^{MCM/WT}$ mice were treated with 40 mg/kg (i.p.) Tam or vehicle, 3 d before minipumps were implanted for delivery acidified PBS (to control for AngII delivery). Cardiac function/dimensions were measured by echocardiography. **A,** Representative images. **B,** Quantification of echocardiograms. LV, left ventricle; ID, internal diameter; PW, posterior wall, AW anterior wall, IVS, interventricular septum; for each graph, left hand data are Control, right hand data are Tamoxifen. Results are means ± SEM with individual values shown. There were no significant differences between vehicle only and tamoxifen treated mice (t test).

Figure 12: Tamoxifen-treatment of $Cre^{MCM/WT}$ mice (i.e. heterozygous for Myh6-MerCreMer only) had no significant effect on cardiac function/dimensions. Mice wild-type for BRaf and heterozygous for Myh6-MerCreMer were treated with 40 mg/kg (i.p.) Tam or vehicle, 3 d before minipumps were implanted for delivery acidified PBS (to control for AngII delivery). Cardiac function/dimensions were measured by echocardiography. Data show quantification of echocardiograms. LV, left ventricle; ID, internal diameter; PW,

posterior wall, AW anterior wall, IVS, interventricular septum; for each graph, left hand data are Control, right hand data are Tamoxifen. Results are means ± SEM with individual values shown. There were no significant differences between vehicle only and tamoxifen treated mice (t test).

Figure 13: Cardiomyocyte-specific BRaf knock-out modulates changes in gene expression induced by angiotensin II in mouse hearts *in vivo*. $BRaf^{KO/KO}/Cre^{MCM/WT}$ mice were treated with 40 mg/kg (i.p.) Tam or vehicle 3 d before minipumps were implanted for delivery of 0.8 mg/kg/d AngII or vehicle. RNA was extracted from mouse hearts following treatment without vehicle only (Control), with 0.8 mg/kg/d AngII, or with tamoxifen plus AngII (Tam/AngII). mRNA was measured by qPCR for expression of hypertrophy-associated (**A**), early (**B**), cytokine (**C**), fibrosis-associated (**D**) or extracellular matrix (**E**) genes; at each time interval for each gene, left hand data are Control, central data are AngII, right hand data are Tam/AngII. Results are means ± SEM with individual values shown. * $p<0.05$, ** $p<0.005$, *** $p<0.0005$, **** $p<0.0001$ *vs* Control, # $p<0.05$, ## $p<0.005$, #### $p<0.0001$ *vs* AngII (one-way ANOVA with Holm-Sidak's post-test).

Figure 14: Tamoxifen alone had no effect on mRNA expression in hearts from $BRaf^{KO/KO}/Cre^{MCM/WT}$ mice. $BRaf^{KO/KO}/Cre^{MCM/WT}$ mice were treated with 40 mg/kg (i.p.) Tam or vehicle, 3 d before minipumps were implanted for delivery acidified PBS (to control for AngII delivery). mRNA expression was determined by qPCR for hypertrophy-associated genes (**A**), early genes (**B**), cytokines (**C**), fibrosis-associated genes (**D**) and extracellular matrix genes (**E**); at each time interval for each gene, left hand data are Control, right hand data are Tamoxifen. Date were normalised to the housekeeping gene Gapdh and then to means of the vehicle-treated controls. Results are means ± SEM with individual values shown. There were no significant differences between vehicle and tamoxifen-treated mice (one-way ANOVA).

Figure 15: Cardiomyocyte-specific BRaf knock-out increases focal damage and cardiac fibrosis in mouse hearts *in vivo*. $BRaf^{KO/KO}/Cre^{MCM/WT}$ mice were treated with 40 mg/kg (i.p.) Tam or vehicle, 3 d before minipumps were implanted for delivery of 0.8 mg/kg/d AngII or vehicle. Hearts were fixed in formaldehyde and sections stained with haemotoxylin and eosin (H&E, upper panels) or Masson's trichrome (lower panels). Images for each condition were taken from different areas from the same heart section and are representative of the average response.

Figure 16: Dabrafenib inhibits ERK1/2 signalling in in perfused adult rat hearts. Adult male rat hearts were perfused under control conditions (Con), with 5 μM dabrafenib alone (**A**) or with FGF2 (0.5 μg/ml, 10 min) without/with dabrafenib (Dab) (**B**). Protein samples were immunoblotted for phosphorylated (phospho-) or total ERK1/2. Representative blots are in the upper panels with positions of relative molecular mass markers on the right of each image. Densitometric quantification is in the lower panels. In quantification for **A**, left hand data are Control, right hand data are Dabrafenib. In quantification for **B**, left hand data are Control, central data are FGF2, right hand data are Dabrafenib + FGF2. Results are means ± SEM with individual values shown. *$p<0.05$ *vs* control, ## $p<0.005$ *vs* FGF (one-way ANOVA with Holm-Sidak post-test).

Figure 17: Dabrafenib alone had no significant effect on cardiac function/dimensions. C57Bl/6J male mice were treated with vehicle or 3 mg/kg/d dabrafenib for 3 or 7 d. Cardiac function/dimensions were measured by echocardiography. Data show quantification of echocardiograms. LV, left ventricle; ID, internal diameter; PW, posterior wall, AW anterior wall, IVS, interventricular septum; in each graph, left hand data are Control, right hand data are Dabrafenib. Results are means ± SEM with individual values shown. There were no significant differences between vehicle only and dabrafenib-treated mice (t test).

Figure 18: Dabrafenib reduces cardiac hypertrophy induced by angiotensin II in mouse hearts *in vivo*. Echocardiography of hearts from C57BL/6J male mice treated without dabrafenib or AngII (Control), with 0.8 mg/kg/d AngII or with 3 mg/kg/d dabrafenib with AngII. Representative images from individual mice are in (**A**) with enlargement of the posterior wall in (**B**). **C** and **D**, Quantification of echocardiograms taken at 3 (**C**) or 7 (**D**) days. LV, left ventricle; ID, internal diameter; PW, posterior wall; IVS, interventricular septum; in each graph, left hand data are Control, central data are AngII, right hand data are Dabrafenib + AngII. (N.B. Diastolic dimensions are shown; systolic dimensions are provided in *Figure 19*). Results are means ± SEM with individual values shown. *$p<0.05$, **$p<0.005$, ***$p<0.0005$, ****$p<0.0001$ *vs* control, # $p<0.05$, ## $p<0.005$, ### $p<0.0005$ *vs* AngII (one-way ANOVA with Holm-Sidak post-test).

Figure 19: Dabrafenib reduces cardiac hypertrophy induced by angiotensin II in mouse hearts *in vivo*: systolic measurements. C57Bl/6J male mice were treated with vehicle or 3 mg/kg/d dabrafenib) for 3 or 7 d. Cardiac function/dimensions were measured by

echocardiography. Echocardiography of hearts showing systolic measurements. LV, left ventricle; ID, internal diameter; PW, posterior wall, IVS, interventricular septum; in each graph, left hand data are Control, central data are AngII, right hand data are Dabrafenib + AngII. Results are means ± SEM with individual values shown. *p<0.05 , **p<0.005, **** p<0.0001 *vs* Control, # p<0.05 *vs* AngII (one-way ANOVA with Holm-Sidak's post-test).

Figure 20: Dabrafenib modulates changes in gene expression induced by angiotensin II in mouse hearts *in vivo*. C57BL/6J male mice were treated without dabrafenib or AngII (Control), with 0.8 mg/kg/d AngII or with 3 mg/kg/d dabrafenib with AngII. Proteins or RNA were extracted from mouse hearts after 7 d. **A,** Proteins were immunoblotted for phospho- or total ERK1/2. Representative images are shown with densitometirc quantification; quantification data are Control, Dabrafenib, AngII, Dabrafenib + AngII in order from left to right. **B - D,** mRNA expression of hypertrophy-associated (**B**), Cytokines (**C**), fibrosis-promoting and extracellular matrix (**D**) genes was measured by qPCR; in each graph, left hand data are Control, central data are AngII, right hand data are Dabrafenib + AngII. Results are means ± SEM with individual values shown. *p<0.05, **p<0.005, ***p<0.0005, ****p<0.0001 *vs* control, # p<0.05, ## p<0.005 *vs* AngII (one-way ANOVA with Holm-Sidak post-test).

Figure 21: Dabrafenib reduces cardiomyocyte diameter and inhibits cardiac fibrosis induced by angiotensin II in mouse hearts *in vivo*. C57BL/6J male mice were treated without dabrafenib or AngII (Control), with 0.8 mg/kg/d AngII or with 3 mg/kg/d dabrafenib with AngII. **A - D**, Hearts were fixed in formaldehyde and sections stained with haemotoxylin and eosin (H&E) or Masson's trichrome. Representative images are shown with quantification of myocyte area (**C**) and interstitial or perivascular fibrosis (**D**); in each graph, left hand data are Control, central data are AngII, right hand data are Dabrafenib + AngII. Results are means ± SEM with individual values shown. **p<0.005, ***p<0.0005, ****p<0.0001 *vs* control; # p<0.05, ## p<0.005 *vs* AngII (one-way ANOVA with Holm-Sidak post-test). **E**, Schematic representation of the conclusions from this study.

Figure 22: Effects of SB590885 on AngII-induced hypertension. Echocardiography of hearts from C57BL/6J male mice treated without SB590885 or AngII (Control), with 0.8 mg/kg/d AngII or with 0.5 mg/kg/d SB590885 with AngII. Quantification of echocardiograms taken at 7 days. LV, left ventricle; ID, internal diameter; PW, posterior wall; in each graph, left hand data are Control, central data are AngII, right hand data are

SB590885 + AngII. Data for individual mice were normalised to the mean values of the two baseline echocardiograms. Results are means ± SEM with individual values shown. *p<0.05, **p<0.005, ***p<0.0005, ****p<0.0001 *vs* control (one-way ANOVA with Holm-Sidak post-test).

Figure 23: Raf inhibitors inhibit ERK1/2 activation in cultured cardiac myocytes. A-C. Neonatal rat cardiomyocytes were exposed (20 min) to the indicated concentrations of dabrafenib (**A**), vemurafenib (**B**) or PLX7904 (**C**). **D**, Cardiomyocytes were unstimulated or exposed to 10 μM dabrafenib, 30 μM vemurafenib or 10 μM PLX7904 in the absence or presence of 100 nM endothelin 1 (ET-1). **E**, Cardiomyocytes were unstimulated or exposed to 10 μM dabrafenib or 10 μM encorafenib in the absence or presence of 50 nM A61603. Protein samples were immunoblotted for phosphorylated (phospho-) or total ERK1/2. In **A**, Representative blots are in the upper panels with densitometric quantification in the panel. Results are means ± SEM (n=4 independent cell preparations). *p<0.05 relative to no inhibitor (one-way ANOVA with Tukey post-test). **B-D**, Images are representative of n=4 (vemurafenib data), n=2 (dabrafenib, encorafenib) or n=1 (PLX7904) independent myocyte preparations. Positions of relative molecular mass markers on the right of each image.

DETAILED DESCRIPTION OF THE INVENTION

Dabrafenib

N-{3-[5-(2-amino-4-pyrimidinyl)-2-(1,1-dimethylethyl)-1,3-thiazol-4-yl]-2-fluorophenyl}-2,6-difluorobenzenesulfonamide may be referred to as dabrafenib. Dabrafenib has the following structure:

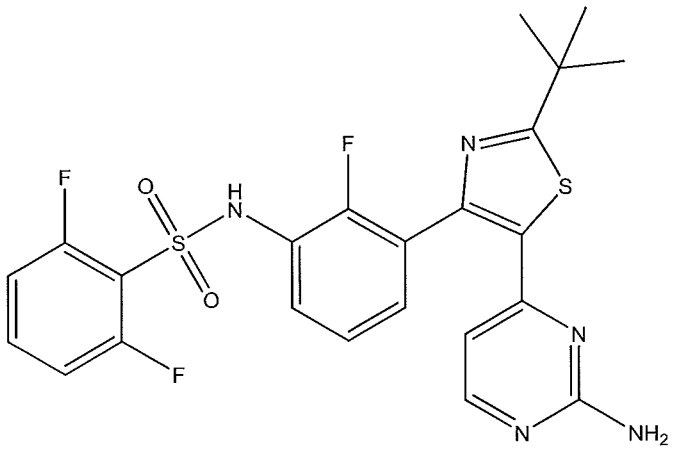

In one aspect, the compound used in the treatment of the invention is dabrafenib or a pharmaceutically acceptable salt thereof. As used herein, a pharmaceutically acceptable salt is a salt with a pharmaceutically acceptable acid or base. Pharmaceutically acceptable acids include both inorganic acids such as hydrochloric, sulphuric, phosphoric, diphosphoric, hydrobromic or nitric acid and organic acids such as citric, fumaric, maleic, malic, ascorbic, succinic, tartaric, benzoic, acetic, methanesulphonic, ethanesulphonic, benzenesulphonic or p-toluenesulphonic acid. Pharmaceutically acceptable bases include alkali metal (e.g. sodium or potassium) and alkali earth metal (e.g. calcium or magnesium) hydroxides and organic bases such as alkyl amines, aralkyl amines and heterocyclic amines.

For the avoidance of doubt, dabrafenib can, if desired, be used in the form of a solvate. Further, for the avoidance of doubt, dabrafenib may be used in any tautomeric form.

BRaf inhibitor

In a further aspect, the compound used in the treatment of the invention may be a BRaf inhibitor, or a pharmaceutically acceptable salt thereof (including, but not limited to, dabrafenib and its pharmaceutically acceptable salts).

As described herein, a BRaf inhibitor is a compound which inhibits BRaf activity. Inhibiting BRaf activity includes reducing BRaf or modulating BRaf.

Small molecule protein kinase inhibitors are classified are classified according to mode of binding to the kinase, assessed by structural analysis of the inhibitor in complex with the relevant kinase, usually using crystallography or related technique. Most protein kinase inhibitors interact with the ATP-binding site containing a DFG motif, the position/orientation of which is crucial. The DFG motif moves inwards ("DFG-in") for the kinase to adopt an active conformation. Type 1 inhibitors bind to the "DFG-in" structure whilst Type 2 inhibitors bind to a "DFG-out" conformation. An active kinase requires inward movement of the αC-helix. Type 1.5 inhibitors bind to the "DFG-in" conformation, but stabilise the enzyme with the helix in an inactive “out” conformation. The BRaf inhibitor for use in the present invention can be a Type 1 BRaf inhibitor. The BRaf inhibitor for use in the present invention can be a Type 1.5 BRaf inhibitor. The BRaf inhibitor for use in the present invention can be a Type 2 BRaf inhibitor.

Specific examples of BRaf inhibitors for use in the treatment or prevention of fibrosis include dabrafenib, vemurafenib, encorafenib, lifirafenib, LY3009120, PLX8394, LXH254, MLN2480, Raf709, TAK632, and PLX7904. Preferably, the BRaf inhibitor used in the treatment of the invention is typically selected from dabrafenib, vemurafenib, encorafenib, lifirafenib, LY3009120, PLX8394, LXH254, or MLN2480. Preferably, the BRaf inhibitor used in the treatment of the invention is dabrafenib. Pharmaceutically acceptable salts of all of these compounds can be used.

For the avoidance of doubt, the BRaf inhibitor can, if desired, be used in the form of a solvate. Further, for the avoidance of doubt, the BRaf inhibitor may be used in any tautomeric form.

Raf inhibitor

In a yet further aspect, the compound used in the treatment of the invention may be a Raf inhibitor, or a pharmaceutically acceptable salt thereof (including, but not limited to, dabrafenib and its pharmaceutically acceptable salts).

As described herein, a Raf inhibitor is a compound which inhibits Raf activity, namely BRaf activity, and/or cRaf activity, and/or ARaf, activity. Inhibiting Raf activity includes reducing Raf or modulating Raf. The Raf inhibitor may inhibit any or all of BRaf, cRaf and ARaf, and may derive its pharmacological efficacy in treating fibrosis via its capacity to inhibit any or all of BRaf, cRaf and ARaf.

Several compounds that are known to inhibit wild-type BRaf also inhibit the other wild-type Raf kinases, in particular wild-type cRaf. *Table 1* provides IC_{50} values for a number of Raf inhibitors showing the level of inhibition of mutated BRaf V600E compared to wild-type BRaf or cRaf.

Table 1: IC_{50} values for inhibition of mutated BRaf V600E vs wild-type (WT) BRaf or cRaf using cell-free assays.

Inhibitor	BRafV600E	WT BRaf	WT cRaf
Dabrafenib	0.7 nM	5.2 nM	6.3 nM
Encorafenib	0.8 nM	1.1 nM	0.6 nM
PLX7904	N/A (~5 nM in cells)	N/A	N/A
PLX8394	3.8 nM	14 nM	23 nM
Vemurafenib	31 nM	100 nM	48 nM

Specific examples of Raf inhibitors for use in the treatment or prevention of fibrosis include dabrafenib, vemurafenib, encorafenib, lifirafenib, LY3009120, PLX8394, LXH254, MLN2480, Raf709, TAK632, and PLX7904. In one currently preferred aspect, the Raf inhibitor used in the treatment of the invention is typically selected from dabrafenib, vemurafenib, encorafenib, or PLX8394. Preferably, the Raf inhibitor used in the treatment of the invention is dabrafenib. Pharmaceutically acceptable salts of all of these compounds can be used.

For the avoidance of doubt, the Raf inhibitor can, if desired, be used in the form of a solvate. Further, for the avoidance of doubt, the Raf inhibitor may be used in any tautomeric form.

Diseases and Conditions

Dabrafenib can inhibit BRaf activity, in addition to cRaf and ARaf activity. Dabrafenib can therefore treat conditions by inhibiting BRaf (alone or in conjunction with cRaf and/or ARaf) activity, in particular fibrosis. This includes cardiac fibrosis, kidney fibrosis, liver fibrosis, pulmonary fibrosis, or muscular fibrosis. Preferably, the fibrosis is cardiac fibrosis.

In a preferred embodiment, the invention provides dabrafenib for use in the treatment or prevention of fibrosis. Preferably, the invention provides dabrafenib for use in the treatment or prevention of fibrosis by inhibiting BRaf activity. More preferably, the invention provides dabrafenib for use in the treatment or prevention of cardiac fibrosis by inhibiting BRaf activity.

Further, other Raf inhibitors can also treat conditions by inhibiting BRaf (and/or Raf) activity, in particular fibrosis. This includes cardiac fibrosis, kidney fibrosis, liver fibrosis, pulmonary fibrosis, or muscular fibrosis. Preferably, the fibrosis is cardiac fibrosis. In a preferred embodiment, the invention provides a Raf inhibitor for use in the treatment or prevention of fibrosis. Preferably, the invention provides a Raf inhibitor for use in the treatment or prevention of cardiac fibrosis.

Patients

Dabrafenib and related BRaf and/or Raf inhibitors can inhibit activity of wild-type BRaf or mutant BRaf. Preferably, the patient treated in the treatment of the invention does not have a

BRaf mutation. Preferably, the patient who does not have a BRaf mutation has only wild-type BRaf.

The patient may be suffering from hypertension, heart failure, cardiac hypertrophy, non-alcoholic steatohepatitis, or muscular dystrophy. Preferably, the patient may be suffering from hypertension, heart failure, or cardiac hypertrophy. More preferably, the patient may be suffering from hypertension.

Pharmaceutical composition

The compounds for use of the invention may be present in a pharmaceutical composition. Typically, the pharmaceutical composition may comprise dabrafenib or a BRaf or Raf inhibitor as described herein and one or more pharmaceutically acceptable carriers, diluents or excipients. The pharmaceutical composition may be as described below.

Pharmaceutical compositions may be administered to the subject by any acceptable route of administration including, but not limited to, inhaled, oral, nasal, topical (including transdermal) and parenteral modes of administration. Oral administration is preferred. Further, the compositions of the invention may be administered in multiple doses per day, in a single daily dose or a single weekly dose. It will be understood that any form of the active agents used in the composition of the invention that is suitable for the particular mode of administration can be used in the pharmaceutical compositions discussed herein.

The pharmaceutical compositions of this invention typically contain a therapeutically effective amount of an active agent. Those skilled in the art will recognize, however, that a pharmaceutical composition may contain more than a therapeutically effective amount, i.e., bulk compositions, or less than a therapeutically effective amount, i.e., individual unit doses designed for multiple administration to achieve a therapeutically effective amount.

Any conventional carrier or excipient may be used in the pharmaceutical compositions of the invention. The choice of a particular carrier or excipient, or combinations of carriers or excipients, will depend on the mode of administration being used to treat a particular subject or type of medical condition or disease state. In this regard, the preparation of a suitable composition for a particular mode of administration is well within the scope of those skilled in the pharmaceutical arts. Additionally, carriers or excipients used in such compositions are commercially available. By way of further illustration, conventional formulation techniques

are described in Remington: The Science and Practice of Pharmacy, 20th Edition, Lippincott Williams & White, Baltimore, Md. (2000); and H. C. Ansel et al., Pharmaceutical Dosage Forms and Drug Delivery Systems, 7th Edition, Lippincott Williams & White, Baltimore, Md. (1999).

Representative examples of materials which can serve as pharmaceutically acceptable carriers include, but are not limited to, the following: sugars, such as lactose, glucose and sucrose; starches, such as corn starch and potato starch; cellulose, such as microcrystalline cellulose, and its derivatives, such as sodium carboxymethyl cellulose, ethyl cellulose and cellulose acetate; powdered tragacanth; malt; gelatin; talc; excipients, such as cocoa butter and suppository waxes; oils, such as peanut oil, cottonseed oil, safflower oil, sesame oil, olive oil, corn oil and soybean oil; glycols, such as propylene glycol; polyols, such as glycerin, sorbitol, mannitol and polyethylene glycol; esters, such as ethyl oleate and ethyl laurate; agar; buffering agents, such as magnesium hydroxide and aluminum hydroxide; alginic acid; pyrogen-free water; isotonic saline; Ringer's solution; ethyl alcohol; phosphate buffer solutions; compressed propellant gases, such as chlorofluorocarbons and hydrofluorocarbons; and other non-toxic compatible substances employed in pharmaceutical compositions. Pharmaceutical compositions are typically prepared by thoroughly and intimately mixing or blending the active agent / active ingredient with a pharmaceutically acceptable carrier and one or more optional ingredients. The resulting uniformly blended mixture may then be shaped or loaded into tablets, capsules, pills, canisters, cartridges, dispensers and the like using conventional procedures and equipment.

The pharmaceutical compositions may be suitable for oral administration. Suitable compositions for oral administration may be in the form of capsules, tablets, pills, lozenges, cachets, dragees, powders, granules; solutions or suspensions in an aqueous or non-aqueous liquid; oil-in-water or water-in-oil liquid emulsions; elixirs or syrups; and the like; each containing a predetermined amount of the active agent.

When intended for oral administration in a solid dosage form (i.e., as capsules, tablets, pills and the like), the composition will typically comprise the active agent and one or more pharmaceutically acceptable carriers, such as sodium citrate or dicalcium phosphate. Solid dosage forms may also comprise: fillers or extenders, such as starches, microcrystalline cellulose, lactose, sucrose, glucose, mannitol, and/or silicic acid; binders, such as carboxymethylcellulose, alginates, gelatin, polyvinyl pyrrolidone, sucrose and/or acacia;

humectants, such as glycerol; disintegrating agents, such as agar-agar, calcium carbonate, potato or tapioca starch, alginic acid, certain silicates, and/or sodium carbonate; solution retarding agents, such as paraffin; absorption accelerators, such as quaternary ammonium compounds; wetting agents, such as cetyl alcohol and/or glycerol monostearate; absorbents, such as kaolin and/or bentonite clay; lubricants, such as talc, calcium stearate, magnesium stearate, solid polyethylene glycols, sodium lauryl sulfate, and/or mixtures thereof; coloring agents; and buffering agents.

Release agents, wetting agents, coating agents, sweetening, flavoring and perfuming agents, preservatives and antioxidants may also be present in the pharmaceutical compositions. Exemplary coating agents for tablets, capsules, pills and like, include those used for enteric coatings, such as cellulose acetate phthalate, polyvinyl acetate phthalate, hydroxypropyl methylcellulose phthalate, methacrylic acid-methacrylic acid ester copolymers, cellulose acetate trimellitate, carboxymethyl ethyl cellulose, hydroxypropyl methyl cellulose acetate succinate, and the like. Examples of pharmaceutically acceptable antioxidants include: water-soluble antioxidants, such as ascorbic acid, cysteine hydrochloride, sodium bisulfate, sodium metabisulfate sodium sulfite and the like; oil-soluble antioxidants, such as ascorbyl palmitate, butylated hydroxyanisole, butylated hydroxytoluene, lecithin, propyl gallate, alpha-tocopherol, and the like; and metal-chelating agents, such as citric acid, ethylenediamine tetraacetic acid, sorbitol, tartaric acid, phosphoric acid, and the like.

Compositions may also be formulated to provide slow or controlled release of the active agent using, by way of example, hydroxypropyl methyl cellulose in varying proportions or other polymer matrices, liposomes and/or microspheres. In addition, the pharmaceutical compositions of the invention may contain opacifying agents and may be formulated so that they release the active agent only, or preferentially, in a certain portion of the gastrointestinal tract, optionally, in a delayed manner. Examples of embedding compositions that can be used include polymeric substances and waxes. The active agent can also be in micro-encapsulated form, if appropriate, with one or more of the above-described excipients.

Suitable liquid dosage forms for oral administration include, by way of illustration, pharmaceutically acceptable emulsions, microemulsions, solutions, suspensions, syrups and elixirs. Liquid dosage forms typically comprise the active agent and an inert diluent, such as, for example, water or other solvents, solubilizing agents and emulsifiers, such as ethyl alcohol, isopropyl alcohol, ethyl carbonate, ethyl acetate, benzyl alcohol, benzyl benzoate,

propylene glycol, 1,3-butylene glycol, oils (e.g., cottonseed, groundnut, corn, germ, olive, castor and sesame oils), glycerol, tetrahydrofuryl alcohol, polyethylene glycols and fatty acid esters of sorbitan, and mixtures thereof. Suspensions may contain suspending agents such as, for example, ethoxylated isostearyl alcohols, polyoxyethylene sorbitol and sorbitan esters, microcrystalline cellulose, aluminium metahydroxide, bentonite, agar-agar and tragacanth, and mixtures thereof.

When intended for oral administration, the pharmaceutical compositions of the invention may be packaged in a unit dosage form. The term "unit dosage form" refers to a physically discrete unit suitable for dosing a subject, i.e., each unit containing a predetermined quantity of the active agents calculated to produce the desired therapeutic effect either alone or in combination with one or more additional units. For example, such unit dosage forms may be capsules, tablets, pills, and the like.

Compositions of the invention can also be administered parenterally (e.g., by subcutaneous, intravenous, intramuscular, or intraperitoneal injection). For such administration, the active agents are provided in a sterile solution, suspension, or emulsion. Exemplary solvents for preparing such formulations include water, saline, low molecular weight alcohols such as propylene glycol, polyethylene glycol, oils, gelatin, fatty acid esters such as ethyl oleate, and the like. A typical parenteral formulation is a sterile pH 4-7 aqueous solution of the active agents. Parenteral formulations may also contain one or more solubilizers, stabilizers, preservatives, wetting agents, emulsifiers, and dispersing agents. These formulations may be rendered sterile by use of a sterile injectable medium, a sterilizing agent, filtration, irradiation, or heat.

Compositions of the invention can also be administered transdermally using known transdermal delivery systems and excipients. For example, the active agents can be admixed with permeation enhancers, such as propylene glycol, polyethylene glycol monolaurate, azacycloalkan-2-ones and the like, and incorporated into a patch or similar delivery system. Additional excipients including gelling agents, emulsifiers and buffers, may be used in such transdermal compositions if desired.

Compositions of the invention may be suitable for inhaled administration, which will typically be in the form of an aerosol or a powder, for instance a dry powder composition.

Such compositions are generally administered using well-known delivery devices, such as a nebulizer inhaler, a dry powder inhaler, or a metered-dose inhaler.

Dosage

A therapeutically effective amount of a compound of the invention is administered to a patient. In the treatments according to the invention, dabrafenib or a Raf inhibitor as described herein or the pharmaceutically acceptable salt thereof may be provided in any suitable dosage. A typical dose is from about 0.001 to 50 mg per kg of body weight, for example 0.01 to 10 mg, according to the activity of the specific compound, the age, weight and conditions of the subject to be treated, the type and severity of the disease and the frequency and route of administration. The amount of dabrafenib or Raf inhibitor present in a single dose may be from 1 μg to 50 mg, from 1 μg to 10 mg, from 1 μg to 1 mg, from 1 μg to 500 μg, from 1 μg to 100 μg or from 1 μg to 50 μg (i.e. 0.001 mg to 0.050 mg). Alternatively, the amount of dabrafenib or BRaf inhibitor present in a single dose may be from 1 μg to 50 mg, from 10 μg to 50 mg, from 100 μg to 50 mg or from 250 μg to 50 mg. The dose of dabrafenib or Raf inhibitor may be from 1 μg/kg to 500 μg/kg, or from 50 μg/kg to 250 μg/kg (kg as weight of patient). A dose may be administered as often as required. This may be as and when a dose is required, or may follow a routine such as three or more times daily, twice daily, once daily, three or more times weekly, twice weekly, or once weekly. Preferably, dabrafenib is administered orally at a dose of 150 mg, twice daily (i.e. ~3-5 mg/kg/d).

The following Examples illustrate the invention and may assist in illuminating the scientific principles underlying the mechanism of action of the active agents described herein for treating fibrosis.

EXAMPLES

Example 1 – BRaf signalling promotes cardiomyocyte hypertrophy

Overview

Aims: Raf kinases (BRaf, cRaf, ARaf) lie upstream of the extracellular signal-regulated kinases 1/2 (ERK1/2). ERK1/2 promote cardiomyocyte hypertrophy and cytoprotection, but the role of BRaf in the adult heart has until now been unclear. BRaf mutations cause cancer

and Raf inhibitors are used clinically but some activate ERK1/2 via the Raf paradox, and the cardiac consequences have not been established. The aim of this study was to determine if activation of BRaf→ERK1/2 signalling promotes cardiac hypertrophy.

Methods and Results: A mouse model was established for cardiomyocyte-specific tamoxifen-inducible heterozygous knock-in of the activating $BRaf^{V600E}$ mutation into the endogenous gene. Tamoxifen-treatment increased ERK1/2 cascade signalling with increased hypertrophic gene expression from 24 h. Echocardiography detected increases in ejection fraction and fractional shortening from 7 d, with significantly increased left ventricular posterior wall (LVPW) thickness by 10 d. This was associated with increased cardiomyocyte cross-sectional area without detectable fibrosis. The Type-1 Raf inhibitor, SB590885, activated ERK1/2 signalling in rat perfused hearts and isolated cardiomyocytes via the Raf paradox, promoting cardiomyocyte hypertrophy. *In vivo*, SB590885 (0.5 mg/kg/d, 3 d) increased LVPW thickness and, as with $BRaf^{V600E}$ knock-in, this was associated with increased cardiomyocyte cross-sectional area without increased fibrosis, probably because of a selective effect on cardiomyocytes rather than fibroblasts.

Conclusions: Direct activation of cardiomyocyte BRaf→ERK1/2 signalling, or paradoxical activation of the pathway by the Type-1 Raf inhibitor, SB590885, promotes cardiomyocyte hypertrophy. These data identify a new paradigm for ERK1/2 signalling in the heart, and activation of the pathway by Raf paradox-inducers may provide short-term benefit in heart failure.

Translational perspective: Heart failure and cancer are the leading causes of mortality in Western society. Since mutated BRaf activates the extracellular signal-regulated kinases 1/2 (ERK1/2) and causes cancer, Raf inhibitors have been developed as cancer therapies. However, ERK1/2 are cardioprotective in the heart, promoting cardiomyocyte hypertrophy. This study demonstrates a direct and significant role for BRaf in promoting cardiomyocyte hypertrophy. Moreover, the Type-1 Raf inhibitor SB590885 activates ERK1/2 in cardiomyocytes via a Raf paradox signalling mechanism to induce cardiomyocyte hypertrophy. This new paradigm for ERK1/2 signalling in the heart, raises the possibility that Raf paradox-inducers may provide short-term benefit for heart failure patients.

Introduction

Heart failure and cancer are the leading causes of morbidity and mortality in Western society. Drugs are increasingly available to treat cancer patients, but therapeutic targets for cancer may be required for normal cardiac function, and cardiotoxicity of cancer therapies is an increasing problem. The extracellular signal-regulated kinase 1/2 (ERK1/2) pathway increases cell proliferation and is a target for cancer, but is also cardioprotective and promotes hypertrophy (i.e. growth in the absence of proliferation) in contractile cardiomyocytes. BRaf is one of three Raf kinases (the others being ARaf and cRaf) that phosphorylate and activate downstream kinases (MKK1/2), which phosphorylate and activate ERK1/2. Oncogenic BRaf mutations [particularly of BRaf(Val600) commonly mutated to $BRaf^{V600E}$] are associated with ~15% of all cancers with high rates in melanoma (40-60%). Raf inhibitors are already used clinically. These were intended to have specificity for $BRaf^{V600E}$, but IC_{50} values for $BRaf^{V600E}$ *vs* wild-type BRaf or cRaf indicate modest selectivity at best. Use of these "first generation" Raf inhibitors is limited because cancer cells become resistant to the drugs and because of paradoxical activation of ERK1/2 signalling in cells with activated Ras.

Unlike most cells, mammalian cardiomyocytes are terminally-differentiated from birth. To accommodate an increased workload (e.g. in hypertension), adult cardiomyocytes hypertrophy, increasing in size and myofibrillar content. This leads to compensated cardiac hypertrophy, but prolonged stress may cause decompensation and heart failure as cardiomyocytes die. All three Raf kinases are expressed in cardiomyocytes. Hypertrophic stimuli activate cRaf and some (e.g. endothelin-1) also activate ARaf. Studies in genetically-modified mice indicate cRaf is required for cardiac hypertrophy, but there are no further studies of ARaf. One report suggested BRaf may be pro-hypertrophic, but BRaf was not studied directly, the conclusions relying on use of an inhibitor (SB590885) at a concentration (10 μM) likely to inhibit all Raf isoforms and unlikely to be specific only for Raf kinases. Here, it was established that BRaf signalling promotes cardiomyocyte hypertrophy using a mouse model with cardiomyocyte-specific knock-in of an activating mutation (V600E) into the endogenous BRaf gene. It was further demonstrated that paradoxical activation of ERK1/2 in cardiomyocytes by the Type-1 Raf inhibitor, SB590885, promotes hypertrophy.

Methods

Ethics statement: Animals were housed at the BioResource Unit at University of Reading (UK registered with a Home Office certificate of designation). All procedures were in

accordance with UK regulations and the European Community Directive 86/609/EEC for animal experiments. Neonatal rats were culled by schedule 1 (cervical dislocation) for which additional approval and licences are not required according to UK regulations. Adult male rats and all mice were housed with water and food *ad libitum* with a 12:12 light/dark cycle. Work was undertaken in accordance with local institutional animal care committee procedures (University of Reading) and the U.K. Animals (Scientific Procedures) Act 1986. Wild-type C57Bl/6J mice, and Sprague-Dawley adult and neonatal (2-4 d) rats were from Charles River (UK).

***In vivo* mouse studies:** Genetically-modified mice were from Jackson Laboratories. Mice with a floxed cassette for Cre-induced knock-in of the $BRaf^{V600E}$ mutation (B6.129P2(Cg)-*Braf*^{tm1Mmcm}/J, strain no. 017837) were maintained on a C57Bl/6J background. Myh6-MERCreMER mice expressing tamoxifen-activated Cre under control of the mouse Myh6 promoter (Tg(Myh6-cre)1Jmk/J, strain no. 009074) were backcrossed against the C57Bl/6J background for at least 4 generations. $BRaf^{V600E/WT}/Cre^{MCM/WT}$ double heterozygous mice and single heterozygous $Cre^{MCM/WT}$ littermates were generated for experimentation. Recombination was induced with a single dose of tamoxifen (40 mg/kg i.p.; Sigma-Aldrich) with vehicle only controls (corn oil; Sigma-Aldrich). Alzet osmotic pumps were used to deliver SB590885 (0.5 mg/kg/d; Selleck Chemicals) dissolved in DMSO/PEG [50% (v/v) DMSO, 20% (v/v) polyethylene glycol 400, 5% (v/v) propylene glycol, 0.5% (v/v) Tween 80] or DMSO/PEG alone to male C57Bl/6J mice (8 wks). Mice were culled by CO_2 inhalation with cervical dislocation. Hearts were snap-frozen in liquid N_2 or fixed in 10% formalin for histology. Echocardiography was performed on anaesthetised mice (maintained with 1.5% isoflurane delivered via a nose cone) using a Vevo 2100 system and MS400 18-38 MHz transducer (Visualsonics). Left ventricular (LV) cardiac function and dimensions was assessed from short axis M-mode images with the axis at the mid-level of the LV at the level of the papillary muscles. Data analysis (Vevo LAB version 1.7.1) was performed by independent assessors blinded to intervention. Please see *Further Methodology* section for full details of methodology plus information on genotyping, confirmation of recombination, minipump preparation and implantation, sample preparation and histology.

Adult rat heart perfusions and cell cultures: Hearts from adult male Sprague–Dawley rats were perfused retrogradely (37°C, 70 mmHg) with 15 min equilibration. SB590885 in DMSO or DMSO alone was added at the end of the equilibration period and perfusions

continued for a further 15 min. Neonatal rat ventricular myocytes (NRVMs) were cultured from 2-4 d Sprague-Dawley rats. For immunoblotting or qPCR, cardiomyocytes were plated at 4×10^6 cells per 60 mm dish. After 18 h myocytes were beating spontaneously. For immunostaining, cardiomyocytes were plated at 1×10^6 cells per 35 mm dish containing glass coverslips. The plating medium was withdrawn after 18 h and cells incubated in serum-free maintenance medium (24 h). Human cardiac fibroblasts were grown in fibroblast growth medium-3 (PromoCell). Cells were seeded the day before experimentation at a density to achieve 90% confluence after 24 h and synchronised overnight in M199 medium containing 0.1% (v/v) FCS and 100 units/ml penicillin and streptomycin. See *Further Methodology* section for full details of perfusions, cell cultures and sample preparation.

RNA preparation, qPCR, Raf assays, immunostaining and immunoblotting: See *Further Methodology* section for full details of methods, primers and antibodies.

Statistical analysis: Statistical analysis was performed using GraphPad Prism 7.0.

Further Methodology

In vivo mouse studies: *Source and breeding* - Wild-type C57Bl/6J mice (8 wks) were from Charles River (UK). Genetically-modified mice were from Jackson Laboratories and imported into the UK by Charles River. Mice with a floxed cassette for Cre-induced knock-in of the $BRaf^{V600E}$ mutation (B6.129P2(Cg)-*Braf*^{tm1Mmcm}/J, strain no. 017837) were used. These were purchased as live mice maintained on a C57Bl/6J congenic background. Mice were bred with Myh6-MERCreMER mice expressing nuclear-localised tamoxifen-activated Cre recombinase under control of the mouse Myh6 promoter (Tg(Myh6-cre)1Jmk/J, strain no. 009074) backcrossed against the C57Bl/6J background for at least 4 generations. Breeding protocols were used to produce $BRaf^{V600E/WT}/Cre^{MCM/WT}$ double heterozygous mice or single heterozygous MHC^{MCM} mice derived from crosses between the Tg(Myh6-cre)1Jmk/J and B6.129P2(Cg)-*Braf*^{tm1Mmcm}/J to control for tamoxifen-induced Cre activation.

Genotyping - DNA was extracted from ear notches using Purelink genomic DNA (gDNA) mini-kits (Invitrogen) according to the manufacturer's instructions. Briefly, tissue was digested in genomic digestion buffer containing proteinase K (2-4 h, 55°C). Following centrifugation (12,000 x g, 3 min, 18°C), supernatants were incubated with RNAse A (2 min) before addition of genomic lysis binding buffer mixed with an equal volume of ethanol. gDNA was purified using Purelink spin columns and PCR amplified (up to 33 cycles) with

specific primers (see *Table 2* for primer sequences and annealing temperatures) and using GoTaq Hot Start Polymerase (Promega). PCR conditions were 95°C for 3 min, followed by 33 cycles of 95°C denaturation for 30 s, 30 s annealing, elongation at 72°C for 30 s, followed by a 7 min 72°C final extension. PCR products were run on 2% (w/v) agarose gels (45 min, 80V) and visualised under UV light.

Induction and confirmation of recombination - Mice were treated with a single dose of tamoxifen (40 mg/kg i.p.; Sigma-Aldrich) or vehicle. Tamoxifen was dissolved in ethanol and then mixed with corn oil. For confirmation of recombination in the heart, RNA was extracted from heart powders and cDNA prepared as described below. cDNA (4 µl) was subjected to PCR analysis using GoTaq Hot Start Polymerase with specific primers and conditions (*Table 2*). PCR conditions were 95°C for 5 min, followed by 40 cycles of 95°C denaturation for 40 s, 40 s annealing, elongation at 72°C for 60 s, followed by a 7 min 72°C final extension. For $BRaf^{V600E}$, 50% of the resulting product was digested with XbaI (New England Biolabs) (3 h, 37°C). Digested and undigested products were separated by electrophoresis on a 2% (w/v) agarose gel (85 V, 45 min). $BRaf^{V600E}$ knock-in introduces a novel Xba1 site in the PCR product in the cDNA producing an additional product.

Table 2: Primers for genotyping and confirmation of recombination.

Mouse strain	DNA	Forward primer	Reverse primer	Annealing temp.
Genotyping				
$BRaf^{V600E}$	gDNA	TGAGTATTTTTGTGGCAACTGC	CTCTGCTGGGAAAGCGGC	54°C
Cre^{WT}	gDNA	TCTATTGCACACAGCAATCCA	CCAACTCTTGTGAGAGGAGCA	52°C
Cre^{MCM}	gDNA	TCTATTGCACACAGCAATCCA	CCAGCATTGTGAGAACAAGG	52°C
Recombination				
$BRaf^{V600E}$	cDNA	GCTCGGCAGACTGCACAGGG CATGGATTAC	TGAGGCACTCTGCCATTAAT CTCTTCATGGC	64°C

Drug delivery - Drug delivery used Alzet osmotic pumps (models 1007D or 1002; supplied by Charles River), filled according to the manufacturer's instructions in a laminar flow hood using sterile technique. Mice were treated with SB590885 (0.5 mg/kg/d) dissolved in DMSO/PEG mix [50% (v/v) DMSO, 20% (v/v) polyethylene glycol 400, 5% (v/v) propylene glycol, 0.5% (v/v) Tween 80] or DMSO/PEG alone. SB590885 was from SelleckChem and vehicle components were from Sigma-Aldrich. Minipumps were incubated overnight in sterile PBS (37°C) prior to implantation. Implantation was performed under continuous

inhalation anaesthesia using isoflurane (induction at 5%, maintenance at 2-2.5%) mixed with 2 l/min O_2. A 1 cm incision was made in the mid-scapular region and mice were given 0.05 mg/kg (s.c.) buprenorphine (Vetergesic, Ceva Animal Health Ltd.) to repress any post-surgical discomfort. Minipumps were implanted portal first in a pocket created in the left flank region of the mouse. Wound closure used a simple interrupted suture with polypropylene 4-0 thread (Prolene, Ethicon). Mice were recovered singly and returned to their home cage once fully recovered.

Cardiac ultrasound - Echocardiography was performed on anaesthetised mice using a Vevo 2100 imaging system equipped with a MS400 18-38 MHz transducer (Visualsonics). Mice were anaesthetised in an induction chamber with isoflurane (5% flow rate) with 1 l/min O_2 then transferred to the heated Vevo Imaging Station. Anaesthesia was maintained with 1.5% isoflurane delivered via a nose cone. Left ventricular cardiac function and structure was assessed from short axis M-mode images with the axis placed at the mid-level of the left ventricle at the level of the papillary muscles. Baseline scans were taken prior to experimentation (-7 to -3 days). Further scans were taken at intervals following minipump implantation. Imaging was completed within 30 min. Data analysis (Vevo LAB version 1.7.1) was performed by independent assessors blinded to intervention. Data were gathered from two scans taken from each time point, taking mean values across 5 cardiac cycles for each scan. Mice were recovered singly and transferred to the home cage once fully recovered.

Tissue harvesting and processing - Mice were culled by schedule 1 (CO_2 followed by cervical dislocation). Hearts were excised quickly, washed in PBS, dried and snap-frozen in liquid N_2 or fixed for histology.

Histology and assessment of myocyte size and fibrosis: Histological analysis was performed on hearts subjected to *in situ* perfusion fixation with 10% formalin. Hearts were immersed in 70% (v/v) ethanol, embedded in paraffin and sectioned at 10 μm. Sections were de-waxed using xylene and re-hydrated through sequential washes in decreasing ethanol gradients (100%, 100%, 90%, 75%, 50%) to distilled water. Sections were stained using kits for hematoxylin and eosin (H&E, Sigma) or Masson's trichrome (Polysciences). For H&E staining, sections were submerged in Harris hematoxylin, differentiated in 1% acid alcohol, 'blued' in saturated lithium carbonate, and counterstained in eosin Y solution. For Masson's trichrome staining, sections were incubated in Bouin's fixative (60 min, 60°C) then processed

through Weigert's iron hematoxylin, Biebrich Scarlet-acid Fuchsin, and aniline blue with 1% acetic acid differentiation stains. Sections were rapidly dehydrated to xylene and mounted in DPX for image capture using a Nikon slide scanner.

For analysis of myocyte cross-sectional area, cells within the LV (excluding endocardial regions) were chosen at random and outline traced using NDP.view2 software (Hamamatsu). Only cells with a single nucleus that were clearly in cross-section were included in the analysis. For assessment of fibrosis, 20× images of the entire LV were exported and the collagen fraction calculated as the ratio between the sum of the total area of fibrosis (blue colour) to the sum of the total tissue area (including the myocyte area) for the entire image using Image J. For investigating the pattern of left ventricular fibrosis, images were sub-divided between those which included vessels (for perivascular fibrosis) and those void of vessels (for interstitial fibrosis). All histological and data analysis was performed by independent assessors blinded to treatment groups.

Adult rat heart perfusions: Adult male (300-350 g) Sprague–Dawley rats (Charles River) were anaesthetised with a lethal intraperitoneal dose of Euthatal (pentobarbital sodium, 60 mg/kg). After complete anaesthesia was induced, a saphenous vein was exposed and heparin (1000 U/kg) administered intravenously. The chest cavity was opened and the heart and lungs were removed into modified ice-cold KHBBS (25 mM $NaHCO_3$, 119 mM NaCl, 35 mM KCl, 2.5 mM $CaCl_2$, 1.2 mM $MgSO_4$, 1.2mM KH_2PO_4 equilibrated with 95% O_2/5% CO_2) whilst the heart was still beating. Surrounding tissues were removed from the heart before aortic cannulation and perfusion. Hearts were perfused retrogradely (37°C at 70 mmHg) as described previously with a 15 min equilibration period. SB590885 or dabrafenib (SelleckChem) (1/1000 dilution) was added at the end of the equilibration period and all perfusions continued for a further 15 min. Hearts were 'freeze-clamped' between aluminium tongs cooled in liquid nitrogen and pulverized under liquid N_2 in a pestle and mortar. The powders were stored at −80°C.

Cell cultures: Neonatal rat ventricular myocytes (NRVMs) were prepared and cultured from 2-4 d Sprague-Dawley rats (Charles River) essentially as previously described. Ventricles were dissected and dissociated by serial digestion at 37°C with 0.44 mg/ml (6800 U) Worthington Type II collagenase (supplied by Lonza) and 0.6 mg/ml pancreatin (Sigma-Aldrich, cat. No. P3292) in sterile digestion buffer (116 mM NaCl, 20 mM HEPES, 0.8 mM Na_2HPO_4, 5.6 mM glucose, 5.4 mM KCl and 0.8 mM $MgSO_4$, pH 7.35). The first digestion

supernatant (5 min, 37°C, 160 cycles/min in a shaking waterbath) was discarded. Cell suspensions from subsequent digestions (4×25 min, 37°C 136 cycles/min shaking) were recovered by centrifugation (5 min, 60×g) and the cell pellet resuspended in plating medium (Dulbecco's modified Eagle's medium (DMEM)/medium 199 [4:1 (v/v)]) containing 15% (v/v) foetal calf serum (FCS; Life Technologies) and 100 units/ml penicillin and streptomycin. Cells were pre-plated on plastic tissue culture dishes (30 min) to remove non-cardiomyocytes. Non-adherent cardiomyocytes were collected and viable cells counted by Trypan Blue (Sigma-Aldrich) exclusion using a haemocytometer. For immunoblotting or qPCR, viable cardiomyocytes were plated at a density of 4×10^6 cells/dish on 60 mm Primaria dishes pre-coated with sterile 1% (w/v) gelatin (Sigma-Aldrich). After 18 h myocytes were beating spontaneously. For immunostaining experiments, cardiomyocytes were plated at 1×10^6 cells/dish on 35 mm Primaria dishes containing glass coverslips pre-coated with sterile 1% (w/v) gelatin followed by laminin (20 µg/ml in PBS; Sigma-Aldrich). For all experiments, the plating medium was withdrawn after 18 h and cells were incubated in serum-free maintenance medium (DMEM/medium [4:1 (v/v)] containing 100 units/ml penicillin and streptomycin) for a further 24 h.

Human cardiac fibroblasts (PromoCell) were grown in Fibroblast growth medium-3 (FGM3, PromoCell). Cells were seeded the day before experimentation (at a density to achieve 90% confluence after 24 h) and synchronised overnight in M199 medium containing 0.1% (v/v) FCS and 100 units/ml penicillin and streptomycin.

RNA preparation and qPCR: Total RNA was prepared using RNA Bee (AMS Biotechnology Ltd) with 1 ml per 4×10^6 NRVMs or 10-15 mg mouse heart powder. RNA was prepared according to the manufacturer's instructions, dissolved in nuclease-free water and purity assessed from the A_{260}/A_{280} measured using an Implen NanoPhotometer (values of 1.8–2.1 were considered acceptable). RNA concentrations were determined from the A_{260} values. Quantitative PCR (qPCR) analysis was performed as previously described. Total RNA (2 µg) was reverse transcribed to cDNA using High Capacity cDNA Reverse Transcription Kits with random primers (Applied Biosystems) according to the manufacturer's instructions. qPCR was performed using an ABI Real-Time PCR 7500 system (Applied Biosystems). Optical 96-well reaction plates were used with iTaq Universal SYBR Green Supermix (Bio-Rad Laboratories Inc.) according to the manufacturer's instructions. Primers for mouse *Col4a1* (forward: 5'- CTGGCACAAAAGGGACGAG-3';

reverse: 5'- ACGTGGCCGAGAATTTCACC-3'), *ARaf* (forward: 5'-AGCATCCAGGATCTGTCTGG-3'; reverse: 5'- ACCTGCATGAGGCTGGAGTC-3'), *BRaf* (forward: 5'- GGCCAGGCTCTGTTCAATG -3'; reverse: 5'-CTCTTTGCTGAAGGGCATCT-3') and *cRaf* (forward: 5'-AGTTAGAGCCGAGCGGACTT-3'; reverse: 5'- ACTCCAAAGCCATTGCTGAT-3') were from Invitrogen by Thermo Fisher Scientific. *Gapdh* was used as the reference gene for the study using proprietory primers for rat and mouse from PrimerDesign. Other genes were studied using custom primers from PrimerDesign (*Table 3*). Results were normalized to *Gapdh*, and relative quantification was obtained using the ΔCt (threshold cycle) method; relative expression was calculated as $2^{-\Delta\Delta Ct}$, and normalised to vehicle or time 0.

Table 3: Custom qPCR primers (PrimerDesign)

Gene Symbol	Accession No.	Product (bp)	Position	Sense Primer (5'→3')	Antisense Primer (5'→3')
Rat genes					
Atf3	NM_012912	132	993-1124	AGCAGGATCGCACTAATGGG	ACAACTTCAATGATGATGAATGTTCTCAC
Ctgf	NM_022266	131	796-926	CTATGATGCGAGCCAACTGC	GAGACGACTCTGCTTCTCCAG
Dusp2	NM_00101208	110	1235-1344	ACTTGCGGAAATTAATTGAACTCTAAA	ACATGGTTTCTGCTTGTCACAG
Dusp5	NM_133578	97	1970-2066	CCTTGGACTTTGGCATGGTTT	GGGTCTGACAACTTTCTGAATGA
Dusp6	NM_053883	75	740-814	AGCGACTGGAATGAGAACACA	GCAGCCCTCGTCTTTGAGT
Egr1	NM_012551	116	1049-1164	TCAGTCGTAGTGACCACCTTAC	GGTATGCCTCTTGCGTTCATC
Fos	NM_022197	104	223-326	GGGACAGCCTTTCCTACTACC	GGCACTAGAGACGGACAGATC
Nppb	NM_031545.1	133	309-441	CCAGGAGAGACTTCGAAATTCCA	TGCAGCCAGGAGGTCTTCC
Myc	NM_012603	93	524-616	CGTTATTTGAAGCCTGAATTTCCT	TCATAGTTCCTGTTAGCGAAGC
Fosl1	NM_012953	138	319-456	GTCCAGCAGCAGAAGTTCCA	GGGACTGTACTGGGGATAGGT
Mouse genes					
Atf3	NM_007498	125	329 - 453	ACTGGTATTTGAGGATTTTGCTAAC	TGTTGTTGACGGTAACTGACTC
Col1a1	NM_007742	141	3396 - 3536	TCGTGGCTTCTCTGGTCTC	CCGTTGAGTCCGTCTTTGC
Ctgf	NM_010217	101	1,159 - 1,259	GCACACCGCACAGAACCA	ATGGCAGGCACAGGTCTTG
Ddr2	NM_022563.2	112	6646-6757	GCACTTGGTGAATTAATTAGAATCCTG	GGACAACTAAATGGTCCCTCCC
Dusp5	NM_00108539	117	412- 528	GAGTGCTGTGTGGATGTGAA	CTGGTCATAGGCTGGTCTGT
Egr1	NM_007913	95	1,125 - 1,219	GCCTTCGCTCACTCCACTA	GCTGGGATTGGTAGGTGGTA
Fos	NM_010234	112	853 - 964	CTTCACCCTGCCCCTTCTC	CGGAAACAAGAAGTCATCAAAGG
IL11	NM_00129042	120	254-373	TGACGGAGATCACAGTCTGGA	CGGAGGTAGGACATCAAGTCTAC
IL6	NM_031168	106	57 - 162	TCCATCCAGTTGCCTTCTTG	GGTCTGTTGGGAGTGGTATC
Jun	NM_010591	82	2,264 - 2,345	CCTAACATTCGATCTCATTCAGTATTA	CTACAGAAGCAATCTACAGTCTCTA
Lox	NM_010728	102	1556-1657	GACATTCGCTACACAGGACAT	AACACCAGGTACGGCTTTATC
Myc	NM_00117735	93	1,638 - 1,730	AACAACCGCAAGTGCTCCA	GTTCCTCCTCTGACGTTCCAA
Myh7	NM_080728	113	4,411 - 4,523	GAGATCGAGGACCTGATGG	TCATACTTCTGCTTCCACTCA
Nppa	NM_008725	98	197 - 294	GATGGATTTCAAGAACCTGCTAGA	CTTCCTCAGTCTGCTCACTCA

NppB	NM_008726	104	438 - 541	TCCAGCAGAGACCTCAAAATTC	CAGTGCGTTACAGCCCAAA
Timp1	NM_011593	84	414-497	TACGCCTACACCCCAGTCAT	GCCCGTGATGAGAAACTCTTC

Sample preparation: For analysis of protein kinases in total extracts, cells were washed with ice-cold PBS and scraped into 150 µl Buffer A [20 mM β-glycerophosphate (pH 7.5), 50 mM NaF, 2 mM ethylenediamine tetraacetic acid (EDTA), 1% (v/v) Triton X-100, 5 mM dithiothreitol] containing protease and phosphatase inhibitors [10 mM benzamidine, 0.2 mM leupeptin, 0.01 mM trans-epoxy succinyl-l-leucylamido-(4-guanidino)butane, 0.3 mM phenylmethylsulfonyl fluoride, 4 µM microcystin]. Rat or mouse heart powders were extracted in 8 vol (relative to powder weight) Buffer A plus inhibitors. Samples were vortexed and extracted on ice (10 min). Extracts were centrifuged (10,000×g, 4°C) for 5 or 10 min for NRVMs or heart powders, respectively. The supernatants were removed, a sample was taken for protein assay and the rest boiled with 0.33 vol SDS-polyacrylamide gel electrophoresis (SDS-PAGE) sample buffer [0.33 M Tris-HCl pH 6.8, 10% (w/v) SDS, 13% (v/v) glycerol, 133 mM dithiothreitol, 0.2 mg/mL bromophenol blue]. Protein concentrations were determined by BioRad Bradford assay using bovine serum albumin (BSA) standards.

Cytosolic and nuclear extracts were prepared essentially by the method of Dignam et al (Dignam *et al.*, Nucleic Acids Res., (1983), 11:1475-1489). Cells were washed in ice-cold PBS and harvested into 150 µl of hypotonic buffer (10 mM Hepes, pH 7.9, 10 mM KCl, 1.5 mM $MgCl_2$, 0.3 mM Na_3VO_4) containing protease and phosphatase inhibitors. Samples were centrifuged (10,000×g, 4°C, 5 min) and the supernatant (cytosolic) fractions boiled with 50 µl of sample buffer. The pellets were resuspended in 50 µl of nuclear extraction buffer (20 mM Hepes pH 7.9, 420 mM NaCl, 1.5 mM $MgCl_2$, 0.2 mM EDTA, 25% (v/v) glycerol, 0.3 mM Na_3VO_4) containing protease and phosphatase inhibitors and extracted on ice for 1 h with occasional vortex-mixing. The samples were centrifuged (10,000×g, 4°C, 5 min) and the supernatant nuclear extracts boiled with 20 µl sample buffer.

For analysis of Col1a1, heart powders were extracted in Buffer A plus inhibitors as described above and centrifuged (10,000×g, 4°C, 10 min). The pellets were resuspended in 8 Vol Buffer B (10 mM HEPES, pH 7.9, 400 mM KCl, 1.5 mM $MgCl_2$, 0.3 mM Na3VO4 5 mM dithiothreitol) containing protease and phosphatase inhibitors to remove contractile proteins. Samples were vortexed, incubated on ice (10 min) and then centrifuged (10,000 × g, 10 min, 4°C). The pellets were further extracted in 8 vol SDS-PAGE sample buffer diluted 1:1 with Buffer A without bromophenol blue. Samples were boiled for 5 min and centrifuged (12,000

× g, 10 min, 4°C). The supernatants were used to assess collagen content. Protein concentrations were determined using a BCA protein assay (Thermo Scientific). Remaining samples were boiled with 0.33 volumes of diluted (1:1) SDS-PAGE sample buffer containing bromophenol blue.

Raf kinase assays: Assays were conducted largely as described in Clerk *et al.*, Mol. Cell. Biol., (2001), 21:1173-1184. Cells (4×10^6) were washed with ice-cold PBS, scraped into 150 µl buffer C [20 mM Tris-HCl pH 7.4, 2 mM EDTA, 100 mM KCl, 10% (v/v) glycerol, 1% (v/v) Triton X-100, 0.5 % 2-mercaptoethanol, 10 mM benzamidine, 5 mM NaF, 0.2 mM Na_3VO_4] containing protease and phosphatase inhibitors, and centrifuged (10,000 × g, 5 min, 4°C). A sample (10 µl) was taken for immunoblotting of total extracts and boiled with an equal volume of sample buffer. The remaining sample was equally distributed for immunoprecipitation of BRaf or cRaf. Samples were incubated (18 h, 4°C with rotation) with antibodies (2 µg) pre-bound to protein G-Sepharose (30 µl of a 1:1 slurry equilibrated in buffer C; Sigma-Aldrich). Samples were centrifuged (10,000 × g, 5 min, 4°C) and supernatants boiled with 0.33 vol sample buffer. Pellets were washed 3 times in buffer C, then with 300 µl buffer D [30 mM Tris-HCl pH 7.5, 0.1 mM EGTA, 0.1 % (v/v) 2-mercaptoethano), 0.03% Brij 35, 10 mM magnesium acetate, 20 mM *n*-octyl β-D-glucopyranoside, 200 µM ATP] and then resuspended in 30 µl buffer D. Assays were initiated by addition of 0.2 µg GST-MKK1. Following incubation (10 min, 30°C) assays were terminated by addition of 5 µl 0.5 M EDTA pH 8.0 and placed on ice. Sample buffer (15 µl) was added and samples boiled prior to immunoblotting (20 µl).

Immunoblot analysis: Proteins were separated by SDS-PAGE on 10% (MKK1/2, ERK1/2) or 8% (Raf isoforms for Raf immunoprecipitates) (w/v) polyacrylamide resolving gels with 6% stacking gels, and transferred electrophoretically to nitrocellulose using a BioRad semi-dry transfer cell (10 V, 60 min) as described (Marshall *et al.*, PLoS. One., (2010), 5:e10027). For collagen, extracts (10 µg) were separated by SDS-PAGE using 4-15% Mini-PROTEAN® TGX precast gels (BioRad, cat. no. 4561086). Proteins were transferred to nitrocellulose using a BioRad semi-dry transfer cell (12 V, 1h) using a modified transfer buffer for high molecular weight proteins [36.5 mM Tris-HCl, 115.5 mM Glycine, 0.65 mM SDS, 10% (v/v) methanol]. Proteins were detected as previously described using primary antibodies as indicated in *Table 4*. Bands were detected by enhanced chemiluminescence using ECL Prime Western Blotting detection reagents with visualisation using an ImageQuant LAS4000

system (GE Healthcare). ImageQuant TL 8.1 software (GE Healthcare) was used for densitometric analysis.

Table 4: Antibodies used for immunoblotting and immunostaining. CST, Cell Signaling Technologies; SCBT, Santa Cruz Biotechnology Inc.; BD, BD Transduction Labs.

Protein	Source	Cat. no.	Host	Dilution
Phospho-ERK1/2(T202/Y204)	CST	4377	Rabbit	1/1000
Total ERK1/2	CST	4695	Rabbit	1/1000
Phospho-MKK1/2(S217/221)	CST	9154	Rabbit	1/1000
Total MKK1/2	CST	8727	Rabbit	1/1000
Phospho-cRaf(S338)	CST	9427	Rabbit	1/1000
Phospho-BRaf(S445)	CST	2696	Rabbit	1/1000
Total cRaf	BD	610152	Mouse	1/1000
Total BRaf	SCBT	sc-5284	Mouse	1/1000
Total ARaf	SCBT	sc-408	Rabbit	1/500
Collagen 1A1	CST	84336	Rabbit	1/1000
GAPDH	CST	5174	Rabbit	1/1000
Anti-Mouse immunoglobulins/HRP	Dako	P0260	Rabbit	1/5000
Anti-Rabbit immunoglobulins/HRP	Dako	P0448	Goat	1/5000
Troponin T	Stratech Scientific	MS-295-P1	Mouse	1/40
Anti-Mouse immunoglobulins/AlexaFluor 488	Invitrogen	A-11001	Goat	1/200

Immunostaining and planimetry: NRVMs were washed with ice-cold PBS and fixed in 3.7% (v/v) formaldehyde in PBS (10 min, room temperature). Cells were permeabilised with 0.3% (v/v) Triton X-100 (10 min, room temperature) in PBS, and non-specific binding blocked with 1% (w/v) fatty acid free BSA (Sigma-Aldrich UK) in PBS containing 0.1% (v/v) Triton X-100 (10 min, room temperature). All incubations were at room temperature in a humidified chamber, and coverslips were washed three times in PBS after each stage of the immunostaining procedure. Cardiomyocytes were stained with mouse monoclonal primary antibodies to troponin T (60 min) with detection using anti-mouse immunoglobulin secondary antibodies coupled to Alexa-Fluor 488 (60 min). Coverslips were mounted using fluorescence mounting medium (Dako) and viewed with a Zeiss Axioskop fluorescence microscope using a 40× objective. Digital images were captured using a Canon PowerShot G3 camera using a 1.8× digital zoom and cardiomyocyte sizes measured using ImageJ. Images were cropped for presentation using Adobe Photoshop CC 2018.

Results

1) Cardiomyocyte BRaf promotes hypertrophy

BRaf is expressed in cardiomyocytes potentially signalling to ERK1/2 and promoting cardiomyocyte hypertrophy. To assess this, mice were generated for cardiomyocyte-specific knock-in of the activating $BRaf^{V600E}$ mutation into the endogenous gene. Since activating mutations in the ERK1/2 cascade cause developmental cardiac abnormalities, an inducible system was used for gene manipulation in adult cardiomyocytes *in vivo*. Mice with a floxed gene for $BRaf^{V600E}$ knock-in were crossed with mice expressing tamoxifen-inducible Cre regulated by an Myh6 promoter for cardiomyocyte-specific expression. Double heterozygote male mice (i.e. $BRaf^{V600E/MCM}$) were used and recombination induced by a single tamoxifen injection (*Figure 1*). The protocol is shown in *Figure 2A*. To control for Cre activation by tamoxifen, experiments were conducted with single heterozygous $Cre^{MCM/WT}$ mice wild-type for BRaf.

Tamoxifen-treatment of $BRaf^{V600E/MCM}$ mice did not affect expression of any Raf protein (*Figure 1D*). Increased phosphorylation (i.e. activation) was detected of MKK1/2 and ERK1/2 in mouse hearts following cardiomyocyte $BRaf^{V600E}$ knock-in (*Figure 2B*), with increased expression of ERK1/2-dependent early genes (*Fos, Egr1, Myc* and *Ctgf*), and cardiomyocyte-specific hypertrophic markers (*Figure 2, C and D*). Of the latter, B-type natriuretic peptide (*Nppb*) and β-myosin heavy chain (*Myh7*) mRNAs were significantly increased within 1 d, whereas atrial natriuretic factor (*Nppa*) mRNA increased to a lesser degree at later times. Expression of mRNAs encoding proteins associated with fibrosis (*Col1a1, Col4a1, Lox, Timp1, Ddr2, IL-11*) was also increased over 10 d (*Figure 2E*). There were no changes in ERK1/2 signalling in tamoxifen-treated hearts from $Cre^{MCM/WT}$ mice, with minor increases only in *Myh7* and *ARaf* mRNAs (*Figure 3, A and B*). Thus, BRaf→ERK1/2 signalling promotes changes in gene expression consistent with cardiomyocyte hypertrophy.

Echocardiography was used to assess the physiological effects of $BRaf^{V600E}$ knock-in in cardiomyocytes. There were no significant differences in cardiac function/dimensions between $Cre^{MCM/WT}$ mice with/without tamoxifen and vehicle-treated $BRaf^{V600E/MCM}$ mice (*Figure 3C*). Cardiomyocyte $BRaf^{V600E}$ knock-in significantly increased ejection fraction (EF) and fractional shortening (FS) at 7 d, with significant increases in left ventricular (LV) systolic and diastolic posterior wall (PW) thickness over 7-10 d (*Figure 4, A and B*). There was no evidence of cardiac dilatation with no increase in LV internal diameter (ID). The data

are consistent with development of compensated, concentric hypertrophy. The increase in LVPW thickness induced by $BRaf^{V600E}$ knock-in in mouse hearts was associated with increased cardiomyocyte cross-sectional area (*Figure 4, C and D*). Despite changes in mRNA expression of genes associated with fibrosis (*Figure 2E*), there was no histological evidence of increased fibrosis in $BRaf^{V600E}$ knock-in mouse hearts (*Figure 4C*), and no significant change in collagen I (Col1a1) protein (*Figure 4E*). This is indicative of post-transcriptional regulation of fibrotic protein expression. It was hypothesised that activation of endogenous cardiomyocyte BRaf signals through ERK1/2 to induce compensated, concentric cardiac hypertrophy without fibrosis.

2) SB590885 activates ERK1/2 in cardiomyocytes

The data (*Figures 2 and 4*) and previous work (Bogoyevitch *et al.*, J. Biol. Chem., (1995), 270:26303-26310; Muslin *et al.*, Trends Cardiovasc. Med., (2005), 15:225-229) indicate Raf kinases promote cardiac hypertrophy. Raf inhibitors used for cancer may, therefore, inhibit hypertrophy. Conversely, since Type-1 or 1.5 inhibitors paradoxically activate ERK1/2 in proliferating cells (the Raf paradox), such inhibitors may instead promote hypertrophy. The effects were assessed of SB590885, a Type-1 inhibitor with 11-fold higher selectivity for BRaf over cRaf that locks the enzyme in an active conformation. SB590885 activated ERK1/2 in Langendorff-perfused adult rat hearts (*Figure 5A*). A high concentration (10 μM) of SB590885 inhibited ERK1/2 phosphorylation in neonatal rat ventricular myocytes (*Figure 5B*) or human cardiac fibroblasts (*Figure 5C*), although this concentration may not be entirely selective for Raf kinases. Lower concentrations (0.01-0.1 μM) activated ERK1/2 in both cell types, but relative activation in cardiomyocytes was substantially greater than in fibroblasts. Time courses for ERK1/2 activation by SB590885 in cardiomyocytes showed that, although 1 μM SB590885 did not activate ERK1/2 at 20 min (*Figure 5B*), ERK1/2 phosphorylation subsequently increased to a similar level as that seen with 0.1 μM SB590885 at 1 h with significant elevation over at least 8 h (*Figure 5C*). This may result from reducing concentrations of active, available SB590885 as it is metabolised. The overall conclusion was that SB590885 induces significant and sustained activation of ERK1/2 signalling in cardiomyocytes.

The greater responsiveness of cardiomyocytes than fibroblasts to SB590885 could reflect a difference in the ERK1/2 signalling network. In proliferating cells, Raf paradox inducers enhance Raf signalling by increasing Raf dimerization, particularly BRaf/cRaf heterodimer

formation. In cardiomyocytes, SB590885 or endothelin-1 (a potent hypertrophic agonist that activates cRaf) increased MKK1-phosphorylating activity in immunoprecipitated BRaf or cRaf complexes (*Figure 5D*). With SB590885, the increase in activities of BRaf immunocomplexes was not associated with consistent changes in activating phosphorylations of cRaf(S338) or BRaf(S445) (*Figure 5E*) and, although cRaf was readily detected in BRaf immunoprecipitates, there was no significant increase in heterodimerization (*Figure 5D, lower panels*), suggesting the proteins pre-associate. Consequently, because of Raf paradox signalling, Type-1 Raf inhibitors are highly likely to activate ERK1/2 in cardiomyocytes with pro-hypertrophic potential.

3) SB590885 activates ERK1/2-dependent gene expression and promotes cardiomyocyte hypertrophy

Hypertrophic agonists (e.g. endothelin-1) increase activated ERK1/2 in the nucleus without net accumulation of total ERK1/2 and this regulates gene expression. SB590885 behaved similarly although, in contrast to endothelin-1, the degree of nuclear ERK1/2 activity was significantly greater than that in the cytoplasm (*Figure 6A*). SB590885 (0.1 μM, 1 h) increased expression of immediate early genes (*Figure 6B*). This was inhibited by the MKK1/2 inhibitor PD184352, indicating the response was directly caused by increased ERK1/2 signalling. SB590885 promoted cardiomyocyte hypertrophy as shown by increased cell area (*Figure 6C*). To determine if this occurs *in vivo*, mice were treated with SB590885 (0.5 mg/kg/d; 3d) or vehicle, and cardiac function/dimensions assessed by echocardiography. SB590885 increased LVPW thickness in the absence of any significant change in LVID, resulting in an increase in calculated LV mass (*Figure 7, A and B*). This was associated with a significant increase in cardiomyocyte cross-sectional area with no evidence of increased fibrosis (*Figure 7C*). Thus, as with cardiomyocyte $BRaf^{V600E}$ knock-in (*Figures 2 and 4*), activation of ERK1/2 signalling by SB590885 promotes cardiomyocyte hypertrophy.

Discussion

This study demonstrates a direct and significant role for BRaf in promoting cardiomyocyte hypertrophy. Activation of the endogenous gene by heterozygous knock-in of the $BRaf^{V600E}$ mutation was sufficient to induce hypertrophy with changes in hypertrophic gene expression (*Figure 2*) and increased cardiomyocyte size and LVPW thickness *in vivo* (*Figure 4*). The data are consistent with the compensated, concentric hypertrophy seen in mice with

cardiomyocyte-specific expression of constitutively-active MKK1. Both interventions increased ERK1/2 activation, enhanced EF, increased LVPW thickness and did not induce significant fibrosis. The data are also in accord with studies of mice with deletion of ERK1 and/or ERK2 in heart failure models which showed that ERK1/2 signalling is cardioprotective and required for concentric hypertrophy.

In this acute model, EF and FS were particularly increased at 7 d following $BRaf^{V600E}$ knock-in with increases in diastolic LVPW thickness only becoming significant at 10 d (*Figure 4, A and B*). This raises the question of whether the early phases of developing hypertrophy cause the increase contractility or if the effect of ERK1/2 is first on cardiomyocyte contractility which then stimulates hypertrophic growth. It also remains to be established if the prime effect of ERK1/2 on contractility is direct or results from changes in gene expression. With changes in mRNA expression occurring even within 24 h (*Figure 2D*), it is clearly possible that changes in expression of ion channels or contractile proteins may affect FS or EF. However, downstream signalling from ERK1/2 may regulate contractility directly (e.g. activation of p90 ribosomal S6 kinases that phosphorylate NHE1 or myofilament proteins). Further studies to identify the full range of ERK1/2 cascade targets, whether nuclear transcription factors or cytosolic proteins, may provide clarification.

The studies with $BRaf^{V600E/MCM}$ mice provided a clear conclusion with respect to the role of BRaf in cardiomyocytes, but BRaf→ERK1/2 signalling is also important in proliferating cardiac cells including fibroblasts, and inhibitors of ERK1/2 signalling will affect all cell types. Much work has been done to understand the effects of Type-1 and 1.5 inhibitors in proliferating cells. Type-1 inhibitors such as SB590885 bind to Raf kinases in an active conformation and increase Raf dimerization potential. Inhibitor binding to one protomer may prevent inhibitor binding to the other and, in the context of activated Ras, the active protomer activates MKK1/2 and ERK1/2. The responses of terminally-differentiated cells such as cardiomyocytes have been unexplored. SB590885 activated ERK1/2 in perfused hearts at low concentrations (~0.1 μM) but, surprisingly, had a more pronounced effect in cardiomyocytes than fibroblasts (*Figure 5, A and B*). In contrast to studies in proliferating cells, there was no change in BRaf/cRaf heterodimerization (*Figure 5, C and D*), suggesting that cardiomyocytes are primed for Raf paradox signalling. Functionally, as might be expected for an activator of ERK1/2 signalling, SB590885 promoted ERK1/2-dependent changes in gene expression in cardiomyocytes and stimulated cardiomyocyte hypertrophy

(*Figure 6, B and C*). Moreover, SB590885 promoted cardiomyocyte hypertrophy *in vivo* with little evidence of fibrosis (*Figure 7, A-C*), an effect that may be attributed to the greater enhancement of ERK1/2 activity by the drug in cardiomyocytes than fibroblasts (*Figure 5B*).

The data with SB590885 are fully consistent with the data for cardiomyocyte $BRaf^{V600E}$ knock-in (*Figures 2 and 4*), suggesting that activation of ERK1/2 signalling by Raf paradox-inducers such as SB590885 may be a useful therapeutic approach for cardiomyocyte protection or to enhance cardiac function. SB590885 was developed only as a preclinical tool. This or an alternative drug with similar Raf paradox-inducing properties may be useful for cardioprotection or to enhance cardiac function in failing hearts in the short term.

In conclusion, the data establish that activation of cardiomyocyte BRaf promotes hypertrophy, BRaf exists in preformed complexes with cRaf in cardiomyocytes and the Type-1 inhibitor SB590885 activates ERK1/2 in cardiomyocytes to induce cardiomyocyte hypertrophy. A schematic representation of this paradigm is in *Figure 7D*.

Example 2 – Cardiac adaptation to angiotensin II in mice requires cardiomyocyte BRaf, and the Raf inhibitor, dabrafenib, inhibits cardiomyocyte hypertrophy and cardiac fibrosis

Overview

Aim: Raf kinases activate extracellular signal-regulated kinases 1/2 (ERK1/2) that are cardioprotective and promote cardiac hypertrophy. Activation of BRaf in cardiomyocytes promotes hypertrophy, but its role in a pathophysiological setting has not been established. The aim of this study was to determine if cardiac adaption to hypertension requires cardiomyocyte BRaf and whether it is inhibited by the Raf inhibitor, dabrafenib.

Methods and Results: A mouse model was established for cardiomyocyte-specific tamoxifen-inducible homozygous knock-out of BRaf. Cardiomyocyte-specific BRaf knock-out alone did not affect cardiac dimensions/function (assessed by echocardiography) or mRNA expression. Mice were treated with angiotensin II (AngII; 0.8 mg/kg/d, 7 d) to induce hypertension. AngII-induced increased left ventricular wall thickness and decreased internal diameter were moderated by cardiomyocyte BRaf knock-out. Most AngII-induced changes in cardiac mRNA expression were also inhibited. However, cardiomyocyte BRaf knock-out did not reduce interstitial/perivascular fibrosis induced by AngII, and caused areas of focal

damage with loss of cardiomyocytes and enhanced fibrosis/inflammation. Dabrafenib is a Raf inhibitor used for cancer. In mice, 3 mg/kg/d dabrafenib alone did not affect cardiac function/dimensions, but inhibited AngII-induced hypertrophy and changes in cardiac mRNA expression. At a cellular level, dabrafenib inhibited the increase in cardiomyocyte size induced by AngII and, in contrast to cardiomyocyte BRaf knock-out, almost eliminated cardiac fibrosis without any evidence of focal damage.

Conclusions: Cardiomyocyte BRaf is required for cardiac adaptation to AngII-induced hypertension. However, targeting Raf kinases in all cardiac cells with inhibitors such as dabrafenib may be a viable therapeutic option for reducing cardiac hypertrophy and fibrosis in hypertension.

Translational perspective: BRaf activates extracellular signal-regulated kinases 1/2 that are cardioprotective and promote cardiac hypertrophy. Activation of BRaf in cardiomyocytes promotes hypertrophy, but its role in a pathophysiological setting was until now unknown. Here, it was established that BRaf is required for cardiac adaptation to hypertension induced by angiotensin II in mice since loss of cardiomyocyte BRaf compromised the adaptive response enhancing focal damage with loss of cardiomyocytes and increased fibrosis. However, the Raf inhibitor, dabrafenib, inhibited hypertension-induced cardiomyocyte hypertrophy, attenuated interstitial and perivascular fibrosis and did not damage the myocardium. The data suggest that targeting cardiac Raf kinases, irrespective of cell type, with inhibitors such as dabrafenib may be a viable therapeutic option for reducing cardiac hypertrophy and fibrosis in hypertension.

Introduction

Heart failure is an increasing cause of morbidity and mortality worldwide, with hypertension as a major contributing factor. Initially, the heart adapts to the increased work-load to maintain cardiac output. This is achieved in part by hypertrophy of terminally-differentiated contractile cardiomyocytes which increase in size, adapting and increasing the myofibrillar apparatus. In the longer term, this is not sustained, contractile function is compromised and heart failure develops. Pathological changes include cardiomyocyte cell death, and capillary rarefaction. This is associated with inflammation and increased fibrosis. Consequently, strategies to reduce cardiomyocyte death, improve contractility, increase angiogenesis and reduce fibrosis are all necessary to treat heart failure.

The extracellular signal regulated kinase 1/2 (ERK1/2) cascade is a key growth-promoting pathway in all cells. It is best characterised in proliferating cells in which ERK1/2 activation promotes cell division. ERK1/2 are phosphorylated/activated by MKK1/2 that are phosphorylated/activated by upstream Raf kinases (ARaf, BRaf, cRaf) or, in the context of inflammation, Cot/Tpl2. Raf kinases are regulated at multiple levels. Of particular importance, activation requires interaction with activated Ras which induces a conformational change in Raf proteins. They also operate as homo- or heterodimers and are subject to activating and inhibitory phosphorylations. Mutations that activate ERK1/2 cause cancer. Oncogenic mutations are highly prevalent in BRaf, and BRaf inhibitors (e.g. dabrafenib) are in clinical use. Dabrafenib was developed to target oncogenic $BRaf^{V600E/K}$ (IC_{50} 0.7 nM), but also inhibits wild-type BRaf and cRaf (IC_{50} of 5.2 and 6.3 nM, respectively). As a Type 1.5 inhibitor, dabrafenib binds to the "DFG-in" active conformation, but stabilises the kinase in the "αC-helix out" inactive conformation of Raf and may, paradoxically, activate ERK1/2 at low concentrations. This is potentially because it binds to one partner in a Raf dimer, locking the other in an active conformation that can activate MKK1/2 in the presence of activated Ras (the Raf paradox). At high concentrations, both partners are inhibited.

In the heart, the ERK1/2 cascade promotes cardiomyocyte hypertrophy and, independent of this, is potently cardioprotective. All Raf kinases are activated in cultured cardiomyocytes by hypertrophic stimuli such as endothelin-1 (Example 1). *In vivo*, cardiomyocyte-specific expression of dominant-negative cRaf in mice increases cardiomyocyte apoptosis, and leads to cardiomyopathy in response to pressure-overload, indicating that cRaf is cardioprotective. The studies described elsewhere herein demonstrated that activation of endogenous BRaf in cardiomyocytes (via genetic manipulation or a Raf paradox-inducer) promotes hypertrophy (Example 1). Here, the role of BRaf in cardiac adaptation to hypertension induced by angiotensin II (AngII) was investigated. Cardiomyocyte-specific BRaf knock-out compromised cardiac hypertrophy induced by AngII with reduced left ventricular (LV) wall thickness, but this was associated with increased focal cardiac damage and fibrosis indicating that, on balance, cardiomyocyte BRaf signalling is necessary for cardiomyocyte adaptation. However, the Raf inhibitor, dabrafenib, reduced cardiomyocyte hypertrophy and cardiac fibrosis induced by AngII, with no indication of focal damage or evidence of cardiotoxicity. Thus, despite a requirement for BRaf in cardiomyocytes, global inhibition of Raf in the heart

is beneficial. It is concluded that dabrafenib and other related Raf kinase inhibitors may be therapeutically useful for reducing cardiac fibrosis.

Methods

Animals were housed at the BioResource Unit at University of Reading (UK registered with a Home Office certificate of designation). All procedures were in accordance with UK regulations and the European Community Directive 86/609/EEC for animal experiments. Adult male rats and all mice were housed with water and food *ad libitum* with a 12:12 light/dark cycle. Work was undertaken in accordance with local institutional animal care committee procedures and the U.K. Animals (Scientific Procedures) Act 1986. C57Bl/6J mice, and Sprague-Dawley rats were from Charles River (UK). Genetically-modified mice were from Jackson Laboratories. Mice homozygous for floxed BRaf and heterozygous for Cre ($BRaf^{KO/KO}/Cre^{MCM/WT}$), together with heterozygous Cre littermates ($BRaf^{WT/WT}/Cre^{MCM/WT}$) were used. Hearts from adult male Sprague–Dawley rats were perfused retrogradely (37°C, 70 mmHg). Dabrafenib was added during the equilibration period and perfusions continued with/without 0.5 µg/ml basic fibroblast growth factor (bFGF).

***In vivo* mouse studies:** *Source and breeding:* Wild-type C57Bl/6J mice were purchased from Charles River (UK) at 7 wks. Genetically-modified mice were from Jackson Laboratories and imported into the UK by Charles River. Floxed mice were used for Cre-induced BRaf gene deletion (129-*Braf*^{tm1Sva}/J, strain no. 006373) that were cryoresuscitated. These mice were on a 129T2/SvEmsJ background prior to cryopreservation and were then backcrossed against the C57Bl/6J background at UoR for at least 4 generations prior to experimentation. Control experiments were conducted with wild-type littermates. These mice were bred with Myh6-MerCreMer mice expressing nuclear-localised tamoxifen-activated Cre recombinase under control of the mouse Myh6 promoter (B6.FVB(129)-*A1cf*$^{Tg(Myh6\text{-}cre/Esr1*)1Jmk}$/J; strain 005657). These were maintained on a C57Bl/6J background at Jackson Laboratories and were backcrossed against the C57Bl/6J background at UoR for at least 4 further generations. Breeding protocols were used to produce $BRaf^{KO/KO}/Cre^{MCM/WT}$ mice (i.e. homozygous for floxed BRaf and heterozygous for Cre^{MCM}) for experimentation. Additional studies were conducted with $BRaf^{WT/WT}/Cre^{MCM/WT}$ mice (heterozygous for Cre only) generated from the wild-type littermates from the floxed BRaf line.

Genotyping: DNA was extracted from ear notches using Purelink genomic DNA (gDNA) mini-kits (Invitrogen) according to the manufacturer's instructions. Briefly, tissue was digested in genomic digestion buffer containing proteinase K (overnight, 55°C). Following centrifugation (12,000 × g, 3 min, 18°C), supernatants were incubated with RNAse A (2 min) before addition of genomic lysis binding buffer mixed with an equal volume of ethanol. gDNA was purified using Purelink spin columns and PCR amplified with specific primers (see *Table 5* for primer sequences and annealing temperatures) using GoTaq Hot Start Polymerase (Promega). PCR conditions were 95°C for 3 min, followed by 33 cycles of 95°C denaturation for 30 s, 30 s annealing, elongation at 72°C for 30 s, followed by a 7 min 72°C final extension. PCR products were run on 2% (w/v) agarose gels (80V) and visualised under UV light.

Table 5: Primers for genotyping and confirmation of recombination.

Mouse strain	DNA	Forward primer	Reverse primer	Annealing temp.
Genotyping				
$BRaf^{KO}$	gDNA	GCATAGCGCATATGCTCACA	CCATGCTCTAACTAGTGCTG	57°C
Cre^{WT}	gDNA	TCTATTGCACACAGCAATCCA	CCAACTCTTGTGAGAGGAGCA	52°C
Cre^{MCM}	gDNA	TCTATTGCACACAGCAATCCA	CCAGCATTGTGAGAACAAGG	52°C
Recombination				
$BRaf^{KO}$	cDNA	TTGATTTTGAGCCTGGCCCAGTG	GTGCAGTCTGCCGAGCAATATC	57°C

Induction and confirmation of recombination: Mice were treated with a single dose of tamoxifen (40 mg/kg i.p.; Sigma-Aldrich) or vehicle. Tamoxifen was dissolved in ethanol and then mixed with corn oil. For confirmation of recombination, RNA was extracted from tissue powders and cDNA prepared as described below. cDNA (4 µl) was subjected to PCR analysis using GoTaq Hot Start Polymerase with specific primers and conditions (*Table 5*).

Drug delivery: Drug delivery used Alzet osmotic pumps (models 1007D or 1002; supplied by Charles River), filled according to the manufacturer's instructions in a laminar flow hood using sterile technique. Mice were treated with angiotensin II (AngII, 0.8 mg/kd/d) or vehicle (acidified PBS) without or with dabrafenib (3.0 mg/kg/d) dissolved in DMSO/PEG mix [50% (v/v) DMSO, 20% (v/v) polyethylene glycol 400, 5% (v/v) propylene glycol, 0.5% (v/v) Tween 80] or DMSO/PEG alone. AngII was from Merck, dabrafenib was from SelleckChem and vehicle components were from Sigma-Aldrich. Separate minipumps were used for AngII and dabrafenib delivery. Minipumps were incubated overnight in sterile PBS (37°C) prior to implantation. Implantation was performed under continuous inhalation

anaesthesia using isoflurane (induction at 5%, maintenance at 2-2.5%) mixed with 2 l/min O_2. A 1 cm incision was made in the mid-scapular region and mice were given 0.05 mg/kg (s.c.) buprenorphine (Vetergesic, Ceva Animal Health Ltd.) to repress any post-surgical discomfort. Minipumps were implanted portal first in a pocket created in the left flank region of the mouse. Wound closure used a simple interrupted suture with polypropylene 4-0 thread (Prolene, Ethicon). Mice were recovered singly and returned to their home cage once fully recovered.

Cardiac ultrasound: Echocardiography was performed on anaesthetised mice using a Vevo 2100 imaging system equipped with a MS400 18-38 MHz transducer (Visualsonics). Mice were anaesthetised in an induction chamber with isoflurane (5% flow rate) with 1 l/min O_2 then transferred to the heated Vevo Imaging Station. Anaesthesia was maintained with 1.5% isoflurane delivered via a nose cone. Left ventricular cardiac function and structure was assessed from short axis M-mode images with the axis placed at the mid-level of the left ventricle at the level of the papillary muscles. Baseline scans were taken prior to experimentation (-7 to -3 days). Further scans were taken following minipump implantation. Imaging was completed within 30 min. Data analysis (Vevo LAB version 1.7.1) was performed by independent assessors blinded to intervention. Data were gathered from two scans taken from each time point, taking mean values across 5 cardiac cycles for each scan. Mice were recovered singly and transferred to the home cage once fully recovered.

Tissue harvesting and processing: Mice were culled by schedule 1 (CO_2 followed by cervical dislocation). Hearts were excised quickly, washed in PBS, dried and snap-frozen in liquid N_2 or fixed for histology.

Histology and assessment of myocyte size and fibrosis: Histological analysis was performed on hearts subjected to *in situ* perfusion fixation with 10% formalin. Following immersion in 70% (v/v) ethanol, hearts were embedded in paraffin and sectioned at 10 μm. Sections were de-waxed using xylene and re-hydrated through sequential washes in decreasing ethanol gradients (100%, 100%, 90%, 75%, 50%) to distilled water. Sections were stained using kits for hematoxylin and eosin (H&E, Sigma) or Masson's trichrome (Polysciences). For H&E staining, sections were submerged in Harris hematoxylin, differentiated in 1% acid alcohol, 'blued' in saturated lithium carbonate, and counterstained in eosin Y solution. For Masson's trichrome staining, sections were incubated in Bouin's fixative (60 min, 60°C) then processed through Weigert's iron hematoxylin, Biebrich Scarlet-

acid Fuchsin, and aniline blue with 1% acetic acid differentiation stains. Sections were rapidly dehydrated to xylene and mounted in DPX for image capture using a Nikon slide scanner.

For analysis of myocyte cross-sectional area, cells within the left ventricle (excluding endocardial regions) were chosen at random and outline traced using NDP.view2 software (Hamamatsu). Only cells with a single nucleus that were clearly in cross-section were included in the analysis. For assessment of fibrosis, 20× images of the entire left ventricle were exported and the collagen fraction calculated as the ratio between the sum of the total area of fibrosis (blue colour) to the sum of the total tissue area (including the myocyte area) for the entire image using Image J. For investigating the pattern of left ventricular fibrosis, images were sub-divided between those which included vessels (for perivascular fibrosis) and those void of vessels (for interstitial fibrosis). All histological and data analysis was performed by independent assessors blinded to treatment groups.

Adult rat heart perfusions: Adult male (300-350 g) Sprague–Dawley rats (Charles River) were anaesthetised with a lethal intraperitoneal dose of Euthatal (pentobarbital sodium, 60 mg/kg). After complete anaesthesia was induced, a saphenous vein was exposed and heparin (1000 U/kg) administered intravenously. The chest cavity was opened and the heart and lungs were removed into modified ice-cold KHBBS (25 mM $NaHCO_3$, 119 mM NaCl, 35 mM KCl, 2.5 mM $CaCl_2$, 1.2 mM $MgSO_4$, 1.2mM KH_2PO_4 equilibrated with 95% O_2/5% CO_2) whilst the heart was still beating. Surrounding tissues were removed from the heart before aortic cannulation and perfusion. Hearts were perfused retrogradely (37°C at 70 mmHg) as described previously (Clerk *et al.*, J. Biol. Chem., (1998), 273:7228-7234) with a 15 min equilibration period with or without dabrafenib (10 μM, Selleck Chemicals). Perfusions were continued for a further 10 min with or without addition of human basic fibroblast growth factor (bFGF, 0.5 μg/ml; Cell Guidance Systems Ltd., UK). Hearts were 'freeze-clamped' between aluminium tongs cooled in liquid nitrogen and pulverized under liquid N_2 in a pestle and mortar. The powders were stored at −80°C.

RNA preparation and qPCR: Total RNA was prepared using RNA Bee (AMS Biotechnology Ltd) with 1 ml per 4×10^6 NRVMs or 10-15 mg mouse heart powder. RNA was prepared according to the manufacturer's instructions, dissolved in nuclease-free water and purity assessed from the A_{260}/A_{280} measured using an Implen NanoPhotometer (values of 1.8–2.1 were considered acceptable). RNA concentrations were determined from the A_{260}

values. Quantitative PCR (qPCR) analysis was performed as previously described (Marshall *et al.*, PLoS One, (2010), 5:e10027). Total RNA (2 µg) was reverse transcribed to cDNA using High Capacity cDNA Reverse Transcription Kits with random primers (Applied Biosystems) according to the manufacturer's instructions. qPCR was performed using an ABI Real-Time PCR 7500 system (Applied Biosystems). Optical 96-well reaction plates were used with iTaq Universal SYBR Green Supermix (Bio-Rad Laboratories Inc.) according to the manufacturer's instructions. Primers were from Invitrogen by Thermo Fisher Scientific or were custom primers from PrimerDesign (*Table 6*). *Gapdh* was used as the reference gene for the study using proprietory primers for rat and mouse from PrimerDesign. Results were normalized to *Gapdh*, and relative quantification was obtained using the ΔCt (threshold cycle) method; relative expression was calculated as $2^{-\Delta\Delta Ct}$, and normalised to vehicle or time 0.

Table 6: qPCR primers

Gene Symbol	Sense Primer (5'→3')	Antisense Primer (5'→3')
Atf3	ACTGGTATTTGAGGATTTTGCTAAC	TGTTGTTGACGGTAACTGACTC
Araf	AGCATCCAGGATCTGTCTGG	ACCTGCATGAGGCTGGAGTC
Braf	GGCCAGGCTCTGTTCAATG	CTCTTTGCTGAAGGGCATCT
Craf	AGTTAGAGCCGAGCGGACTT	ACTCCAAAGCCATTGCTGAT
Col1a1	TCGTGGCTTCTCTGGTCTC	CCGTTGAGTCCGTCTTTGC
Col4a1	CTGGCACAAAAGGGACGAG	ACGTGGCCGAGAATTTCACC
Ctgf	GCACACCGCACAGAACCA	ATGGCAGGCACAGGTCTTG
Ddr2	GCACTTGGTGAATTAATTAGAATCCTG	GGACAACTAAATGGTCCCTCCC
Egr1	GCCTTCGCTCACTCCACTA	GCTGGGATTGGTAGGTGGTA
Fn1	AAGAGGACGTTGCAGAGCTA	AGACACTGGAGACACTGACTAA
IL1b	CAACCAACAAGTGATATTCTCCAT	GGGTGTGCCGTCTTTCATTA
IL11	TGACGGAGATCACAGTCTGGA	CGGAGGTAGGACATCAAGTCTAC
IL6	TCCATCCAGTTGCCTTCTTG	GGTCTGTTGGGAGTGGTATC
Lox	GACATTCGCTACACAGGACAT	AACACCAGGTACGGCTTTATC
Myc	AACAACCGCAAGTGCTCCA	GTTCCTCCTCTGACGTTCCAA
Myh7	GAGATCGAGGACCTGATGG	TCATACTTCTGCTTCCACTCA
Nppa	GATGGATTTCAAGAACCTGCTAGA	CTTCCTCAGTCTGCTCACTCA
Nppb	TCCAGCAGAGACCTCAAAATTC	CAGTGCGTTACAGCCCAAA
Orc2	CGAAAAAGAGTCAAGGT	CCAAGTCACCTGCTTTGT
Postn1	TTCCTCTCCTGCCCTTATATGC	CCTGATCCCGACCCCTGAT
Timp1	TACGCCTACACCCCAGTCAT	GCCCGTGATGAGAAACTCTTC
TNFa	AGCCAGGAGGGAGAACAGA	CAGTGAGTGAAAGGGACAGAAC

Sample preparation for protein analysis: For analysis of protein kinases in total extracts, cells were washed with ice-cold PBS and scraped into 150 µl Buffer A [20 mM β-glycerophosphate (pH 7.5), 50 mM NaF, 2 mM ethylenediamine tetraacetic acid (EDTA), 1% (v/v) Triton X-100, 5 mM dithiothreitol] containing protease and phosphatase inhibitors [10

mM benzamidine, 0.2 mM leupeptin, 0.01 mM trans-epoxy succinyl-l-leucylamido-(4-guanidino)butane, 0.3 mM phenylmethylsulfonyl fluoride, 4 μM microcystin]. Rat or mouse heart powders were extracted in 8 vol (relative to powder weight) Buffer A plus inhibitors. Samples were vortexed and extracted on ice (10 min). Extracts were centrifuged (10,000×g, 4°C) for 5 or 10 min for NRVMs or heart powders, respectively. The supernatants were removed, a sample was taken for protein assay and the rest boiled with 0.33 vol SDS-polyacrylamide gel electrophoresis (SDS-PAGE) sample buffer [0.33 M Tris-HCl pH 6.8, 10% (w/v) SDS, 13% (v/v) glycerol, 133 mM dithiothreitol, 0.2 mg/mL bromophenol blue]. Protein concentrations were determined by BioRad Bradford assay using bovine serum albumin (BSA) standards.

Immunoblot analysis: Proteins were separated by SDS-PAGE on 10% (w/v) polyacrylamide resolving gels with 6% stacking gels, and transferred electrophoretically to nitrocellulose using a BioRad semi-dry transfer cell (10 V, 60 min) as described (Marshall *et al.*, PLoS One, (2010), 5:e10027). Proteins were detected as described by Marshall *et al.* using antibodies as indicated in *Table 7*. Bands were detected by enhanced chemiluminescence using ECL Prime Western Blotting detection reagents with visualisation using an ImageQuant LAS4000 system (GE Healthcare). ImageQuant TL 8.1 software (GE Healthcare) was used for densitometric analysis of the bands.

Table 7: Antibodies used for immunoblotting and immunostaining. CST, Cell Signaling Technologies; SCBT, Santa Cruz Biotechnology Inc.; BD, BD Transduction Labs.

Protein	Source	Cat. no.	Host	Dilution
Phospho-ERK1/2(T202/Y204)	CST	4377	Rabbit	1/1000
Total ERK1/2	CST	4695	Rabbit	1/1000
Total cRaf	BD	610152	Mouse	1/1000
Total BRaf	SCBT	sc-5284	Mouse	1/1000
Total ARaf	SCBT	sc-408	Rabbit	1/500
GAPDH	CST	5174	Rabbit	1/1000
Anti-Mouse immunoglobulins/HRP	Dako	P0260	Rabbit	1/5000
Anti-Rabbit immunoglobulins/HRP	Dako	P0448	Goat	1/5000

Statistical analysis: Data analysis was performed using Microsoft Excel and GraphPad Prism 8.0. Statistical tests used one-way ANOVA with Holm-Sidak post-test or Student t test as indicated (performed using GraphPad Prism 8.0). $p<0.05$ was the minimum level of significance accepted. Statistical analysis was performed using GraphPad Prism 7.0 with two-tailed unpaired t tests, two-tailed one-way ANOVA or two-tailed two-way ANOVA as

indicated. A multiple comparison test was used in combination with ANOVA as indicated. Graphs were plotted with GraphPad Prism 7.0.

Results

1) Cardiomyocyte BRaf is required for cardiac adaptation to hypertension induced by angiotensin II in mice

Activation of cardiomyocyte BRaf promotes hypertrophy (Example 1). To determine if cardiomyocyte BRaf is required for hypertension-induced cardiac hypertrophy, mice with a floxed gene for BRaf knock-out were crossed with mice expressing tamoxifen-inducible Cre regulated by an Myh6 promoter for cardiomyocyte-specific expression, producing mice for inducible cardiomyocyte-specific BRaf knock-out. Male mice homozygous for the floxed BRaf gene and heterozygous for Cre (i.e. $BRaf^{KO/KO}/Cre^{MCM/WT}$) were used. Recombination was induced by a single tamoxifen injection (*Figure 8*). Tamoxifen-treatment of $BRaf^{KO/KO}/Cre^{MCM/WT}$ mice induced a significant decrease in BRaf mRNA and protein (*Figure 9, A-C*). cRaf (not ARaf) protein was also significantly downregulated (discussed below), so the consequences of BRaf knock-out potentially reflect additional loss of cRaf.

$BRaf^{KO/KO}/Cre^{MCM/WT}$ mice were treated without/with tamoxifen, then implanted with minipumps for delivery of 0.8 mg/kg/d AngII. The effects on cardiac function/dimensions were assessed using echocardiography (*Figure 9, D-F*; *Figure 10*). In hearts of $BRaf^{KO/KO}/Cre^{MCM/WT}$ mice that were not tamoxifen-treated, AngII (7 d) significantly increased diastolic and systolic LV posterior wall (PW) and anterior wall (AW) thickness, with some increase in the interventricular septum (IVS). There was some decrease in LV internal diameter (ID), but a significant increase in LVPW:LVID ratio. It was also accompanied by a significant increase in ejection fraction (EF). The increase in LVPW thickness and LVPW/LVID, but not EF or the IVS, was significantly reduced with cardiomyocyte BRaf knock-out following tamoxifen-treatment. Tamoxifen alone did not affect cardiac function/dimensions in $BRaf^{KO/KO}/Cre^{MCM/WT}$ or $BRaf^{WT/WT}/Cre^{MCM/WT}$ mice (*Figures 11 and 12*, respectively). It was concluded that cardiomyocyte BRaf is required for cardiac hypertrophy induced by AngII.

The effects were assessed of cardiomyocyte BRaf knock-out on expression of genes classically associated with hypertrophy (*Figure 13A*). AngII induced expression of *Nppa, Nppb* and *Myh7* mRNAs in hearts from $BRaf^{KO/KO}/Cre^{MCM/WT}$ mice that were not treated with

tamoxifen. The increase in *Nppa* and *Nppb*, but not *Myh7* was inhibited by BRaf knock-out. mRNA expression of the DNA origin of replication protein, *Orc2* (a marker of cellularity), in addition to classic immediate early genes (*Figure 13B*) and cytokines (*Figure 13C*), was increased by AngII within 24 h, for many, this was inhibited in BRaf knockout-out hearts. However, mRNAs for the pro-inflammatory cytokines, IL1β and TNFα, were not inhibited at 7 d, indicative of ongoing inflammation. mRNAs for extracellular matrix proteins and enzymes required for remodelling were upregulated by AngII, though in the absence of any increase in *Ddr2*, a fibroblast marker (*Figure 13, D* and *E*). Interestingly, upregulation of mRNAs for the enzymes (*Lox*, *Timp1*), but not the matrix proteins themselves, was inhibited by BRaf knock-out. Tamoxifen alone did not affect cardiac mRNA expression of the genes studied in $BRaf^{KO/KO}/Cre^{MCM/WT}$ mice (*Figure 14*). Thus, cardiomyocyte BRaf plays a significant role in the cardiac gene expression response to AngII.

To determine the effects of cardiomyocyte BRaf knock-out on AngII-induced cardiac pathology, hearts were fixed and sections stained with H&E or Masson's trichrome. As expected, AngII alone increased interstitial and perivascular fibrosis throughout the heart with some areas of focal damage (*Figure 15*). This was also detected in hearts from mice with cardiomyocyte-specific BRaf knock-out, but these hearts had more extensive focal damage with increased fibrosis and loss of cardiomyocytes. Overall, the data indicate that cardiomyocyte BRaf is required for sustainable adaptation of the heart to hypertension.

2) Dabrafenib acutely inhibits ERK1/2 signalling in perfused adult rat hearts and inhibits AngII-induced cardiac hypertrophy in mice *in vivo*.

Dabrafenib is a Type-1.5 Raf inhibitor that can activate (rather than inhibit) ERK1/2 signalling via the "Raf paradox" in some cancer cells. Data described elsewhere herein (Example 1) showed that ERK1/2 are activated in cardiomyocytes by the Type-1 Raf inhibitor, SB590885, and this promotes hypertrophy. It was determined if dabrafenib activates or inhibits ERK1/2 signalling in Langendorff perfused adult male rat hearts by immunoblotting samples for phosphorylated (activated) ERK1/2. Dabrafenib (5 μM) inhibited basal ERK1/2 phosphorylation and the increase in ERK1/2 phosphorylation induced by FGF2 (*Figure 16*).

In humans, dabrafenib is administered orally at up to 150 mg, twice daily (i.e. ~3-5 mg/kg/d). To assess its effects on cardiac function/dimensions in mice *in vivo*, mice were implanted

with osmotic minipumps for delivery of 3 mg/kg/d dabrafenib or vehicle in the absence/presence of 0.8 mg/kg/d AngII. Cardiac function/dimensions were assessed by echocardiography. Dabrafenib alone had no significant effect on any variable studied (*Figure 17*). In this model (as in $BRaf^{KO/KO}/Cre^{MCM/WT}$ mice, *Figure 9*), AngII alone significantly increased diastolic and systolic LVPW thickness within 3 d, with decreased LVID, producing significant changes in LVPW/LVID ratios indicative of cardiac hypertrophy (*Figure 18, A-C; Figure 19*). These were significantly inhibited by dabrafenib. The increase in EF and FS induced by AngII at 3 d was also inhibited by dabrafenib. At 7 d, the increase in LVPW thickness induced by AngII was still inhibited by dabrafenib (*Figure 18, A, B and D; Figure 19*).

No significant decrease was detected in ERK1/2 signalling in hearts from mice receiving dabrafenib plus AngII compared with AngII alone (*Figure 20A*). However, dabrafenib significantly inhibited the increased expression of *Nppb* induced by AngII at 7 d, but did not affect *Nppa* or *Myh7* (*Figure 20B*). Most of the early genes were no longer upregulated (data not shown), but *Ctgf, IL6, IL1β* and *Tnfα* were all still significantly increased by AngII at 7 d and their expression was inhibited by dabrafenib (*Figure 20C*). Increased expression of fibrosis-associated enzymes and extracellular matrix genes was not significantly inhibited by dabrafenib, but the increase in expression was reduced (*Figure 20C*).

To determine the effects of dabrafenib on AngII-induced hypertrophy at a cellular level, hearts were fixed and sections stained with H&E or Masson's trichrome (*Figure 21, A-D*). AngII increased cardiomyocyte cross-sectional area together with interstitial and perivascular fibrosis. Dabrafenib inhibited the increase in cardiomyocyte size and almost eliminated fibrosis in both interstitial and perivascular regions. Unlike the cardiomyocyte-specific BRaf knockout model (*Figure 15*), there was no increase in focal areas of fibrosis and no obvious cardiomyocyte loss. These effects most likely account for the reduction in cardiac hypertrophy and enhanced function detected by echocardiography (*Figure 18*).

Discussion

This study identifies BRaf as a key component of the cardiomyocyte response to AngII-induced hypertension. Cardiomyocyte BRaf knock-out inhibited cardiac adaptation to AngII (*Figure 9; Figure 10*), resulting in enhanced focal damage with loss of cardiomyocytes and increased connective tissue (*Figure 15*). Cardiomyocyte BRaf knock-out was associated with

loss of cRaf protein (*Figure 9C*), probably because BRaf heterodimerises with cRaf in cardiomyocytes (Example 1), and loss of BRaf presumably destabilized cRaf protein. Of the Raf kinases, BRaf has the greatest MKK1/2-activating activity and this is most likely its main function. However, cRaf (potentially in dimers with BRaf) also inhibits pro-apoptotic kinases, so alternative pathways may contribute to the response. Nevertheless, the data clearly demonstrate that cardiomyocyte BRaf is an essential element required for cardiac adaptation to hypertension. Dabrafenib, a Raf inhibitor used clinically for cancer, also inhibited AngII-induced cardiac hypertrophy (*Figure 18; Figure 19*). In contrast to cardiomyocyte BRaf knock-out, dabrafenib inhibited the increased expression of IL1β and TNFα mRNAs suggesting it had an additive effect to reduce inflammation. Moreover, at a cellular level, dabrafenib inhibited cardiomyocyte hypertrophy and suppressed cardiac fibrosis, while there was no indication of focal damage to the heart (*Figure 21*).

Both models in this study were designed to inhibit BRaf signalling. The difference in response may be explained by the cell-specific nature of the knock-out model in which only the cardiomyocyte response was compromised, compared with a global effect of the inhibitor on all cardiac cells including fibroblasts. Another factor is that the signal is eliminated in genetic model, whilst an inhibitor reduces, rather than abolishes, the signal. Furthermore, dabrafenib may have differential effects in different cell types according to expression of different Raf isoforms. Here, it is a consideration that, unlike proliferating cells, Raf dimers are pre-formed in cardiomyocytes so the cells may respond differently to dabrafenib. A final consideration is potential off-target effects of dabrafenib. No inhibition of ERK1/2 phosphorylation was detected with dabrafenib (*Figure 20A*), so it is not certain that any of its effects are mediated via the canonical BRaf→ERK1/2 pathway. However, the inhibitory effects of dabrafenib on *NppB, Ctgf* and *IL6* mRNA expression (genes for which ERK1/2 signalling is often required) suggest there was inhibition of the signal even though it may be below the level of sensitivity by immunoblotting.

Other studies suggest that ERK1/2 signalling in cardiac fibroblasts contributes to cardiac fibrosis. For example, miR-21 downregulation of Spry1 increases ERK1/2 activity in fibroblasts that enhances cardiac fibrosis. Given the role of ERK1/2 signalling in promoting cell proliferation, it is perhaps not unexpected that the pathway should promote proliferation of cardiac fibroblasts and, thus, fibrosis. However, no increase was detected in expression of *Ddr2* mRNA (a fibroblast marker) with AngII and there was no effect of dabrafenib. IL11

also promotes extracellular matrix production from cardiac fibroblasts via ERK1/2, acting in a post-transcriptional manner. Although an early increase was detected in IL11 (24 h) with AngII in these studies of cardiomyocyte BRaf knock-out (*Figure 13C*), this was largely absent by 7 d, and no change was detected in IL11 mRNA expression in this study of dabrafenib (*Figure 20C*), so it seems unlikely that IL11 plays a significant role, at least in the early phase of the response to AngII.

It has to be considered that the effects of dabrafenib may be due to inhibition of non-ERK1/2 signalling downstream of a BRaf/cRaf heterodimer (discussed above) together with an alternative input into MKK1/2→ERK1/2 (discussed below). Alternatively, it could reflect an off-target effect such as the pro-apoptotic kinase, RIPK3, that is inhibited by dabrafenib at high concentrations. Further studies with different Raf inhibitors are warranted. Here, it is notable that the cancer field has moved towards development of a different class of inhibitor, Type 2 inhibitors (e.g. PLX8394) that bind exclusively to an inactive conformation of the kinase and are viewed as Raf paradox-breakers.

This study has focused only on the early changes in the heart induced by hypertension (3-7 d; *Figure 18*). At 3 d, the heart had largely compensated for additional workload with an increase in LVPW and an associated decrease in LVID with concomitant increase in EF. By 7 d, the response to AngII is already be changing compared with 3 d in that the EF and FS had normalised. Interestingly, EF and FS increased by 7 d in the mice treated with AngII plus dabrafenib.

The data suggest that drugs targeting Raf kinases may be therapeutically useful for reducing cardiac fibrosis (*Figure 21*). However, many cancer therapies, including protein kinase inhibitors, exhibit cardiotoxicity. This applies to drugs that target the ERK1/2 cascade below Raf kinases at the level of MKK1/2 (trametinib, cobimetinib, selumetinib). Trametinib, alone or in combination with dabrafenib, causes hypertension in up to 26% of patients with decreased EF in 7-11% of patients. Meta-analysis of phase II/III trials of selumetinib (an alternative MKK1/2 inhibitor), trametinib and cobimetinib identified increased risk of hypertension and reduced EF with all drugs, establishing that these are on-target effects. Interestingly, similar cardiotoxicity has not been reported for dabrafenib monotherapy. The reasons may relate to the existence of additional inputs into the MKK1/2→ERK1/2 signal such that cardiomyocyte survival is not compromised to the same degree as inhibiting at the level of MKK1/2. In other cells, Cot/Tpl2 (expressed in cardiomyocytes) activates MKK1/2

in some circumstances and is particularly implicated in the inflammatory response. Additionally, α_1-adrenergic agonists (e.g. phenylephrine) and oxidative stress appear to use an alternative input to MKK1/2 in cardiomyocytes rather than Ras-associated Raf kinases, that seems to require phosphoinositide 3' kinase. Indeed, as discussed above, this could be why no significant decrease was detected in ERK1/2 phosphorylation in hearts from mice treated with dabrafenib. Whilst there is no evidence that dabrafenib alone is cardiotoxic, there are side effects which are generally managed by dose reduction. The most severe effect is probably an increase in cutaneous squamous cell carcinoma (~12% of patients). Thus, if dabrafenib were to be used as a therapy for cardiac fibrosis, it may be important to consider dosage monitoring and whether patients have a predisposition for other diseases.

In summary, the data demonstrate that BRaf plays a significant role in cardiac adaptation to AngII-induced hypertension. However, targeting Raf kinases in general with inhibitors such as dabrafenib may be a viable therapeutic option for reducing cardiac hypertrophy and fibrosis in hypertension.

Example 3 – SB590885 and AngII-induced hypertension

The effects of 0.5 mg/kg/d SB590885 on cardiac adaptation induced by 0.8 mg/kg/d AngII (7 d) were assessed using minipumps for delivery of each drug or the relevant vehicle. SB590885 in the presence of AngII significantly increased ejection fraction (EF) and fractional shortening (FS) relative to vehicle only controls or AngII alone (*Figure 22*). However, SB590885 did not significantly affect the changes in systolic or diastolic left ventricle (LV) internal diameter (ID) or posterior wall (PW) thickness or the LVPW/LVID ratio.

Example 4 – effects of vemurafenib and encorafenib on the heart

The effects of vemurafenib and encorafenib (Type 1.5 BRaf inhibitors) on the heart, in addition to the Type 2 Raf inhibitor PLX7904 (related to PLX8394) on the cardiomyocytes were studied and compared with dabrafenib. The concentration-dependency of dabrafenib for inhibition of basal ERK1/2 phosphorylation (i.e. activation) in rat neonatal cardiomyocytes showed significant inhibition at 10 μM but not with lower concentrations (*Figure 23*). Vemurafenib inhibited basal ERK1/2 phosphorylation in cardiomyocytes at 10-30 μM (*Figure 23B*). PLX7904 was most effective at inhibiting basal ERK1/2 phosphorylation at 10 μM, but lower concentrations tested (from 1 nM) had some inhibitor

effect (*Figure 23C*). The inhibitors were tested against hypertrophic agonists, endothelin-1 (ET-1, 100 nM) or the α_1-adrenergic agonist A61603 (50 nM) and all inhibited ERK1/2 phosphorylation (*Figure 23D*).

CLAIMS

1. A compound which is N-{3-[5-(2-amino-4-pyrimidinyl)-2-(1,1-dimethylethyl)-1,3-thiazol-4-yl]-2-fluorophenyl}-2,6-difluorobenzenesulfonamide, or a pharmaceutically acceptable salt thereof, for use in the treatment or prevention of fibrosis in a patient.

2. A compound for use according to claim 1, for use in the treatment or prevention of fibrosis by inhibiting Raf activity, preferably BRaf activity.

3. A compound for use according to claim 1 or 2, wherein the patient does not have a BRaf genetic mutation, and preferably does not have any Raf mutation.

4. A compound for use according to any one of claims 1 to 3, wherein the fibrosis is cardiac fibrosis.

5. A compound for use according to any one of claims 1 to 3, wherein the fibrosis is kidney fibrosis.

6. A compound for use according to any one of claims 1 to 3, wherein the fibrosis is liver fibrosis.

7. A compound for use according to any one of claims 1 to 3, wherein the fibrosis is pulmonary fibrosis.

8. A compound for use according to any one of claims 1 to 3, wherein the fibrosis is muscular fibrosis.

9. A compound for use according to claim 4, wherein the patient is susceptible to, or suffering from, hypertension.

10. A compound for use according to claim 4, wherein the patient is susceptible to, or suffering from, heart failure.

11. A compound for use according to claim 4, wherein the patient is susceptible to, or suffering from, cardiac hypertrophy.

12. A compound for use according to claim 6, wherein the patient is susceptible to, or suffering from, non-alcoholic steatohepatitis.

13. A compound for use according to claim 8, wherein the patient is susceptible to, or suffering from, muscular dystrophy.

14. Use of a compound which is N-{3-[5-(2-amino-4-pyrimidinyl)-2-(1,1-dimethylethyl)-1,3-thiazol-4-yl]-2-fluorophenyl}-2,6-difluorobenzenesulfonamide, or a pharmaceutically acceptable salt thereof, in the manufacture of a medicament for the treatment or prevention of fibrosis as defined in any one of claims 1 to 2 and 4 to 8 in a patient as defined in any one of claims 1, 3 and 9 to 13.

15. A method for the treatment or prevention of fibrosis as defined in any one of claims 1 to 2 and 4 to 8 in a patient as defined in any one of claims 1, 3 and 9 to 13, which method comprises administering to the patient a compound which is N-{3-[5-(2-amino-4-pyrimidinyl)-2-(1,1-dimethylethyl)-1,3-thiazol-4-yl]-2-fluorophenyl}-2,6-difluorobenzenesulfonamide, or a pharmaceutically acceptable salt.

16. A compound which is a Raf inhibitor, or a pharmaceutically acceptable salt thereof, for use in the treatment or prevention of fibrosis in a patient.

17. A compound for use according to claim 16, wherein the patient does not have a BRaf genetic mutation, and preferably does not have any Raf mutation.

18. A compound for use according to claim 16 or 17, wherein the fibrosis is cardiac fibrosis.

19. A compound for use according to claim 16 or 17, wherein the fibrosis is kidney fibrosis, liver fibrosis, pulmonary fibrosis, or muscular fibrosis.

20. A compound for use according to claim 18, wherein the patient is susceptible to, or suffering from, hypertension.

21. A compound for use according to claim 18, wherein the patient is susceptible to, or suffering from, heart failure.

22. A compound for use according to claim 18, wherein the patient is susceptible to, or suffering from, cardiac hypertrophy.

23. A compound for use according to claim 19, wherein the patient is susceptible to, or suffering from, non-alcoholic steatohepatitis or muscular dystrophy.

25. Use of a compound which is a Raf inhibitor, or a pharmaceutically acceptable salt thereof, in the manufacture of a medicament for the treatment or prevention of fibrosis as defined in any one of claims 16 and 18 to 19 in a patient as defined in any one of claims 16, 17 and 20 to 23.

26. A method for the treatment or prevention of fibrosis as defined in any one of claims 16 and 18 to 19 in a patient as defined in any one of claims 16, 17 and 20 to 23, which method comprises administering to the patient a compound which is a Raf inhibitor, or a pharmaceutically acceptable salt.

Fig. 1A

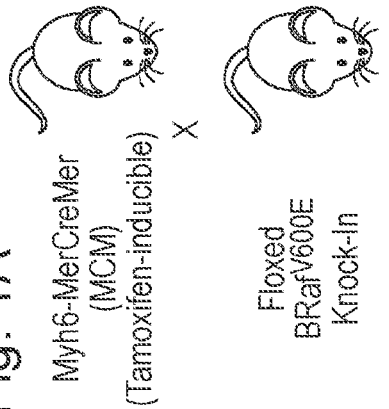

Fig. 1B

Fig. 1C

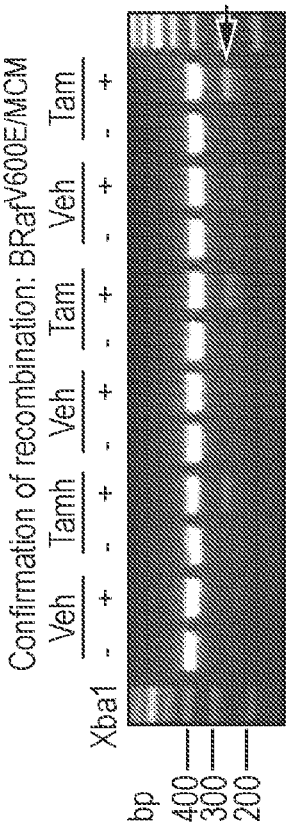

Fig. 1D

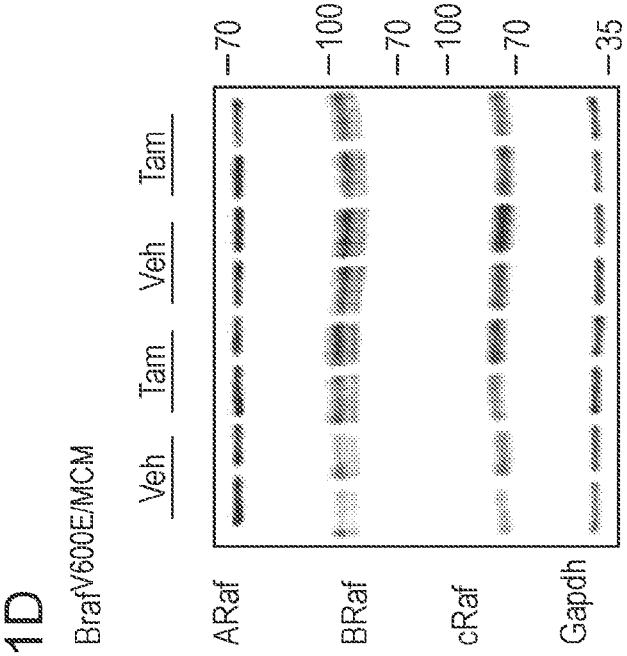

Fig. 2A

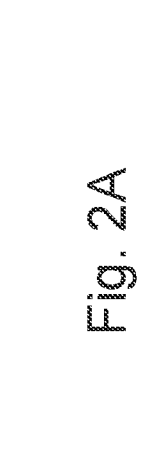

Fig. 2B

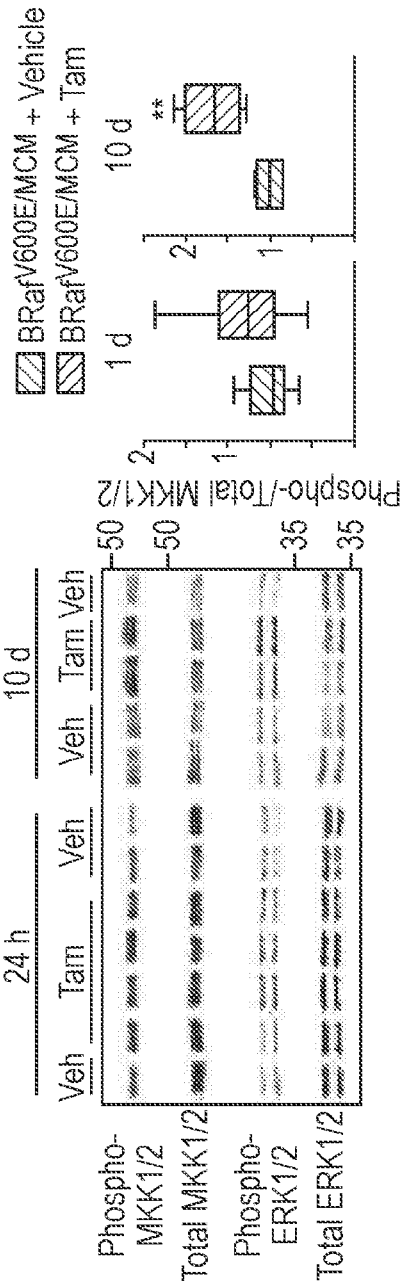

Fig. 2C

Fig. 2D

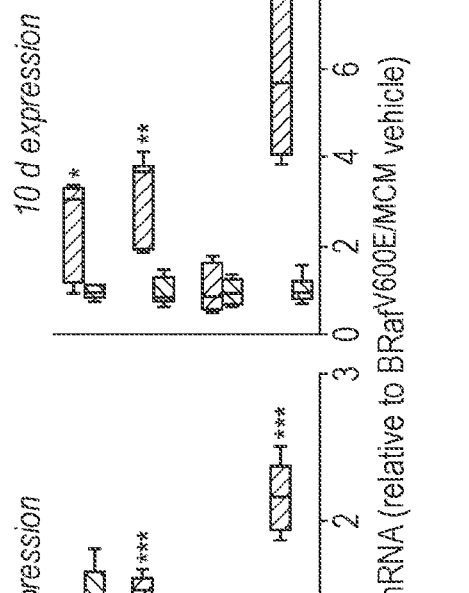

Fig. 2E

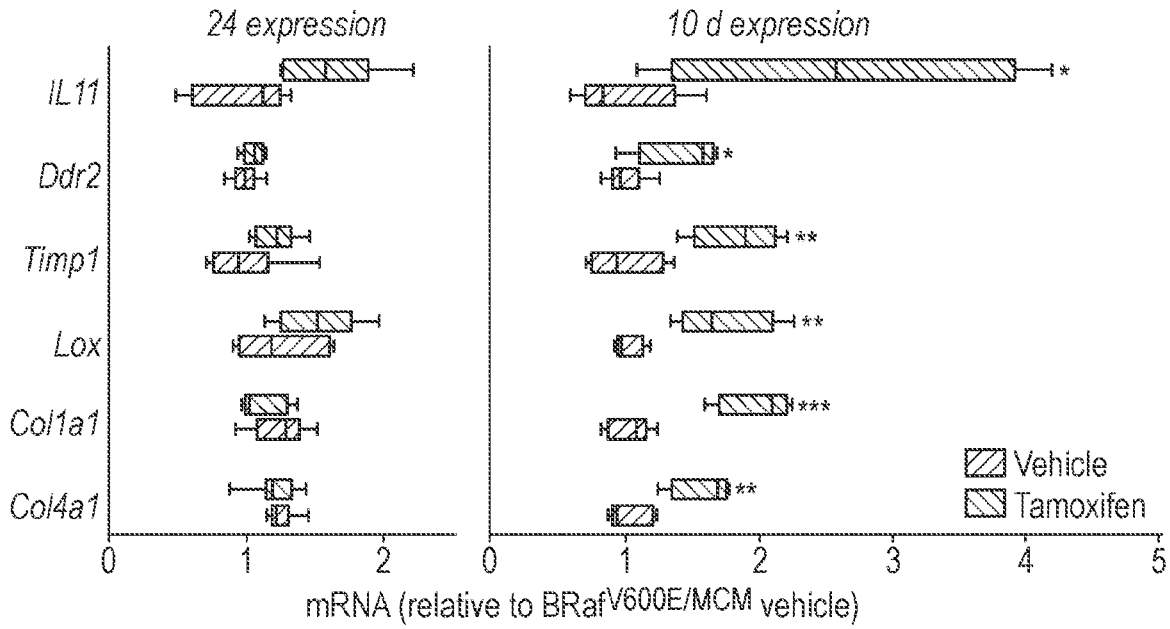
24 expression
10 d expression
IL11
Ddr2
Timp1
Lox
Col1a1
Col4a1
*
*
**
**
***
**
Vehicle
Tamoxifen
0
1
2
0
1
2
3
4
5
mRNA (relative to BRafV600E/MCM vehicle)

Fig. 3A

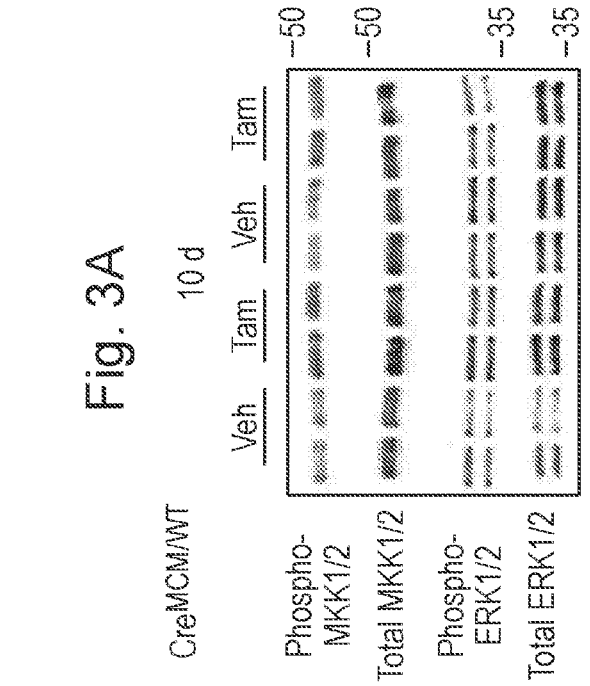
CreMCM/WT
10 d
Veh
Tam
Veh
Tam
Phospho-MKK1/2
Total MKK1/2
Phospho-ERK1/2
Total ERK1/2
50
50
35
35
Phospho-/Total MKK1/2
Phospho-/Total ERK1/2
Veh
Tam
Veh
Tam

Fig. 3B

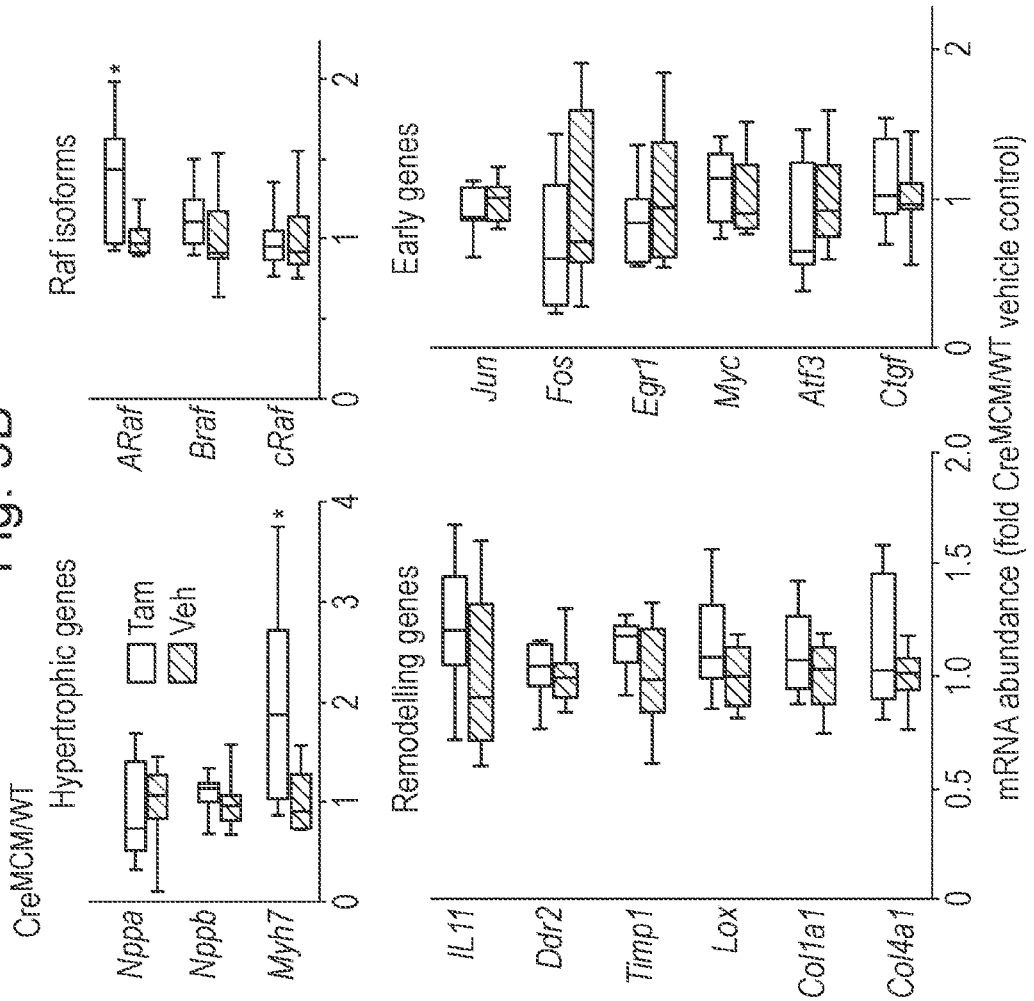
CreMCM/WT
Hypertrophic genes
Tam
Veh
Nppa
Nppb
Myh7
Remodelling genes
Il11
Ddr2
Timp1
Lox
Col1a1
Col4a1
Raf isoforms
ARaf
Braf
cRaf
Early genes
Jun
Fos
Egr1
Myc
Atf3
Ctgf
mRNA abundance (fold CreMCM/WT vehicle control)

Fig. 3C

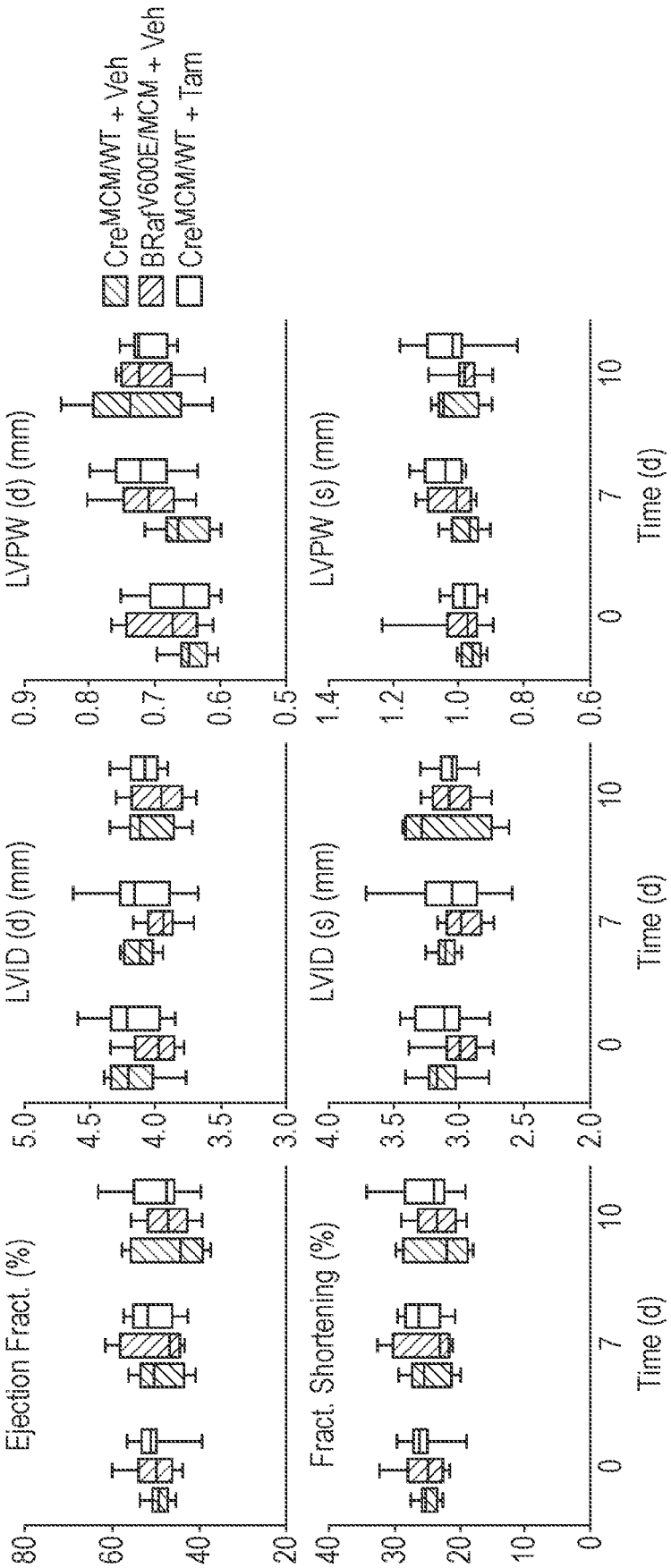
CreMCM/WT + Veh
BRafV600E/MCM + Veh
CreMCM/WT + Tam
Ejection Fract. (%)
Fract. Shortening (%)
LVID (d) (mm)
LVID (s) (mm)
LVPW (d) (mm)
LVPW (s) (mm)
Time (d)

Fig. 4A

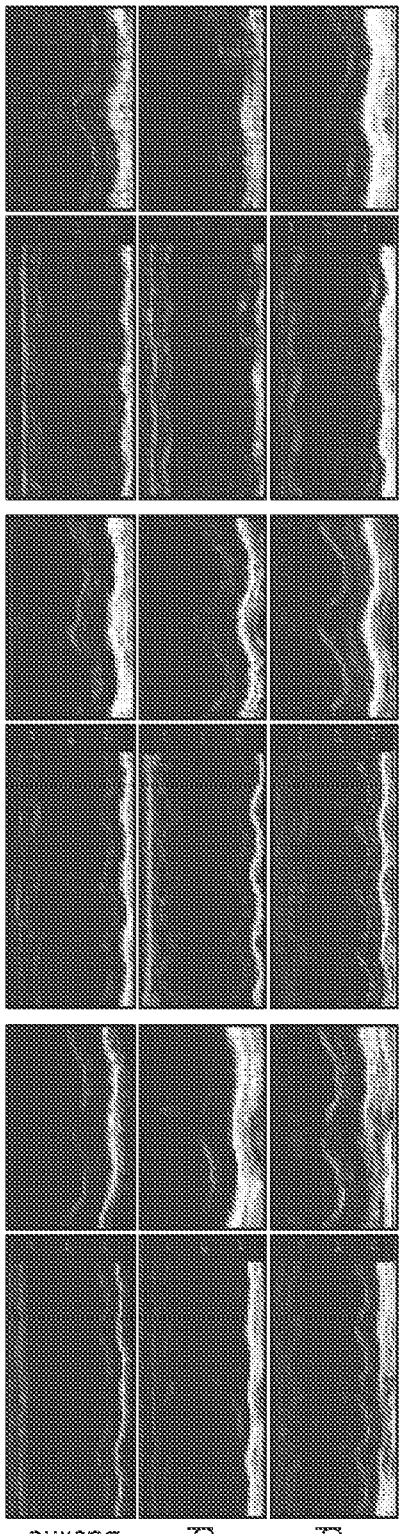
BRafV600E/MCM + Veh
BRafV600E/MCM + Tam
CreBRafV600E/MCM + Tam
Basline
7 d
10 d

Fig. 4B

BRafV600E/MCM + Veh
BRafV600E/MCM + Tam
CreMCM/WT + Tam
Ejection fraction (%)
Fractional shortening (%)
LVID (d) (mm)
LVID (s) (mm)
LVPW (d) (mm)
LVPW (s) (mm)
LVPW/LVID (d)
LVPW/LVID (s)
BL
7 d
10 d

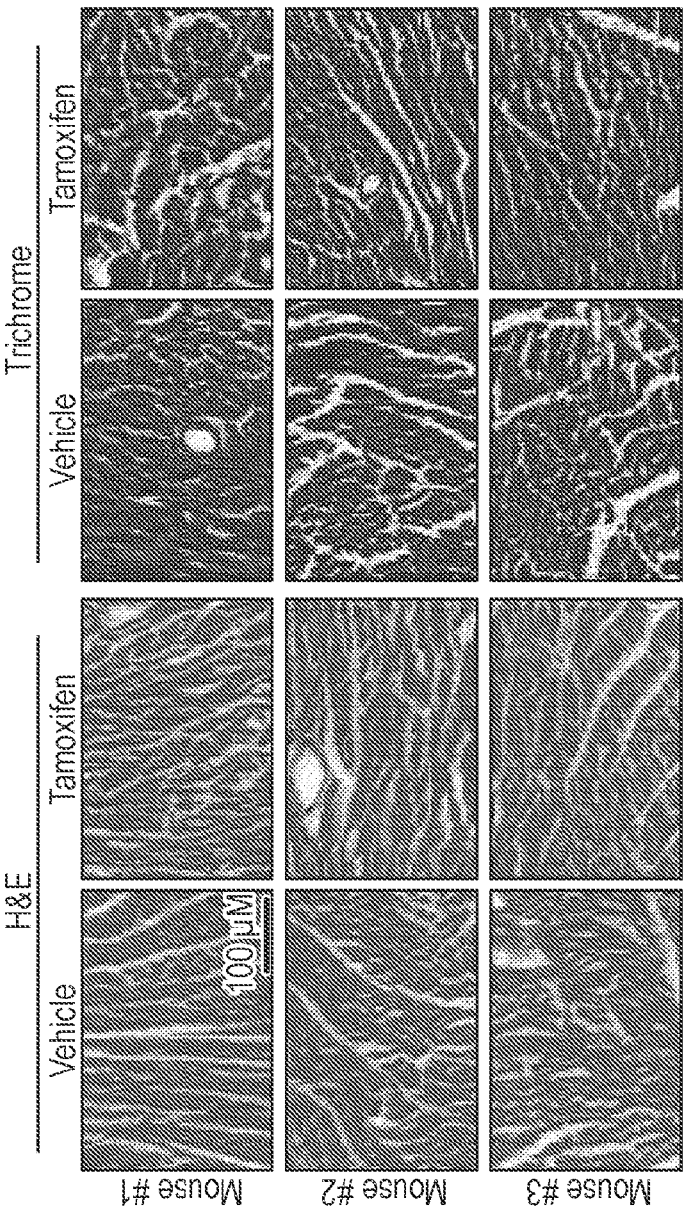

Fig. 4C

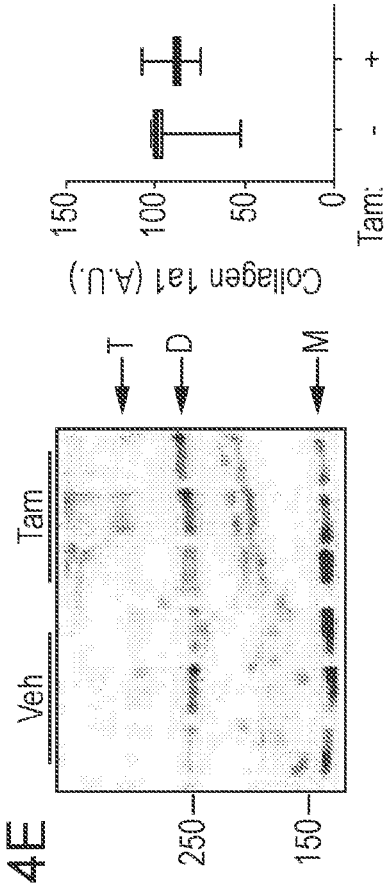

Fig. 4E

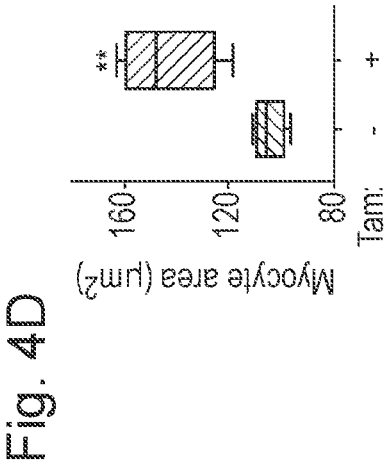

Fig. 4D

Fig. 5A

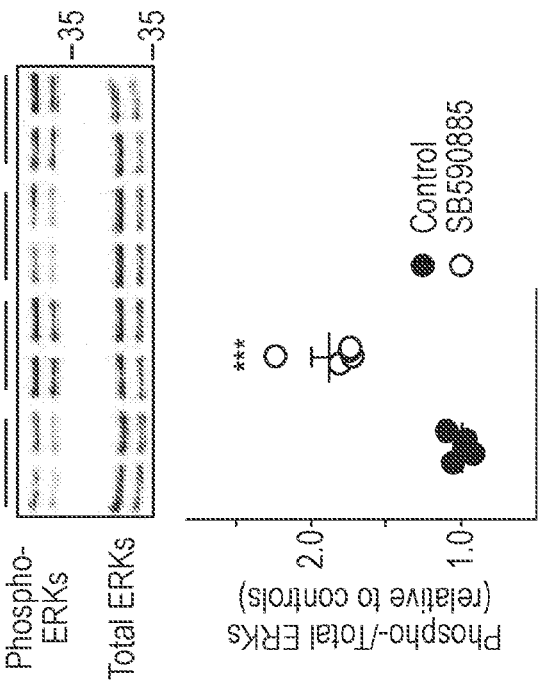

Fig. 5B

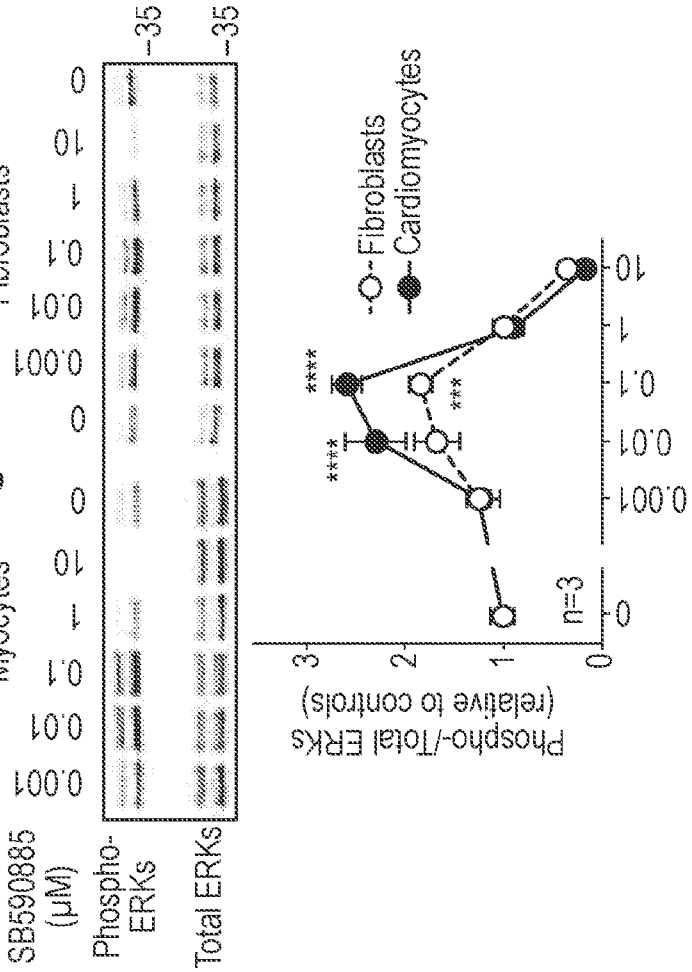

Fig. 5C

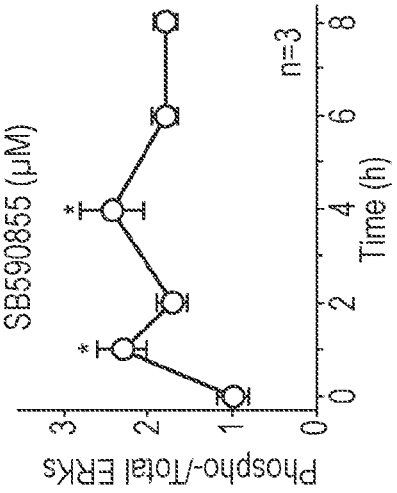

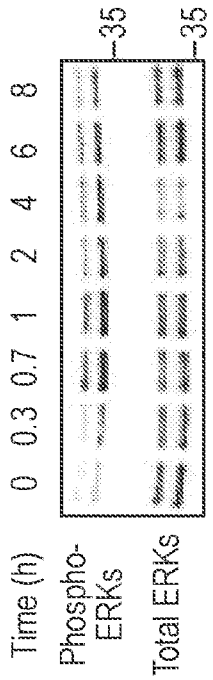

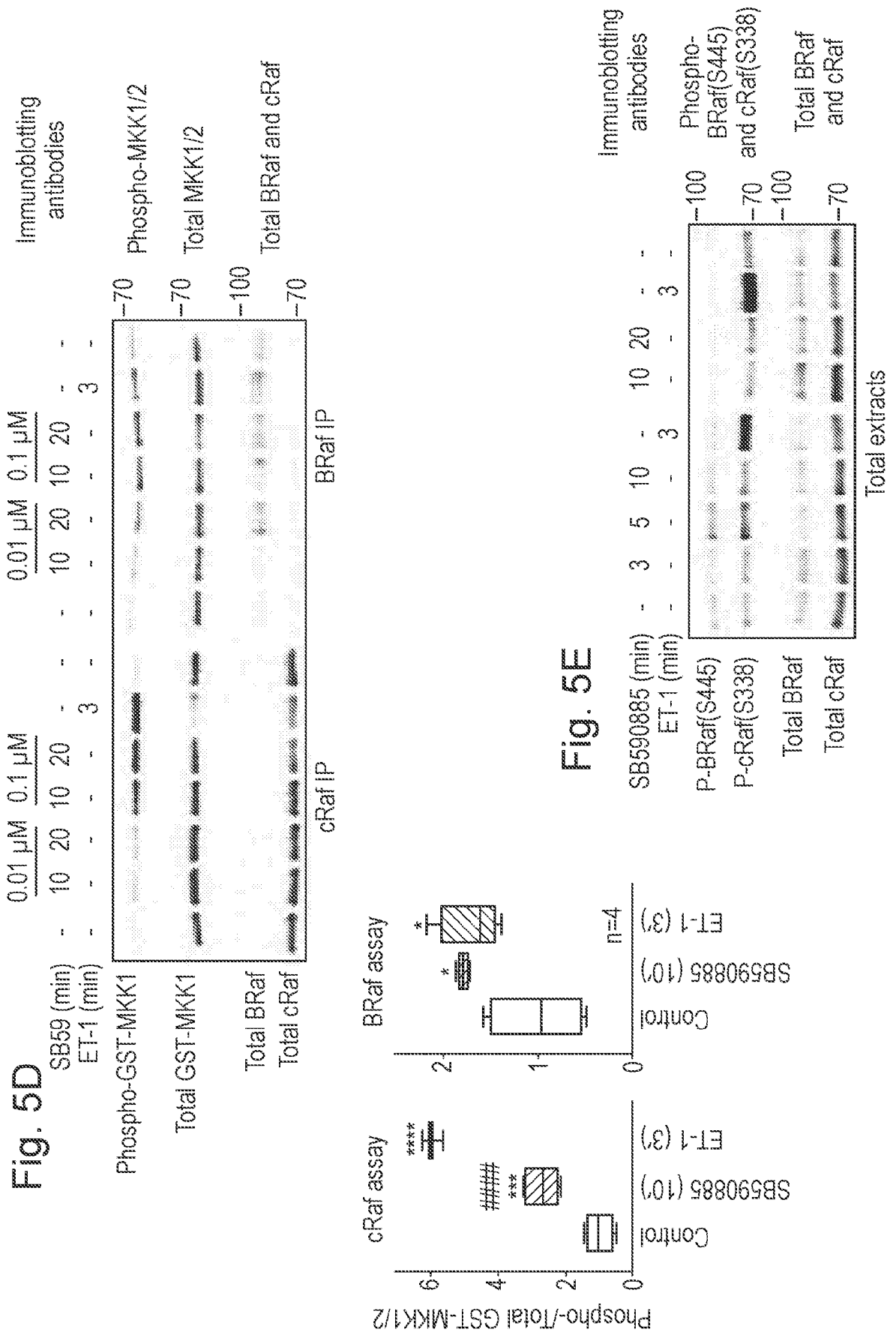
Fig. 5D
SB59 (min) - 0.01 µM 0.1 µM 0.01 µM 0.1 µM
ET-1 (min) - 10 20 10 20 - - 10 20 10 20 - -
3 - - - - 3 - -
Phospho-GST-MKK1
Total GST-MKK1
Total BRaf
Total cRaf
cRaf IP
BRaf IP
Immunoblotting antibodies
Phospho-MKK1/2
Total MKK1/2
Total BRaf and cRaf
70
70
100
70
cRaf assay
BRaf assay
Phospho-/Total GST-MKK1/2
Control
SB590885 (10')
ET-1 (3')
n=4
Fig. 5E
SB590885 (min) - 3 5 10 - 10 20 - -
ET-1 (min) - - - - 3 - - 3 -
P-BRaf(S445)
P-cRaf(S338)
Total BRaf
Total cRaf
Total extracts
Immunoblotting antibodies
Phospho-BRaf(S445) and cRaf(S338)
Total BRaf and cRaf
100
70
100
70

Fig. 6A

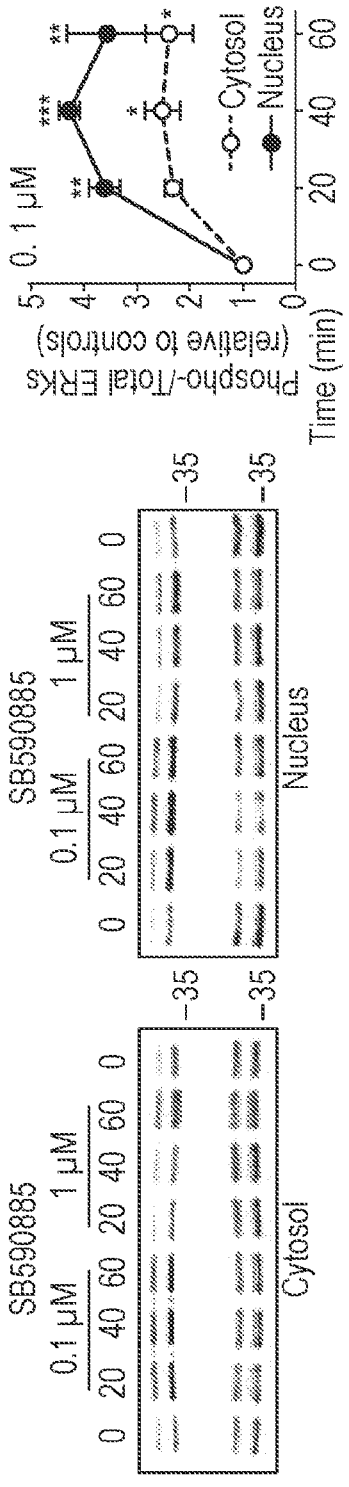

Fig. 6B

Fig. 6C

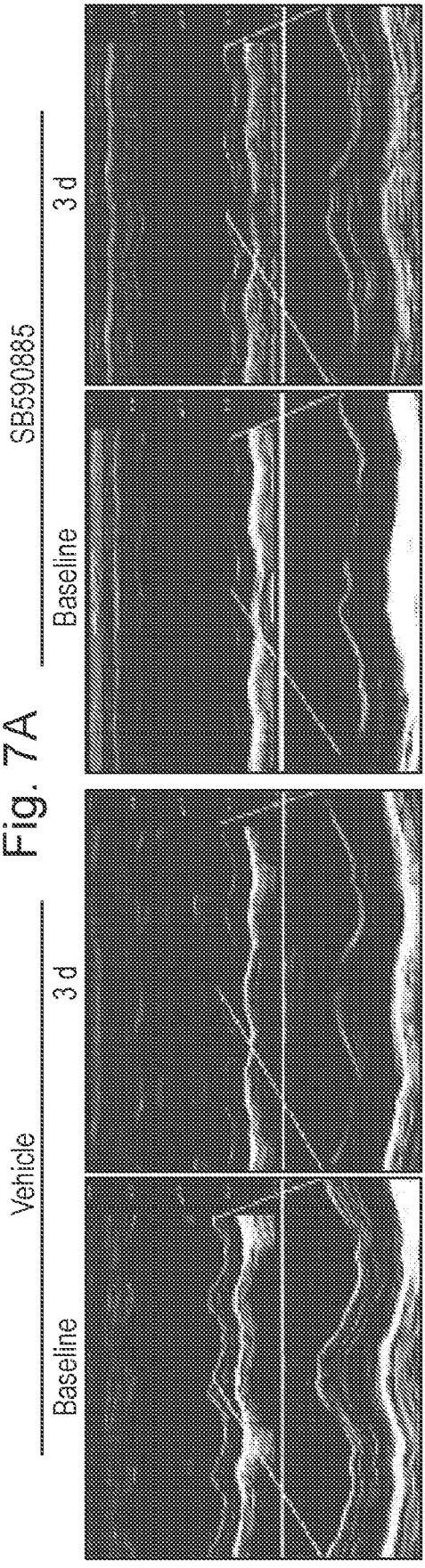
Vehicle
SB590885
Baseline
3 d
Baseline
3 d

Fig. 7A

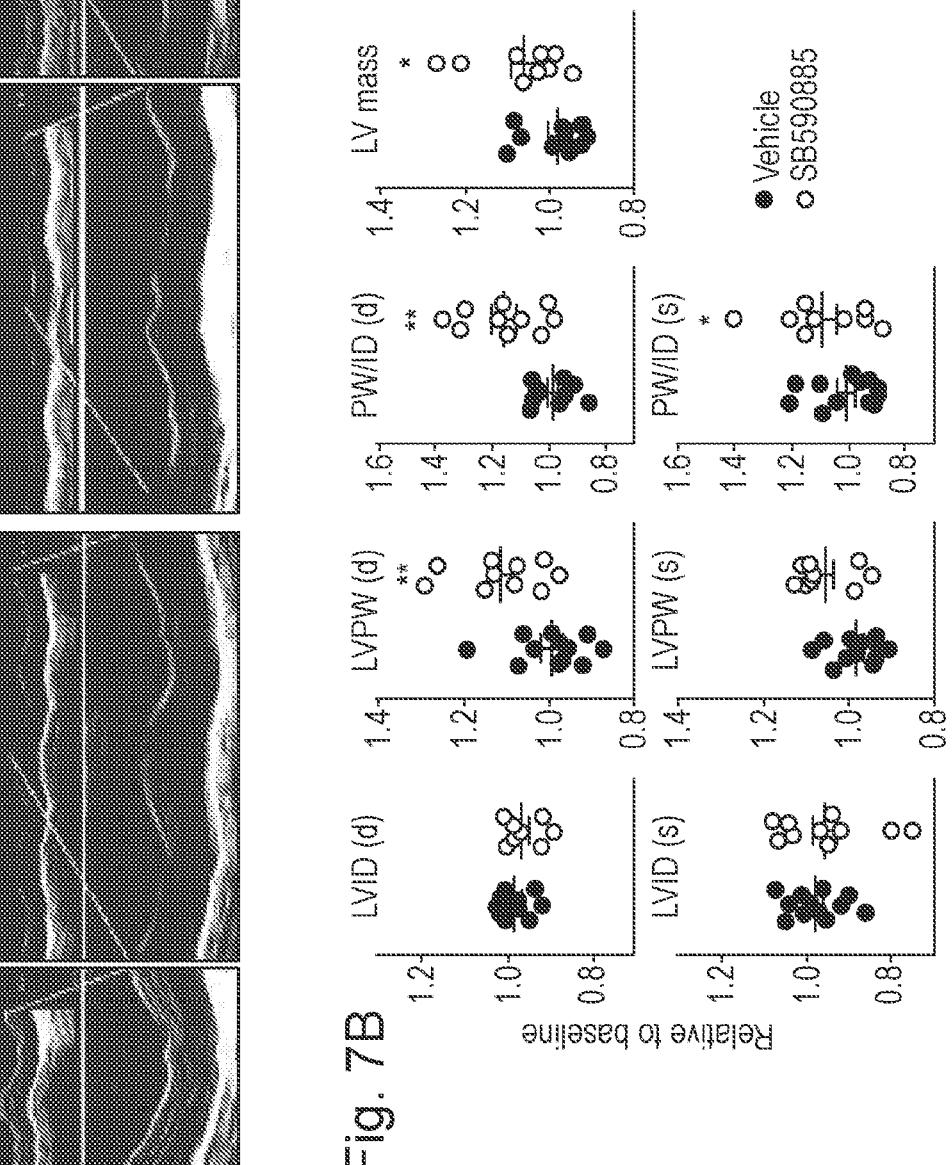
LVID (d)
LVID (s)
LVPW (d)
LVPW (s)
PW/ID (d)
PW/ID (s)
LV mass
Relative to baseline
Vehicle
SB590885

Fig. 7B

Fig. 7C

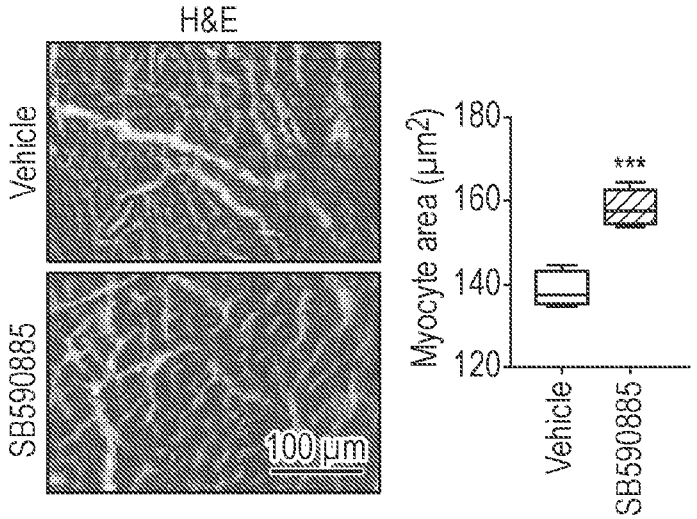
H&E
Vehicle
SB590885
100µm
Myocyte area (µm2)
180
160
140
120
***
Vehicle
SB590885

Fig. 7D

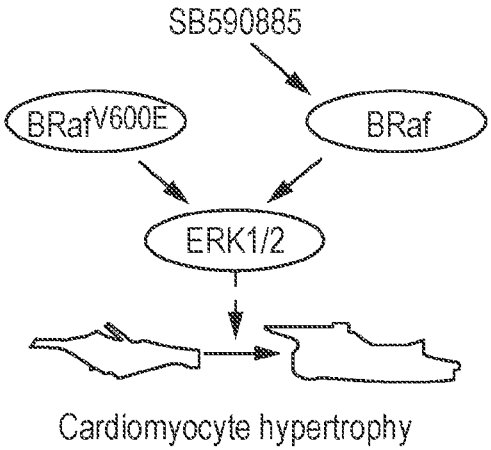
SB590885
BRafV600E
BRaf
ERK1/2
Cardiomyocyte hypertrophy

Fig. 8A

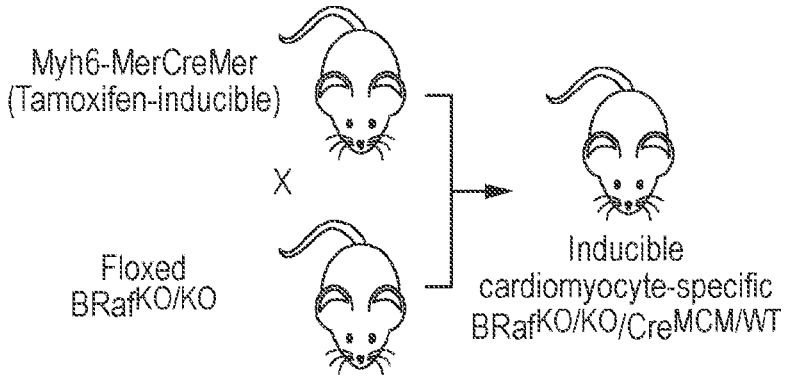

Fig. 8B

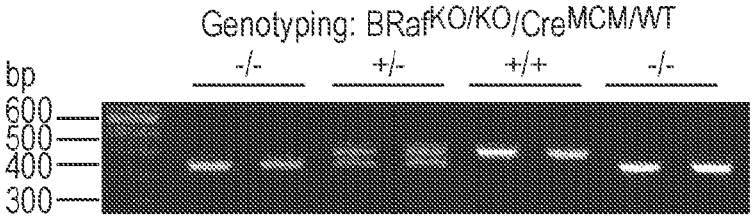

Fig. 8C

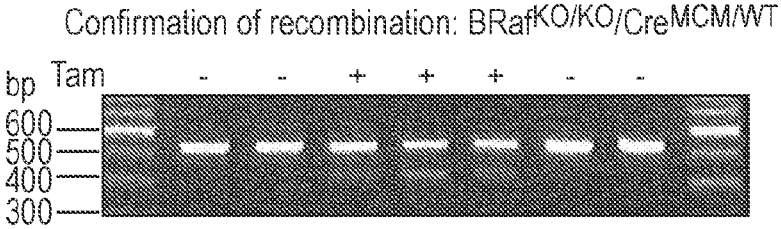


Fig. 9A
BRafKO/KO/CreMCM/WT
AngII (0 d)
Tam (-3 d)
Sacrifice
(1 or 7 d)
Fig. 9B
4 d post-tamoxifen
mRNA (relative to control)
Control
Tamoxifen
ARaf
BRaf
CRaf
Fig. 9C
10 d post-tamoxifen
Con
Tam
Con
Tam
Con
ARaf
BRaf
cRaf
Gapdh
70
100
70
35
Protein (fold control)
Control
Tamoxifen
ARaf
BRaf
CRaf

Fig. 9D
Baseline
7 d
Control
AngII
Tam/AngII
Fig. 9E
7 d

Fig. 9F

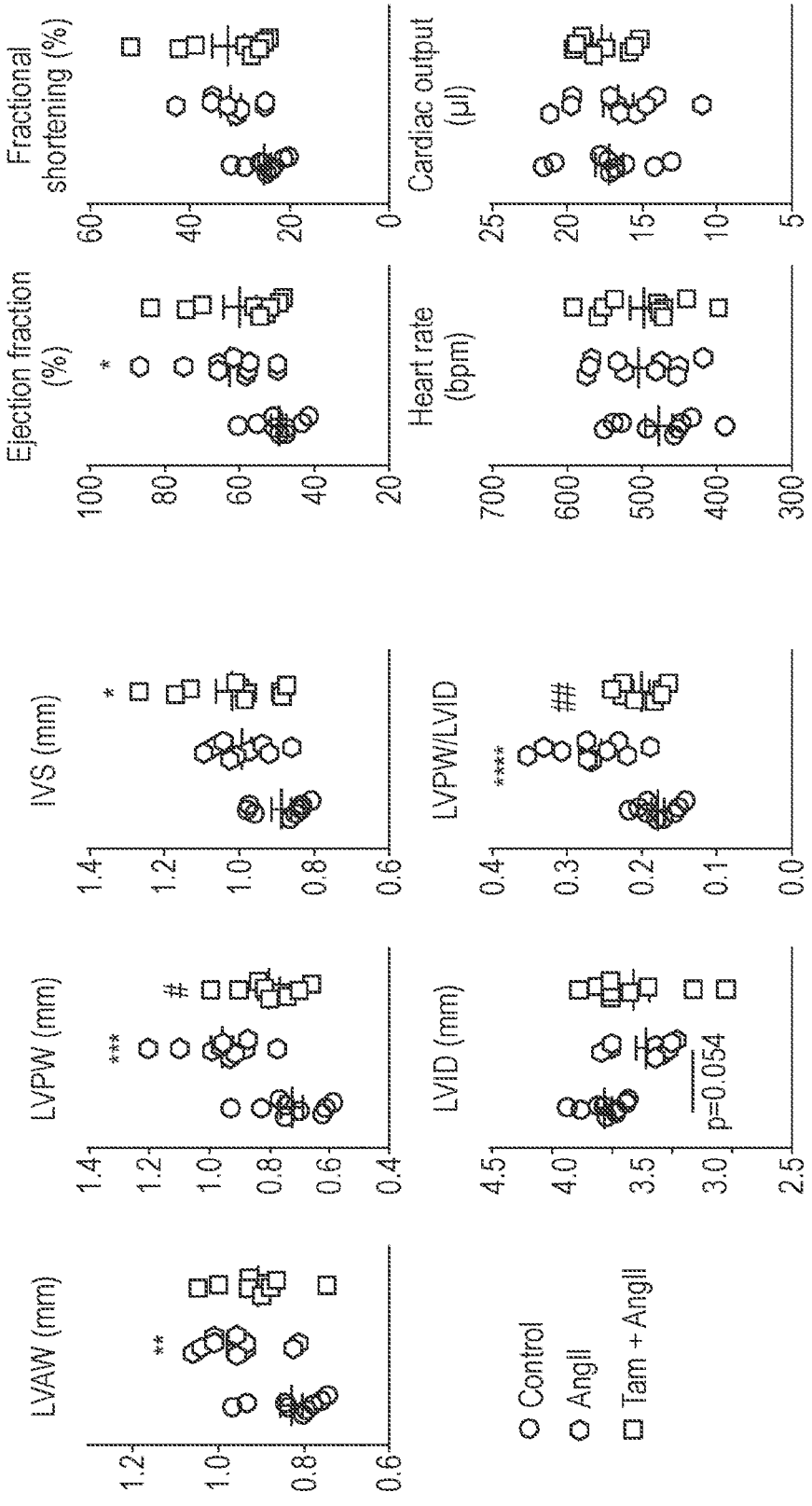
Fractional shortening (%)
Cardiac output (µl)
Ejection fraction (%)
Heart rate (bpm)
IVS (mm)
LVPW/LVID
LVPW (mm)
LVID (mm)
LVAW (mm)
p=0.054
Control
AngII
Tam + AngII

Fig. 10

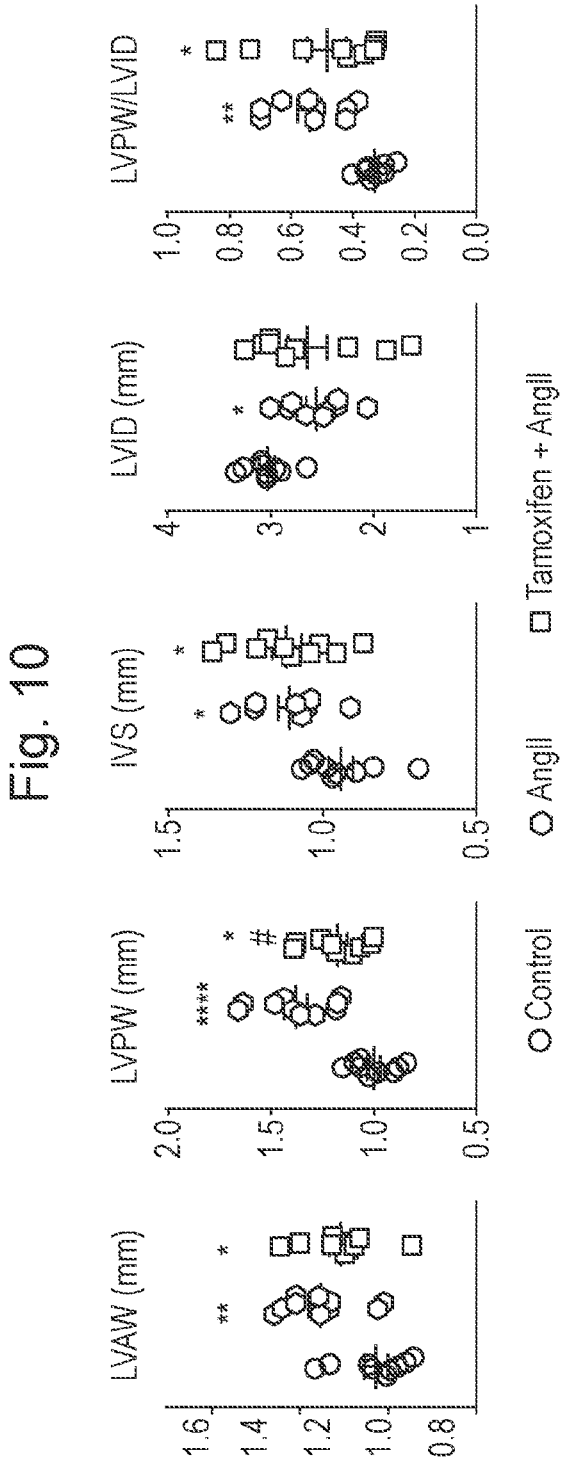
LVAW (mm)
LVPW (mm)
IVS (mm)
LVID (mm)
LVPW/LVID
Control
AngII
Tamoxifen + AngII

Fig. 11A

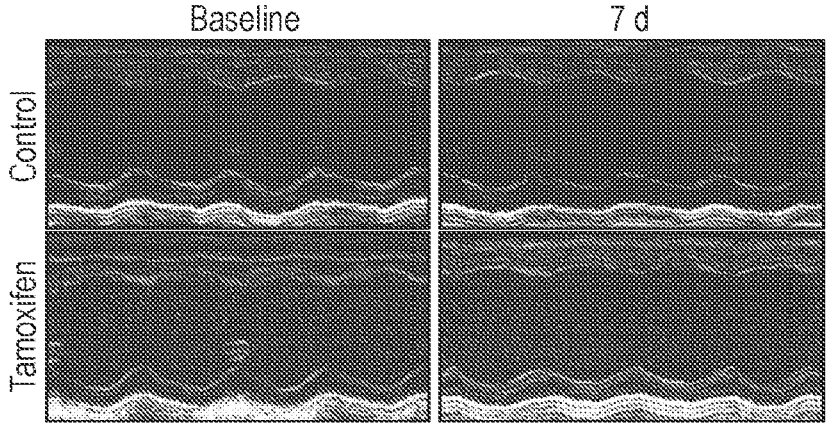

Fig. 11B

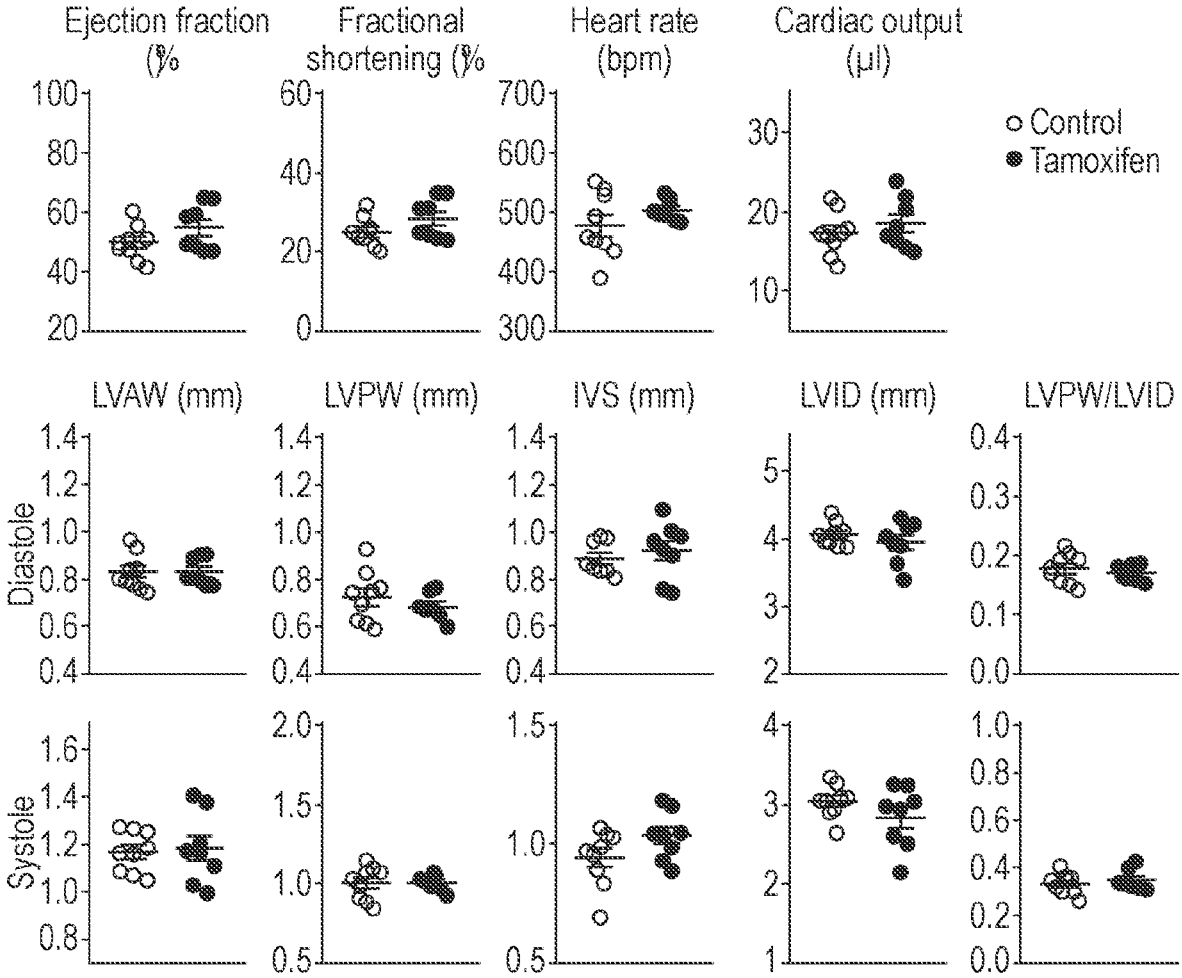

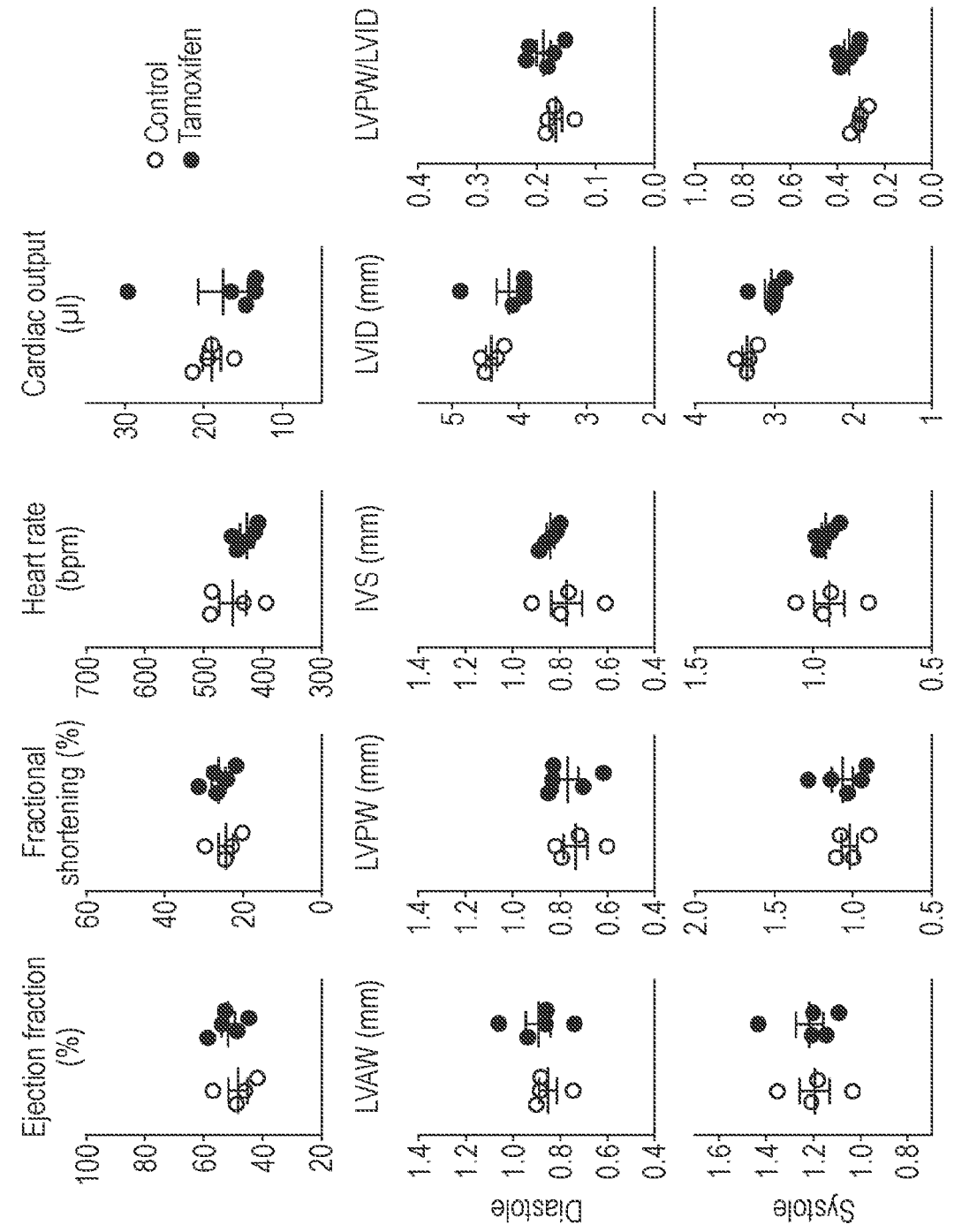
Control
Tamoxifen
Ejection fraction (%)
Fractional shortening (%)
Heart rate (bpm)
Cardiac output (µl)
LVAW (mm)
LVPW (mm)
IVS (mm)
LVID (mm)
LVPW/LVID
Diastole
Systole

Fig. 12

Fig. 13A

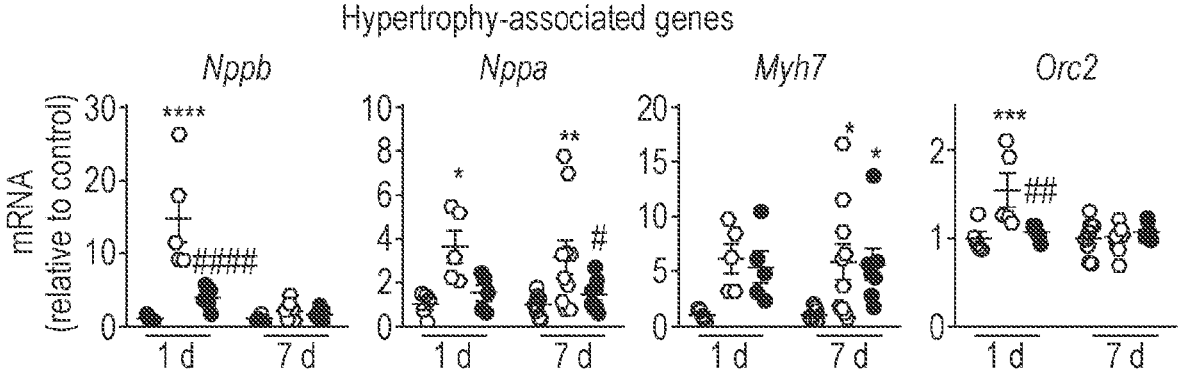

Fig. 13B

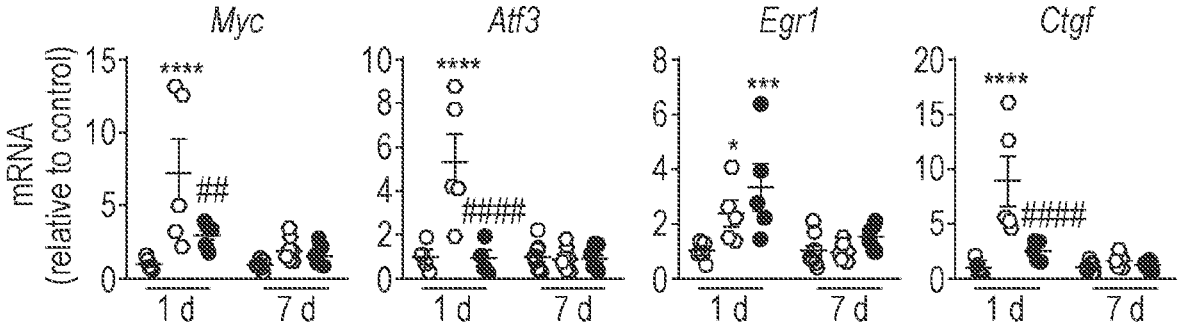

Fig. 13C

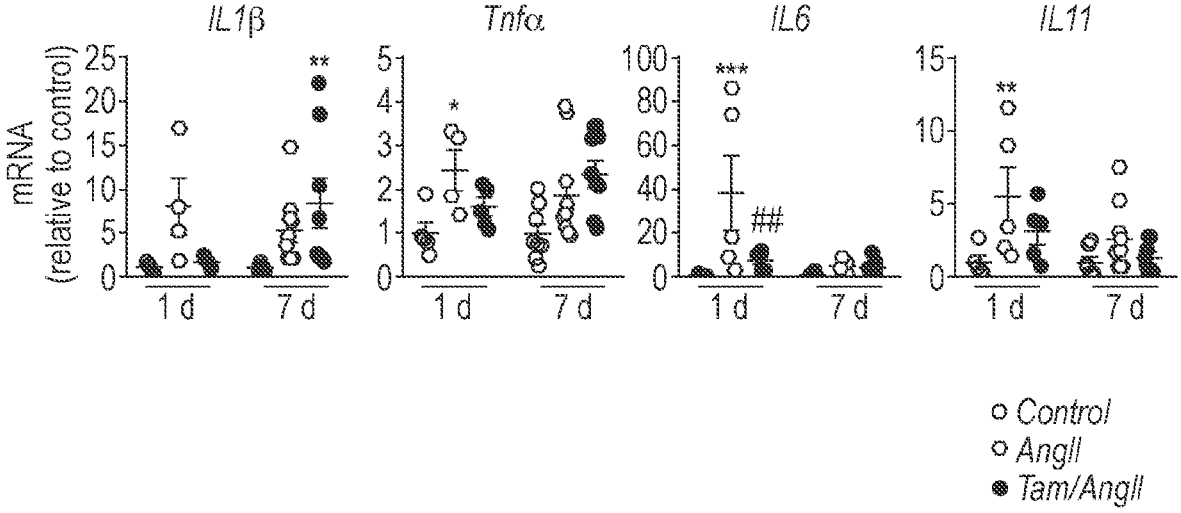

Fig. 13D

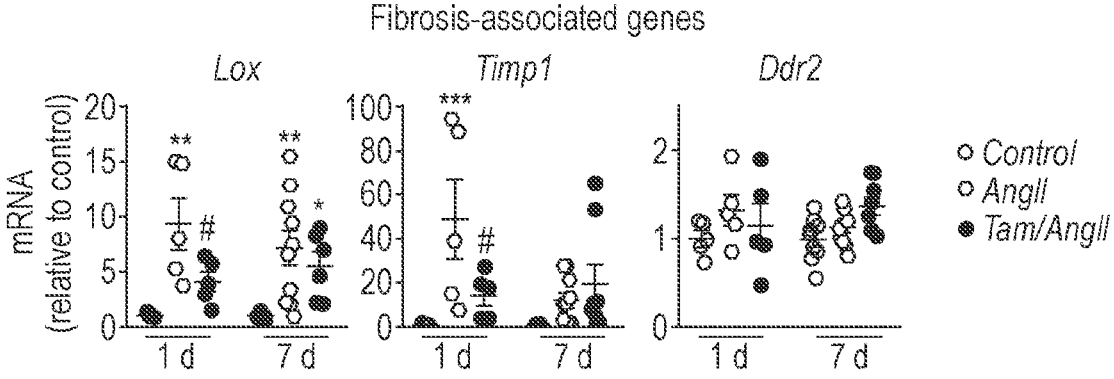

Fig. 13E

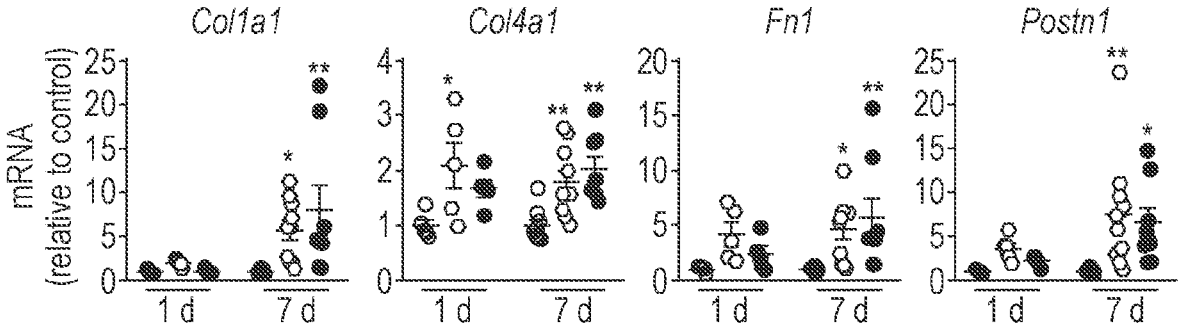

Fig. 14A

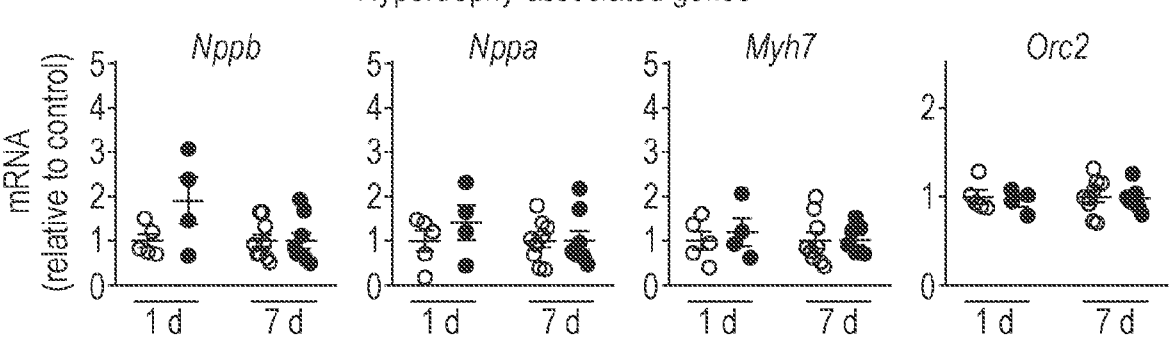

Fig. 14B

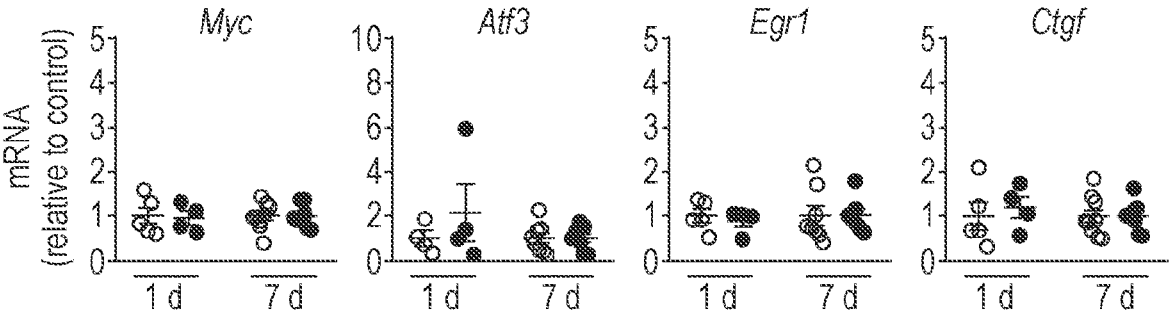

Fig. 14C

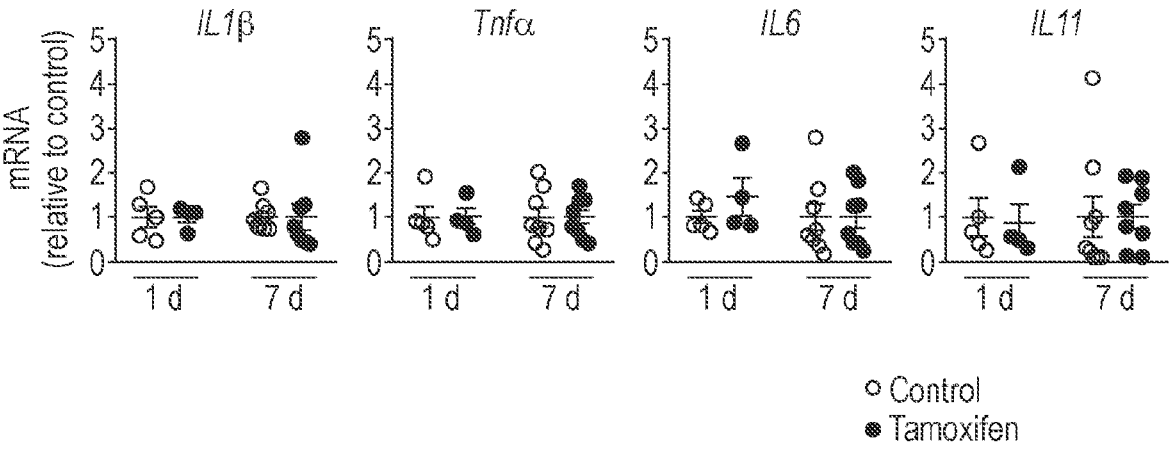

Fig. 14D

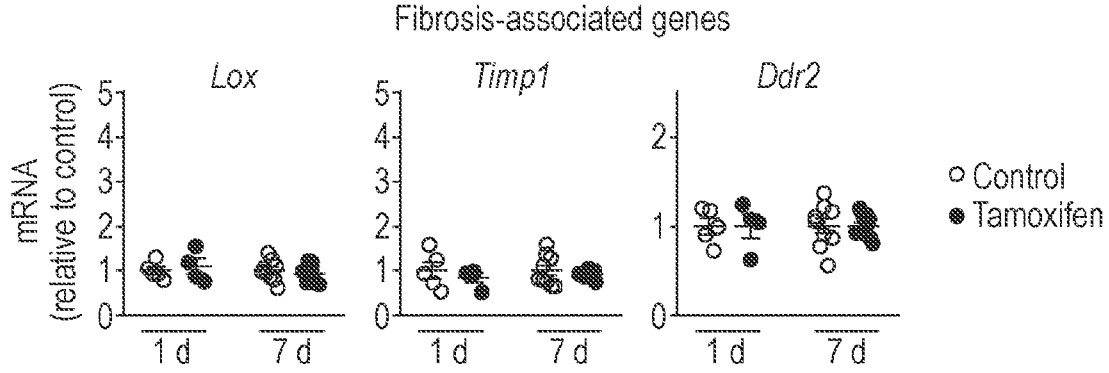

Fig. 14E

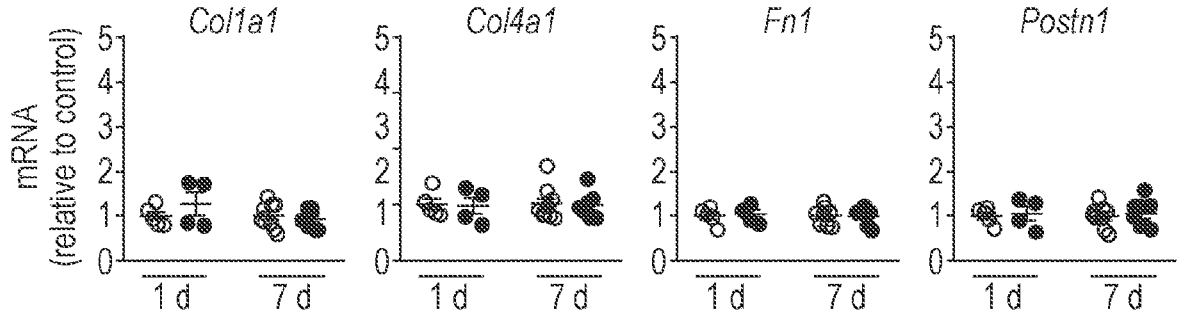

Fig. 15

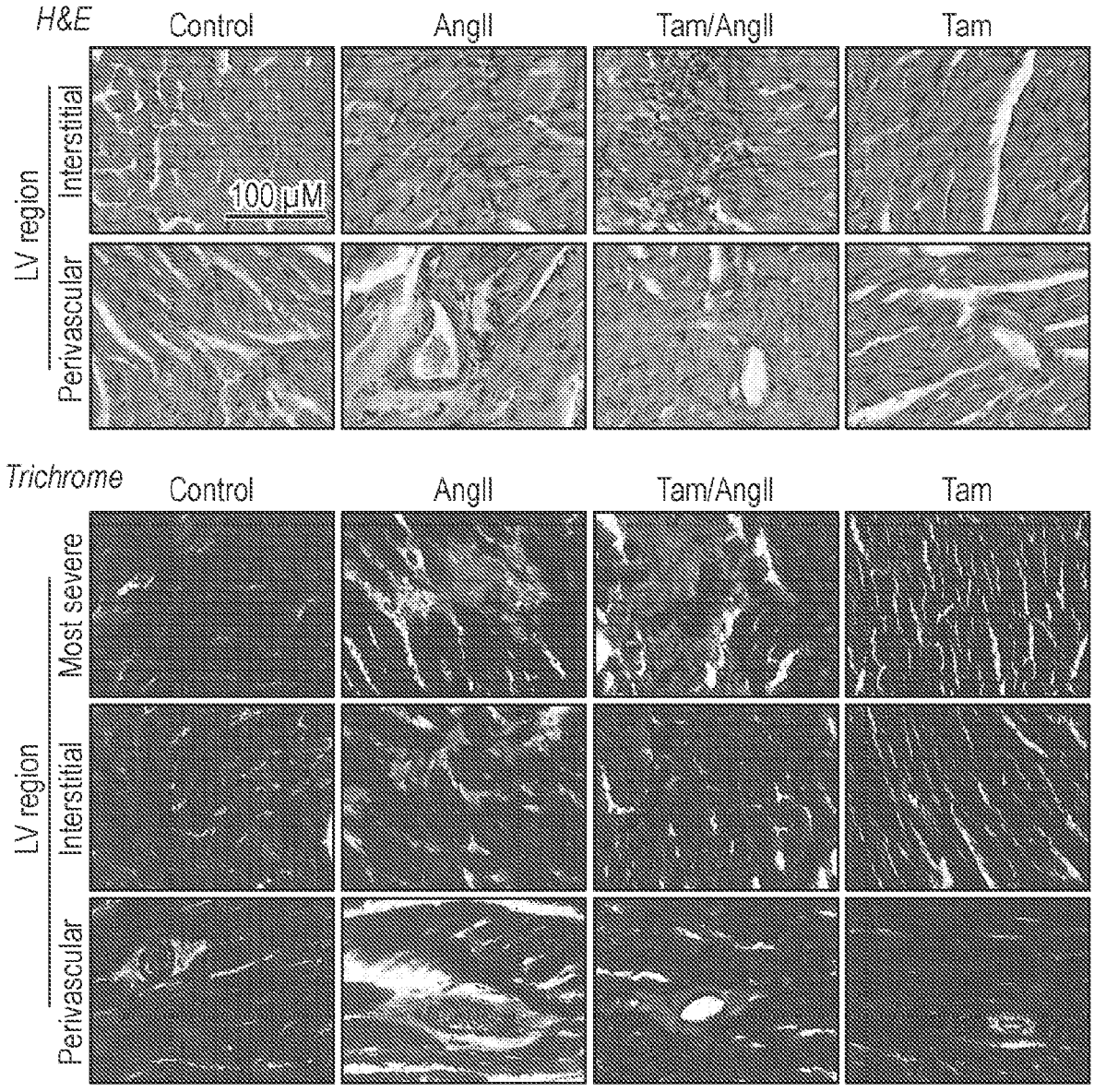
H&E
Control
AngII
Tam/AngII
Tam
LV region
Interstitial
Perivascular
100 µM
Trichrome
Control
AngII
Tam/AngII
Tam
LV region
Most severe
Interstitial
Perivascular

Fig. 16A

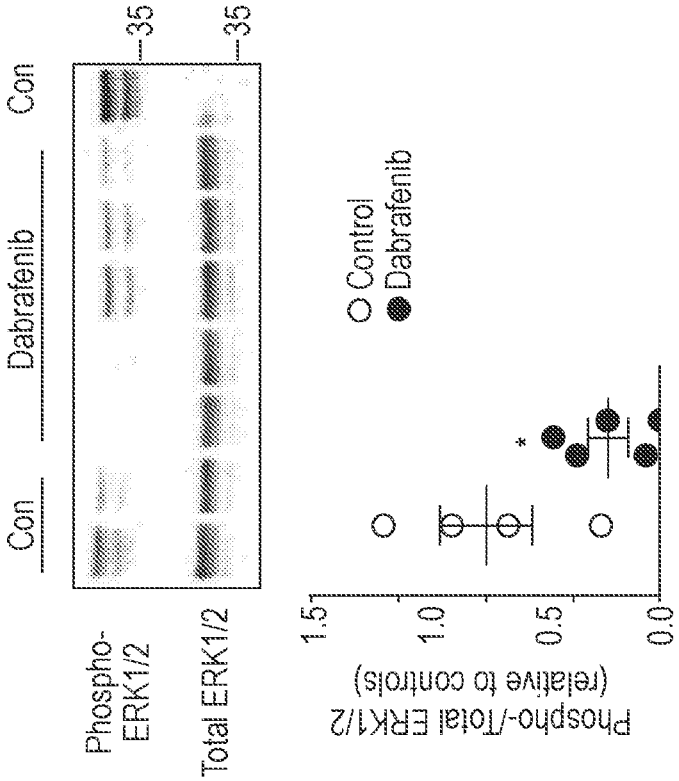

Fig. 16B

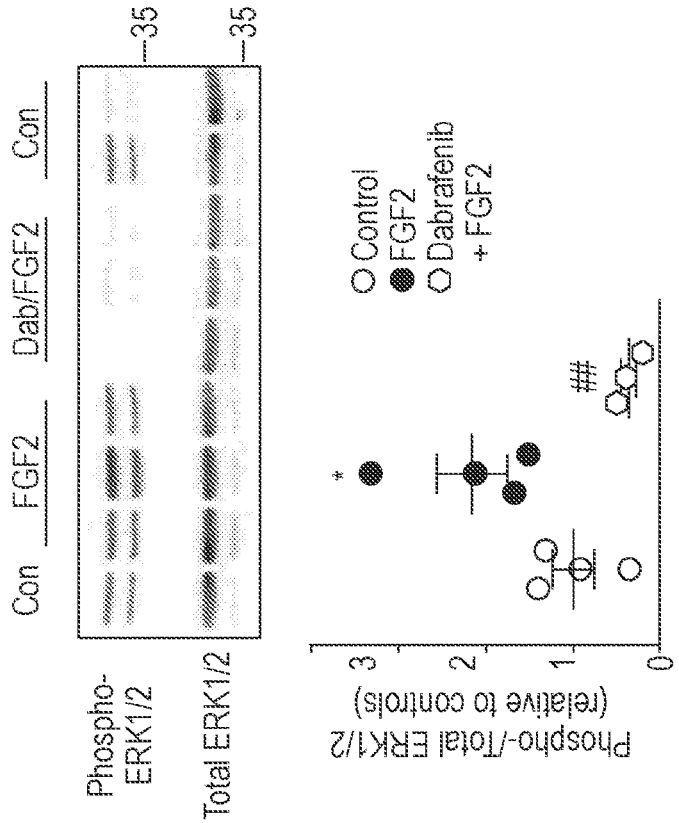

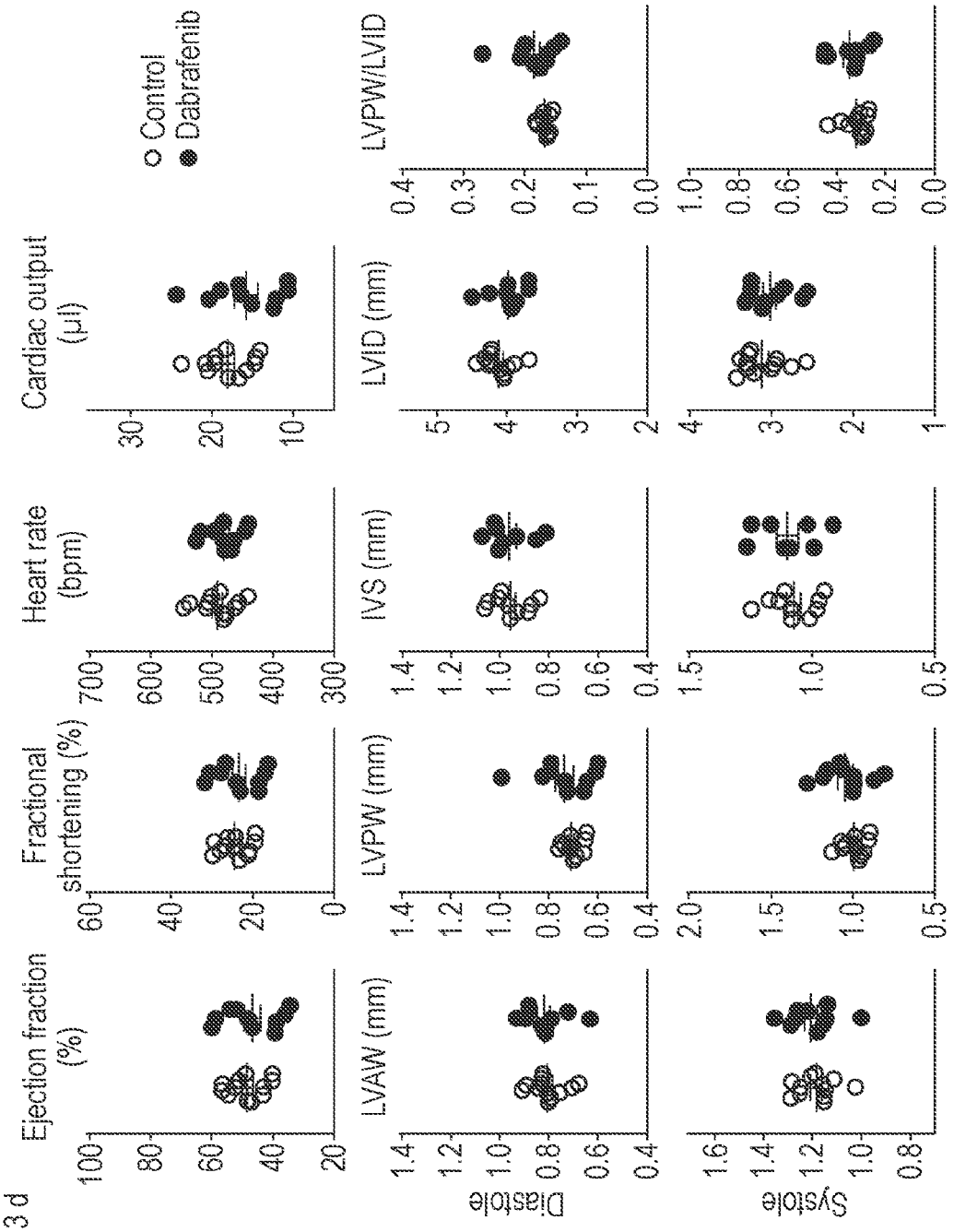
3 d
Ejection fraction (%)
Fractional shortening (%)
Heart rate (bpm)
Cardiac output (µl)
LVAW (mm)
LVPW (mm)
IVS (mm)
LVID (mm)
LVPW/LVID
Diastole
Systole
Control
Dabrafenib

Fig. 17A

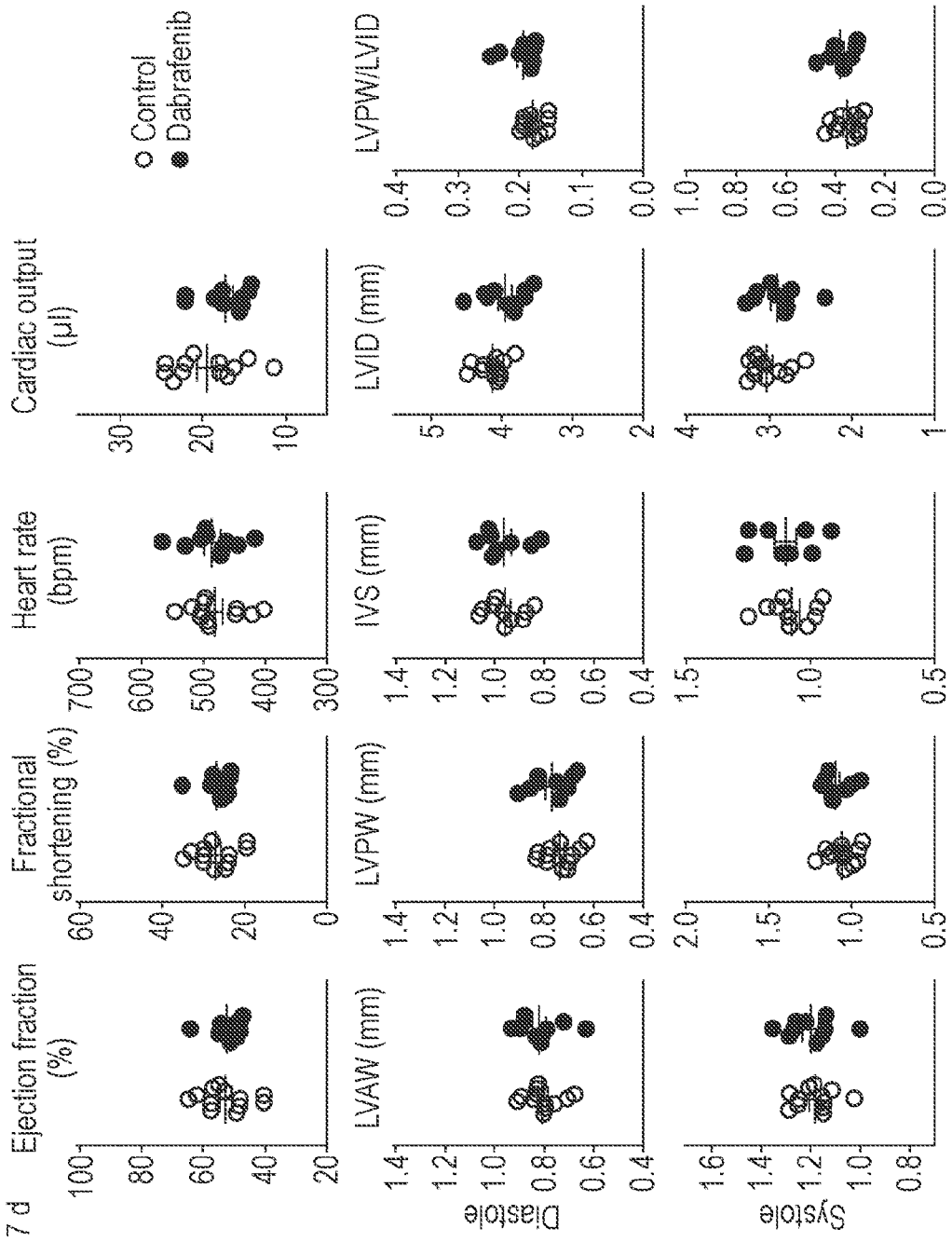
7 d
Ejection fraction (%)
Fractional shortening (%)
Heart rate (bpm)
Cardiac output (µl)
LVAW (mm)
LVPW (mm)
IVS (mm)
LVID (mm)
LVPW/LVID
Diastole
Systole
Control
Dabrafenib

Fig. 17B

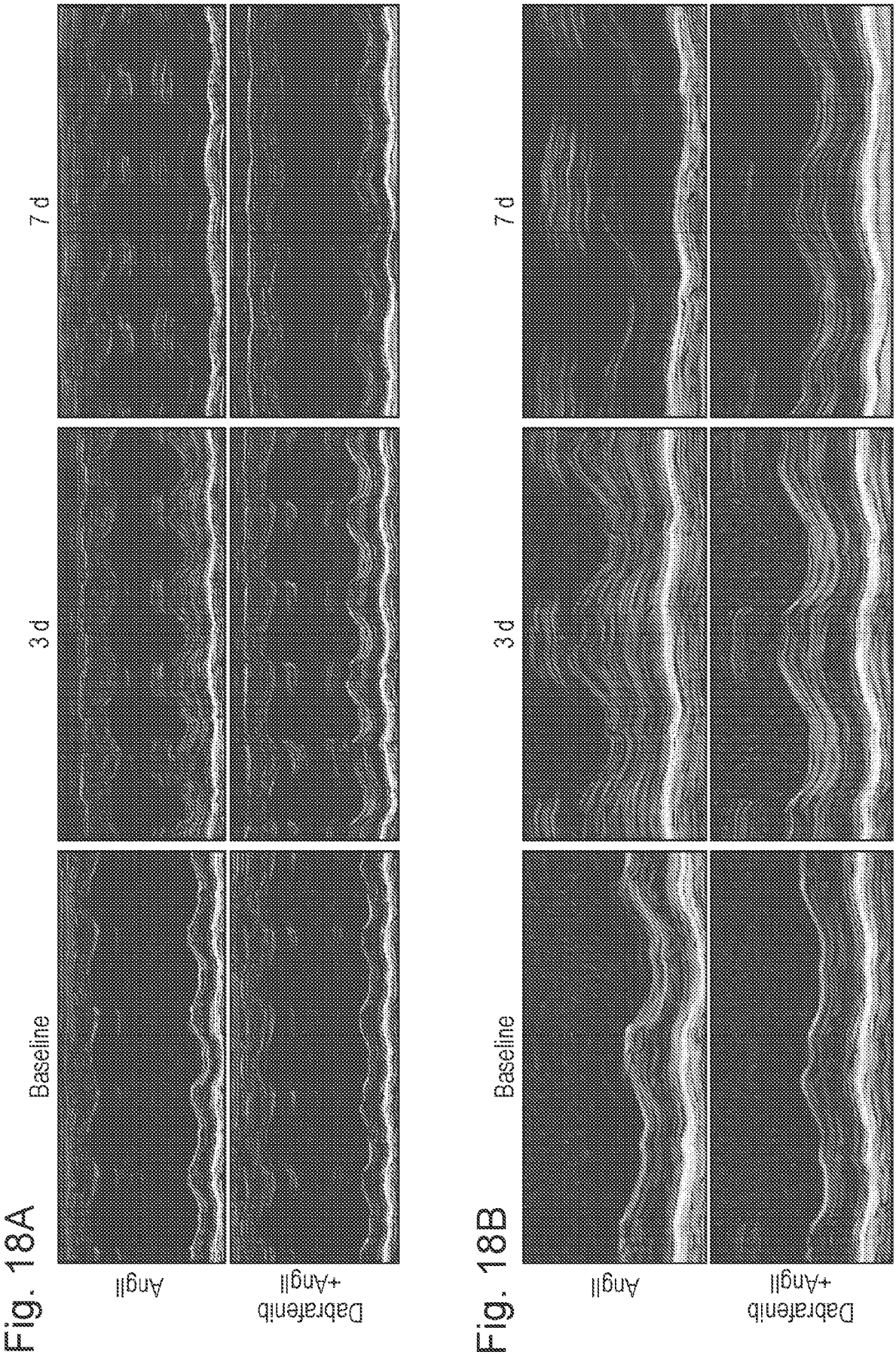

Fig. 18A

Fig. 18B

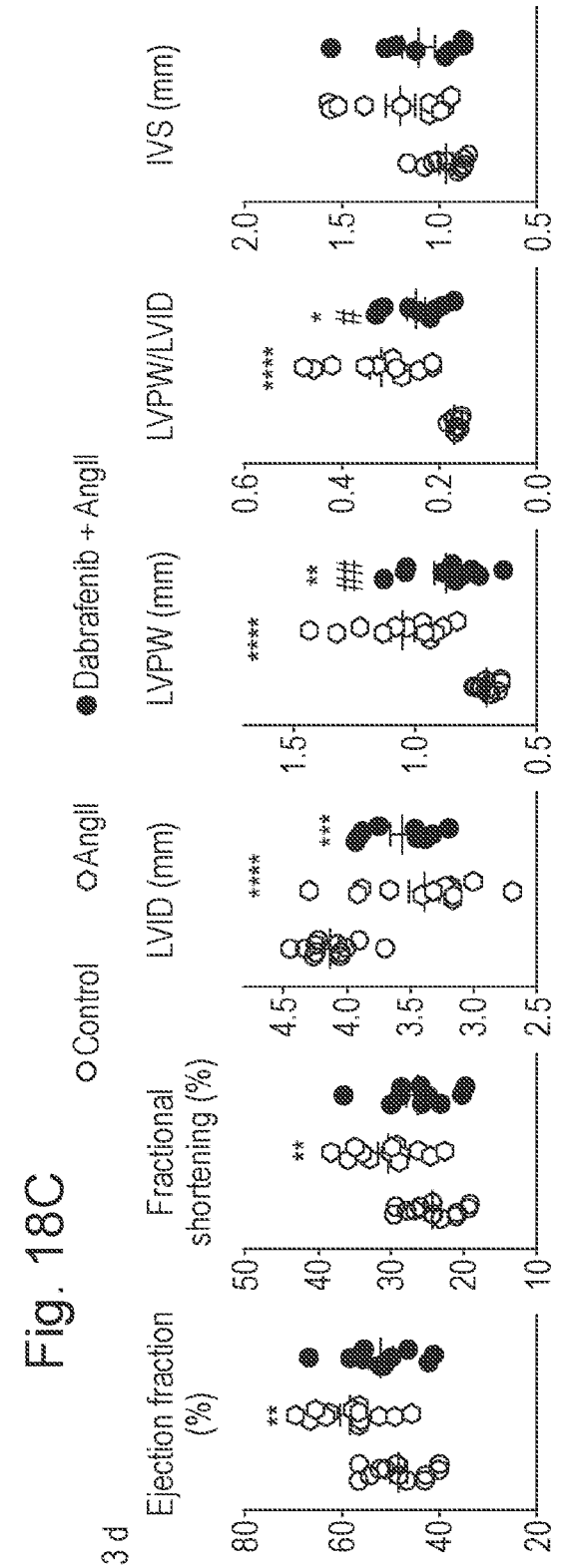
Fig. 18C
Control
Angll
Dabrafenib + Angll
3 d
Ejection fraction (%)
Fractional shortening (%)
LVID (mm)
LVPW (mm)
LVPW/LVID
IVS (mm)

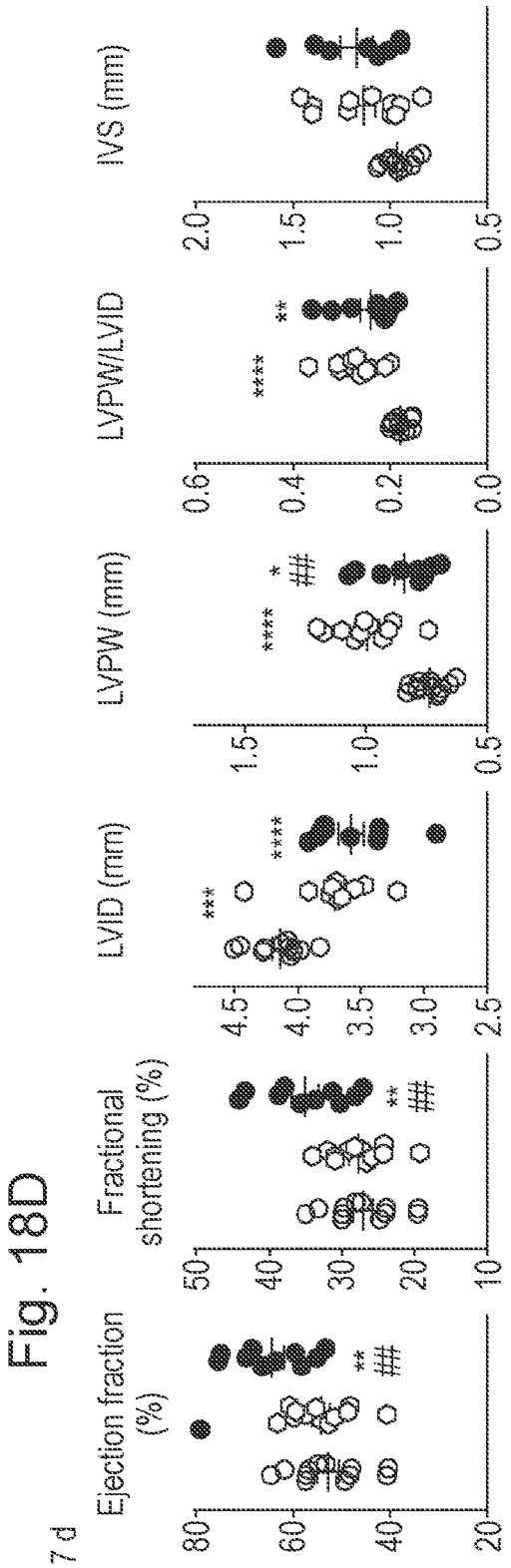
Fig. 18D
7 d
Ejection fraction (%)
Fractional shortening (%)
LVID (mm)
LVPW (mm)
LVPW/LVID
IVS (mm)

Fig. 19

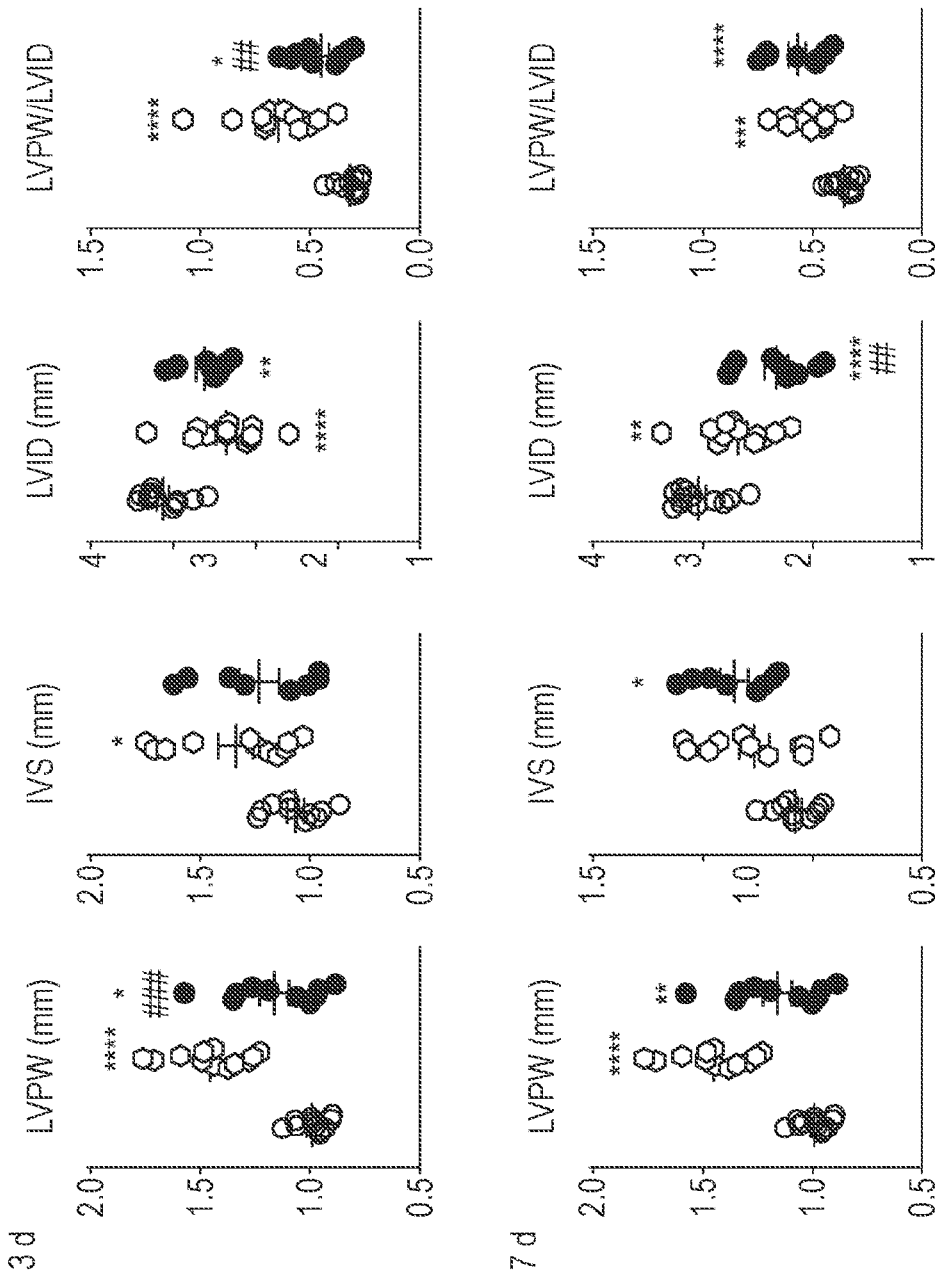

Fig. 20A

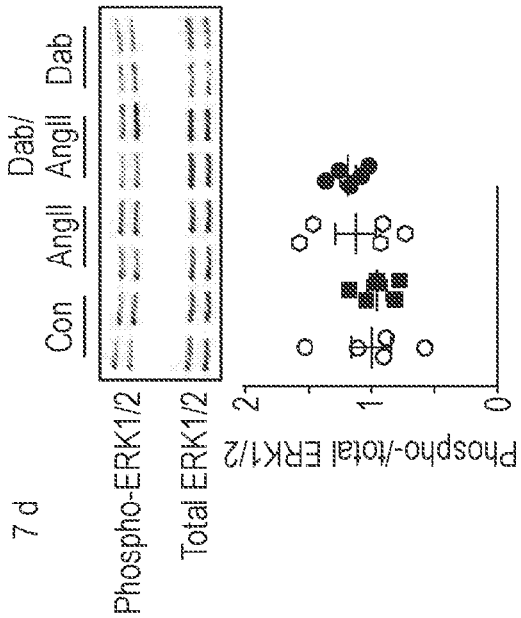

Fig. 20B

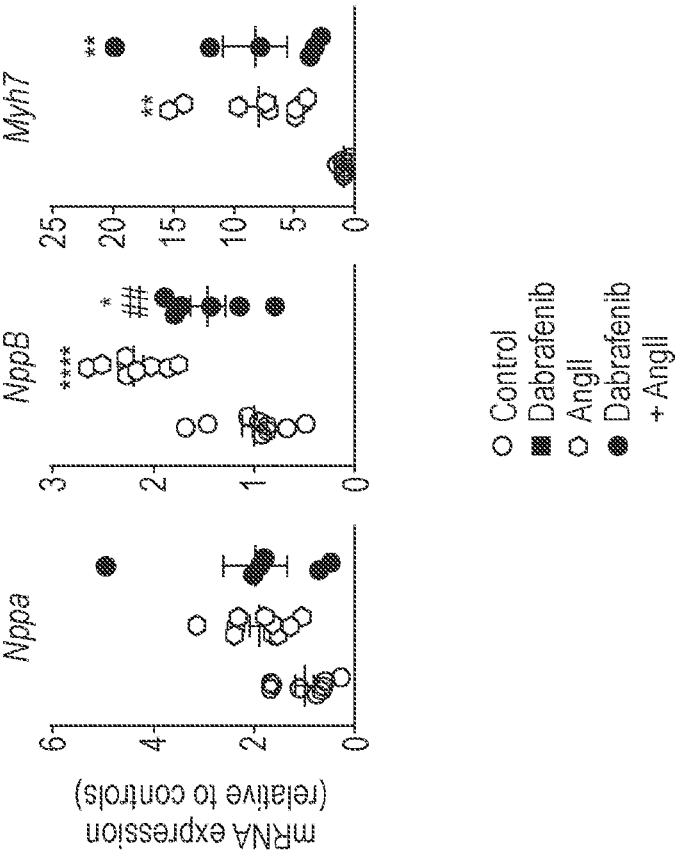

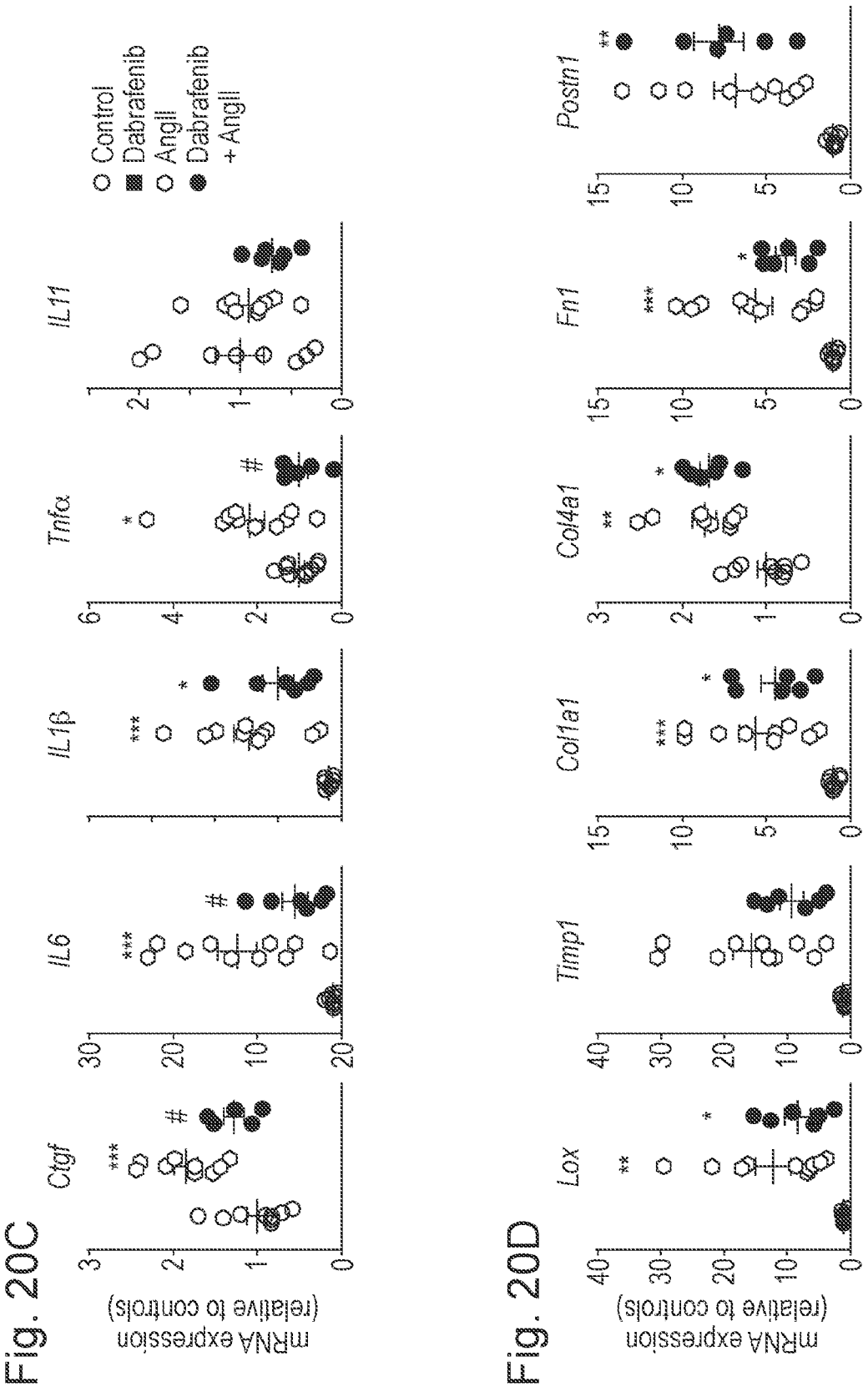

Fig. 20C

Fig. 20D

Fig. 21A

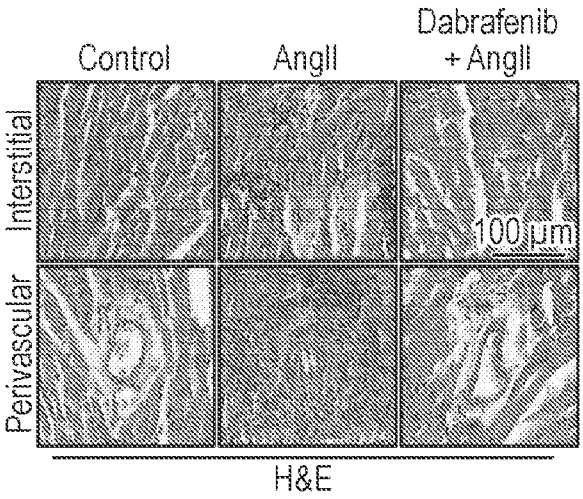

Fig. 21B

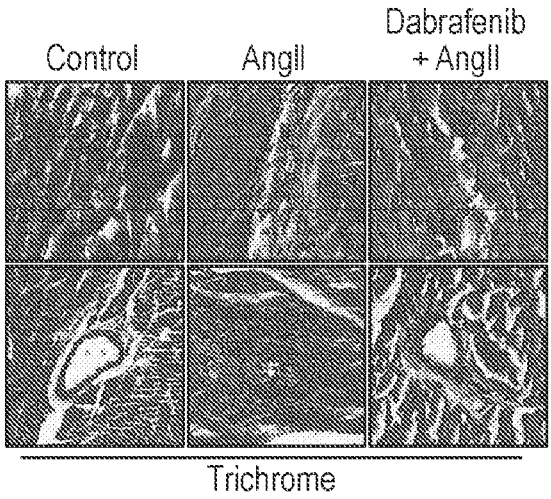

Fig. 21C

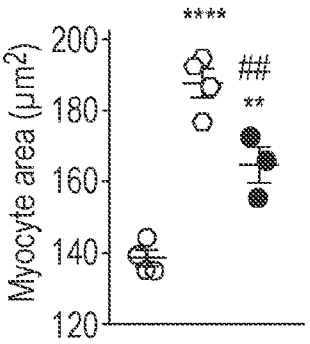

Fig. 21D

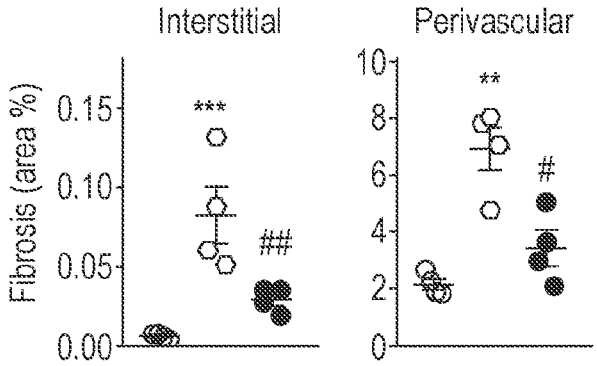

Fig. 21E

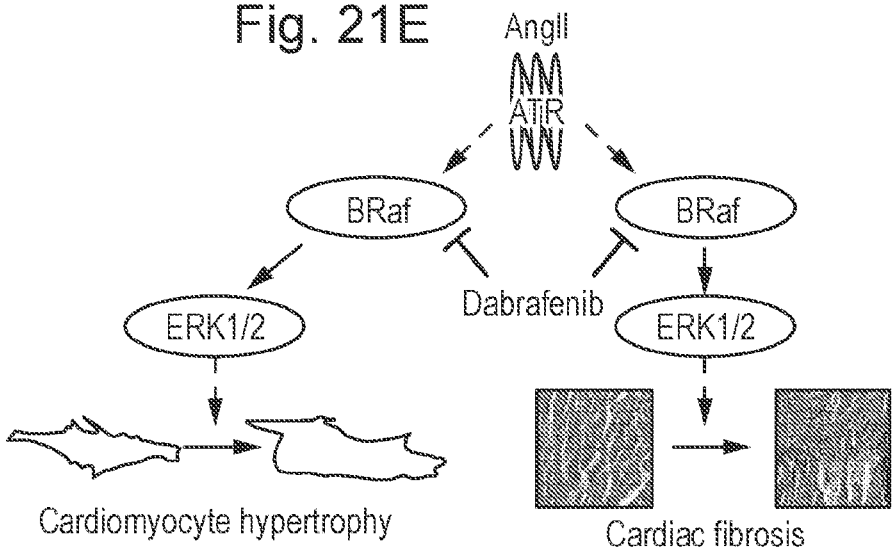

Fig. 22A

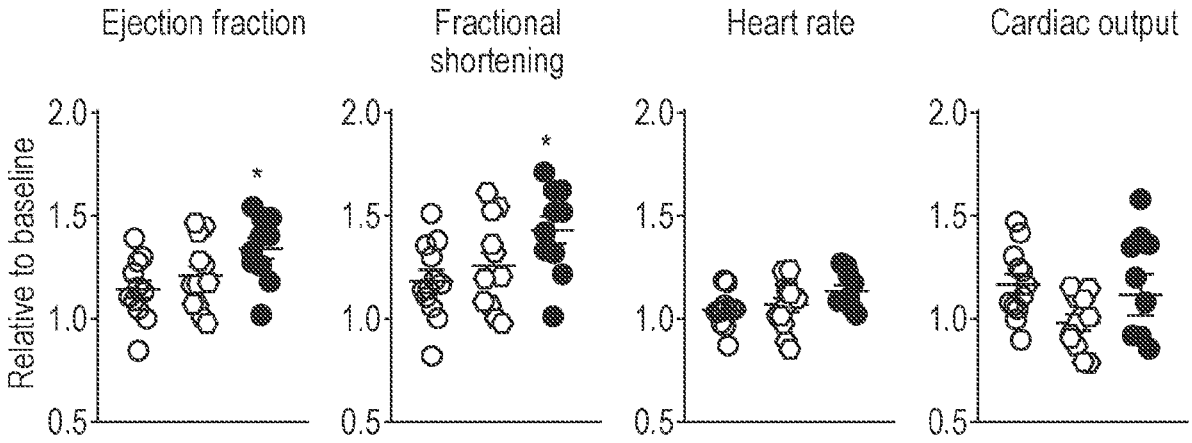

Fig. 22B

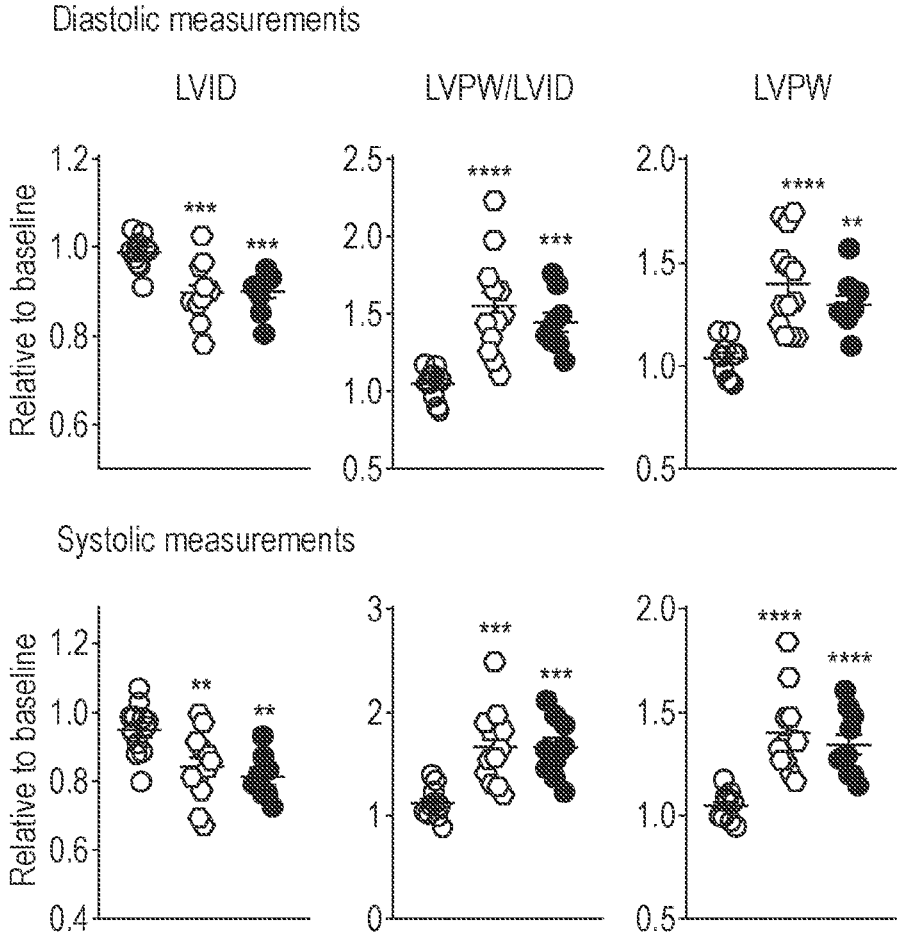

Fig. 23A

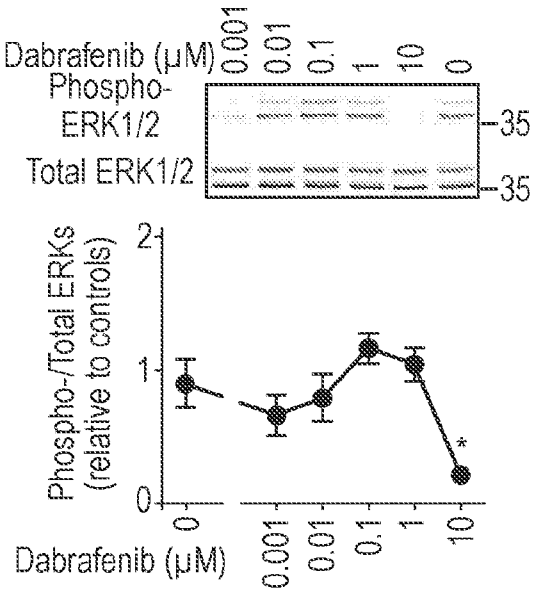

Fig. 23B

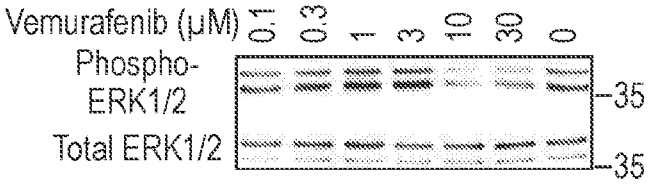

Fig. 23C

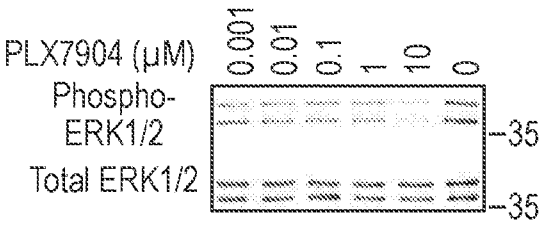

Fig. 23D

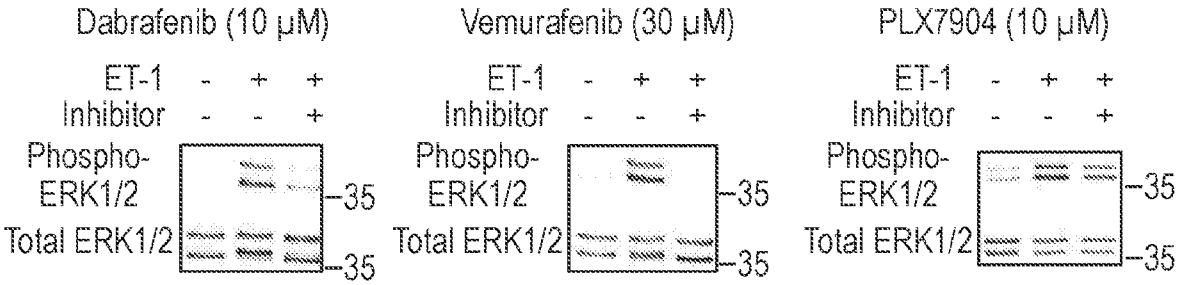

Fig. 23E

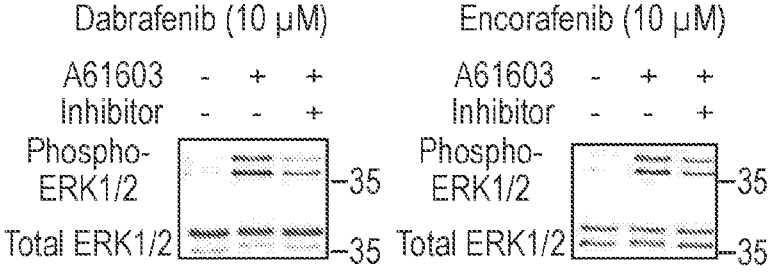

INTERNATIONAL SEARCH REPORT

International application No
PCT/GB2020/050243

A. CLASSIFICATION OF SUBJECT MATTER
INV. A61K31/506 A61K31/437 A61P1/16 A61P9/00 A61P9/04
A61P9/12 A61P11/00 A61P21/00
ADD.
According to International Patent Classification (IPC) or to both national classification and IPC

B. FIELDS SEARCHED

Minimum documentation searched (classification system followed by classification symbols)
A61K A61P

Documentation searched other than minimum documentation to the extent that such documents are included in the fields searched

Electronic data base consulted during the international search (name of data base and, where practicable, search terms used)
EPO-Internal, BIOSIS, EMBASE, WPI Data

C. DOCUMENTS CONSIDERED TO BE RELEVANT

Category*	Citation of document, with indication, where appropriate, of the relevant passages	Relevant to claim No.
X	US 2016/166700 A1 (CHEN YUN-CHING [TW] ET AL) 16 June 2016 (2016-06-16) claims 1,6; example 5	16,17, 19,25,26
X	WO 2014/111584 A1 (GENFIT [FR]) 24 July 2014 (2014-07-24) claims 1,2	16-19, 25,26

-/--

[X] Further documents are listed in the continuation of Box C.

[X] See patent family annex.

* Special categories of cited documents :

"A" document defining the general state of the art which is not considered to be of particular relevance

"E" earlier application or patent but published on or after the international filing date

"L" document which may throw doubts on priority claim(s) or which is cited to establish the publication date of another citation or other special reason (as specified)

"O" document referring to an oral disclosure, use, exhibition or other means

"P" document published prior to the international filing date but later than the priority date claimed

"T" later document published after the international filing date or priority date and not in conflict with the application but cited to understand the principle or theory underlying the invention

"X" document of particular relevance; the claimed invention cannot be considered novel or cannot be considered to involve an inventive step when the document is taken alone

"Y" document of particular relevance; the claimed invention cannot be considered to involve an inventive step when the document is combined with one or more other such documents, such combination being obvious to a person skilled in the art

"&" document member of the same patent family

Date of the actual completion of the international search	Date of mailing of the international search report
23 April 2020	04/05/2020

Name and mailing address of the ISA/	Authorized officer
European Patent Office, P.B. 5818 Patentlaan 2 NL - 2280 HV Rijswijk Tel. (+31-70) 340-2040, Fax: (+31-70) 340-3016	Pacreu Largo, Marta

1

Form PCT/ISA/210 (second sheet) (April 2005)

C(Continuation). DOCUMENTS CONSIDERED TO BE RELEVANT

Category*	Citation of document, with indication, where appropriate, of the relevant passages	Relevant to claim No.
X	AREZOO DARYADEL ET AL: "Multikinase inhibitor sorafenib prevents pressure overload-induced left ventricular hypertrophy in rats by blocking the c-Raf/ERK1/2 signaling pathway", JOURNAL OF CARDIOTHORACIC SURGERY, BIOMED CENTRAL LTD, LO, vol. 9, no. 1, 9 May 2014 (2014-05-09), page 81, XP021188390, ISSN: 1749-8090, DOI: 10.1186/1749-8090-9-81	16-18, 22,25,26
Y	page 7, left-hand column	1-4,10, 11

X	B. BUCHHOLZ ET AL: "The Raf kinase inhibitor PLX5568 slows cyst proliferation in rat polycystic kidney disease but promotes renal and hepatic fibrosis", NEPHROLOGY DIALYSIS TRANSPLANTATION., vol. 26, no. 11, 29 July 2011 (2011-07-29) , pages 3458-3465, XP055688464, GB ISSN: 0931-0509, DOI: 10.1093/ndt/gfr432 abstract	16-26

Y	DANIEL MEIJLES ET AL: "Braf inhibitors, sb590885 and dabrafenib, enhance erk1/2 signalling in cardiomyocytes and promote cardiac hypertrophy", HEART, vol. 103, no. Suppl 5, 5 June 2017 (2017-06-05), pages A146.3-A147, XP055686501, GB ISSN: 1355-6037, DOI: 10.1136/heartjnl-2017-311726.226 abstract	1-15

Y	MEIJLES D N ET AL: "Cardiomyocyte braf promotes hypertrophy and is required for hypertrophic adaptation to hypertension in mice in vivo, but raf inhibitors have differential effects", CIRCULATION RESEARCH 20180801 LIPPINCOTT WILLIAMS AND WILKINS NLD, vol. 123, no. Supplement 1, 1 August 2018 (2018-08-01), XP9520096, ISSN: 1524-4571 abstract	1-15

	-/--	

1

C(Continuation). DOCUMENTS CONSIDERED TO BE RELEVANT

Category*	Citation of document, with indication, where appropriate, of the relevant passages	Relevant to claim No.
Y	MEIJLES DANIEL N ET AL: "Raf Kinase Inhibitors Activate ERK1/2 in Cardiomyocytes, Promoting Cardiac Hypertrophy in vitro and, in the Context of Angiotensin II-Induced Hypertension in Mice, in vivo", CIRCULATION RESEARCH, vol. 121, no. Suppl. 1, 21 July 2017 (2017-07-21), page 470, XP9520095, & BASIC CARDIOVASCULAR SCIENCES SCIENTIFIC SESSIONS OF THE AMERICAN-HEART-ASSOCIATION - PATHWAYS TO CARDIOVASCULAR THERAPEUTICS; PORTLAND, OR, USA; JULY 10 -13, 2017 abstract -----	1-15

INTERNATIONAL SEARCH REPORT

Information on patent family members

International application No
PCT/GB2020/050243

Patent document cited in search report	Publication date	Patent family member(s)	Publication date
US 2016166700 A1	16-06-2016	TW 201620549 A	16-06-2016
		US 2016166700 A1	16-06-2016
WO 2014111584 A1	24-07-2014	AU 2014206781 A1	16-07-2015
		CA 2897258 A1	24-07-2014
		CN 105120855 A	02-12-2015
		DK 2948137 T3	07-01-2019
		EA 201591345 A1	30-11-2015
		EP 2948137 A1	02-12-2015
		ES 2702038 T3	27-02-2019
		HK 1214773 A1	05-08-2016
		HU E042569 T2	29-07-2019
		IL 239715 A	30-06-2019
		JP 6218854 B2	25-10-2017
		JP 2016506913 A	07-03-2016
		KR 20150114497 A	12-10-2015
		LT 2948137 T	27-12-2018
		MD 20150076 A2	30-11-2015
		MX 361565 B	11-12-2018
		PH 12015501566 A1	21-09-2015
		PL 2948137 T3	28-02-2019
		PT 2948137 T	20-12-2018
		SG 11201505281P A	28-08-2015
		SI 2948137 T1	31-01-2019
		TR 201819042 T4	21-01-2019
		US 2015352065 A1	10-12-2015
		US 2017239213 A1	24-08-2017
		WO 2014111584 A1	24-07-2014
		ZA 201505151 B	27-07-2016